UNIVERSITY OF NAPOLI FEDERICO II
Dipartimento di Biologia e Patologia Cellulare e Molecolare "L. Califano"

Doctorate School in Molecular Medicine

Doctorate Program in Molecular Pathology and Physiopathology
Coordinator: Prof. Vittorio Enrico Avvedimento
XXIII Cycle

"FUNCTIONAL AND MOLECULAR EFFECTS OF CHROMOSOME 21 TRISOMY"

IZZO ANTONELLA

Napoli 2010

TABLE OF CONTENTS

LIST OF PUBLICATIONS

1) Conti A, Scala S, Romano M, **Izzo A**, Fabbrini F, Della Ragione F, D'Esposito M, Nitsch L, Calise F and Faiella A "Gene expression profile in liver transplantation and the influence of gene dysregulation occurring in decreased donor grafts" Open Surg J, 2010, 4.
2) **Izzo A**, Genesio R, Ronga V, Nocera V, Marullo L, Cicatiello R, Sglavo G, Paladini D, Conti A and Nitsch L. Prenatal diagnosis of an inverted duplication of chromosome 5p arm with terminal deletion. *In preparation.*

ABSTRACT

Down Syndrome (DS) is the most frequent autosomal aneuploidy that is compatible with post-natal life. The DS phenotype has been attributed to overexpression of chromosome 21 (Hsa21) genes. It is unknown which, and how many, chromosome 21 genes are responsible for each DS phenotypic sign such as mental retardation, cardiac defects, muscle hypotonia, immunological disorders, etc. Hsa21 trisomy has been associated to mitochondrial dysfunction in several DS cells and mouse models suggesting that a mitochondrial dysfunction contributes to DS phenotype. We demonstrated, by microarray analysis and by qRT-PCR, the global upregulation of Hsa21 genes and the dysregulation of genes located on other chromosomes in trisomic fetal hearts at 18-22 weeks of gestation. Downregulation of genes encoding mitochondrial enzymes was a hallmark of trisomic fetal samples.

Molecular, functional and morphological studies of mitochondria in primary lines of fetal fibroblasts were performed in order to evaluate the mitochondrial dysfunction associated to the dysregulation of mitochondrial gene expression in DS.

Molecular analysis of trisomic fibroblasts demonstrated that the upregulation of chromosome 21 genes and the dysregulation of mitochondrial genes also occur in these cells, and that it is not identical to the one observed in fetal hearts.

Functional studies demonstrated a significant reduction of the oxygen consumption rate and of respiratory chain complex I activity in trisomic fibroblasts, a decrease of mtDNA copy number and an increased production of reactive oxygen species.

Furthermore, the mitochondria ultrastructure of trisomic fibroblasts, assessed by electron microscopy, revealed morphological abnormalities like giant mitochondria with irregular shape, evident breaks of both inner and outer membranes and an altered cristae pattern.

These results are indicative of a widespread mitochondrial dysfunction in DS.

To detect the earliest changes in gene expression profile, a new in vitro cell culture model was set up. Human stem cells from euploid as well as from Hsa21 trisomic fetuses were obtained. Both fresh and frozen amniotic fluid cultures were successfully used and the lines obtained appear to be suitable to study the differentiation processes in trisomic vs. euploid cells.

BACKGROUND

1. Down Syndrome

Down Syndrome (DS) is the most frequent autosomal aneuploidy that is compatible with post-natal life. It results from complete or partial trisomy of chromosome 21 (Hsa21) and is characterized by a complex phenotype in which over 80 features occur with various degrees of expression and frequency [Epstein et al. 1991].

Constant features in trisomic subjects are mental retardation, hypotonia, developmental delay, a partial immune deficiency, especially of thymus-dependent system, and an increased risk of leukemia.

Down syndrome is a major cause of congenital heart defects (CHD). It is associated mostly with endocardial cushion defects [Ferencz et al. 1989, Park et al. 1977], the most frequent being atrioventricular canal defects (AVCD) followed by ventricular septal defects (VSD) and tetralogy of Fallot [Park et al. 1977].

DS-CHD critical region

It has been known since half a century that Down syndrome is caused by the presence of an extra copy of chromosome 21. However, the molecular alterations that cause the DS phenotype are still elusive, despite a large amount of studies. Indeed, it is unknown which, and how many, chromosome 21 genes are responsible for each DS phenotypic sign such as mental retardation, cardiac defects, muscle hypotonia, immunologic disorders, etc.

Several attempts to identify the Hsa21 genes that contribute to the DS phenotype have focused on the Down Syndrome Critical Region (DSCR) which spans approximately 5.4 Mb in band 21q22.3 (**Fig. 1**) [Korenberg et al. 1994; Delabar et al. 1993; McCormick et al. 1989; Rahmani et al. 1989]. The DSCR hypothesis predicts that a gene, or some genes, in this region are sufficient to produce the specific DS features when present in three copies. A narrowed region from D21S3 to PFKL in 21q22.3 was also proposed as the candidate region for heart defects (DS-CHD region) [Barlow et al. 2001]. The DSCR hypothesis was tested in mice [Olson et al. 2004] and it was found that trisomy of DSCR alone is necessary but not sufficient for brain DS phenotypes in trisomic mice. These results suggest that the origins of trisomic phenotypes are even more complicated than formerly assumed and that they probably involve multiple gene interactions [Olson et al. 2007]. It has been proposed that the complex phenotypic alterations of DS could result from an interplay between Hsa21 genes and developmentally regulated genes elsewhere on the genome [Reeves 2001] and that the loss of genetic balance in pivotal processes regulating development might increase susceptibility to genetic and environmental insults [Shapiro 1997].

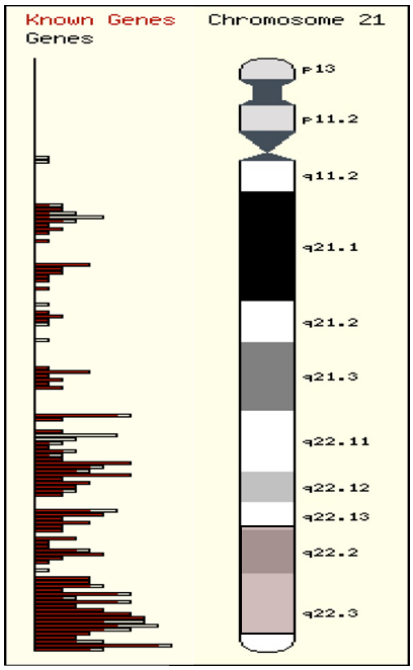

Figure 1. Down Syndrome Critical Region. The DSCR spans approximately 5,4Mb including bands 21q22.2 and 21q22.3 (pink area). This region presents with high gene density.

Mouse models

To understand the molecular mechanisms of phenotypic alterations in DS, the mouse has been used extensively as a model organism, based on the syntenic conservation between human and mouse genomes. Hsa21 presents high sequence omology of about 30 Mb with mouse chromosome 16, including part of DSCR. Other sintenic regions are localized on murine chromosomes 10 and 17.

One group of mouse models was generated to carry Hsa21 or a fragment of it [O'Doherty et al. 2005, Shinohara et al. 2001]. The Tc1 model was obtained introducing into the mouse genome Hsa21 traits with only two small deletions including about 8% of Hsa21 genes. This mouse model shows craniofacial anomalies and cardiac alterations, typical of DS. The morphogenetic defects include ventricular and atrioventricular septal defect, that are due to an incomplete fusion of endocardial cushions [Dunlevy et al. 2010].

Another group of models carries three copies of mouse syntenic regions of Hsa21 in various sizes. Ts65Dn is the most widely used model from this group [Reeves et al. 1995]. Ts65Dn mice are trisomic for ~13.4 Mb of the Hsa21 syntenic region on Mmu16, which contains approximately 99 orthologs of Hsa21 genes and exhibit only few phenotypic features comparable to DS.

Moore (2006) has found that ~8% of Ts65Dn mice develop septal defects which increase their post-natal mortality.
In another mouse model, Dp(16)1Yu/+, the trisomic region spans from 21q11 band to 21q22.3 band thus including part of DS-CHD region. These transgenic mice develop congenital cardiopathy with a similar percentage to those found in DS individuals [Li et al. 2007]: atrioventricular septal defects including Tetralogy of Fallot and atrioventricular canal defect.
Mice trisomic for smaller regions of Mmu16 have also been described. The Ts1Cje mouse is trisomic for ~70 Mmu16 genes extending from, but not including, Sod1 to the Mmu16 telomere [Sago et al. 1998]. These mice showed distinct learning and behavioral deficits, probably caused by abnormalities within the hippocampus that result in abnormal hippocampal function. Olson et al. (2004) produced mice trisomic only for DSCR between Cbr1 and Mx1, containing roughly 33 annotated genes (Ts1Rhr mice), demonstrating that DSCR alone is necessary but not sufficient for brain DS phenotypes in trisomic mice, even though more recently Belichenko et al. (2009) demonstrated that 33 genes mapping to the DSCR are responsible at least for 20 DS features in the mouse Ts1Rhr.
Because of the potential species-specific differences between Hsa21 and the mouse syntenic regions, the transcriptional regulations of the Hsa21 gene orthologs and the interactions of the proteins encoded by these orthologs in a trans-species mouse mutant may be different from those in a mouse mutant carrying three copies of a mouse syntenic region, even if the triplicated regions carry the same orthologous genes in both mutants. Therefore, Yu et al. (2010) decided to generate a mouse model trisomic for all three Hsa21 syntenic regions and to analyze the impact of the simultaneous presence of the three segmental trisomies on the cognitively relevant phenotype. This mouse model, named Dp(10)1Yey/+;Dp(16)1Yey/+;Dp(17)1Yey/+, seems to be the more desiderable genotype for modeling human trisomy 21 and it shows the DS-related abnormalities in the central nervous system, including impairments in learning and hippocampal LTP as well as hydrochephalus. There is no evidence of congenital cardiopathy in this model.
In conclusion, all these models should facilitate better understanding of the mechanisms underlying developmental defects in DS as well as the development of new therapies for the clinical phenotype of the disorder but no one can be considered the perfect one.

Gene expression in DS

It has been postulated that a triplicated chromosome 21 causes an increase in the expression of trisomic genes as a primary dosage effect. This primary dysregulation produces, as secondary effect, the dysregulation of genes mapping on different chromosomes causing the dysregulation of several proteins and consequently the DS phenotype (**Fig. 2**).
In agreement with the above hypothesis, several studies have reported a generalized overexpression of triplicated genes at the mRNA level in mouse

models of DS [Amano et al. 2004; Lyle et al. 2004; Kahlem et al. 2004; Dauphinot et al. 2005]. Interestingly, studies performed on human trisomic tissues indicated that only a subset of Hsa21 genes is over-expressed relative to euploid controls and that the increase in expression may slightly differ from the expected ~1.5-fold [FitzPatrick et al. 2002; Mao et al. 2005, Conti et al. 2007]. Also, the set of over-expressed Hsa21 genes differs across the trisomic cell types [Li et al. 2006]. These findings indicate that other factors (e.g. developmental stage, tissue-specific differences) might also affect gene expression [Sommer and Henrique-Silva 2008].

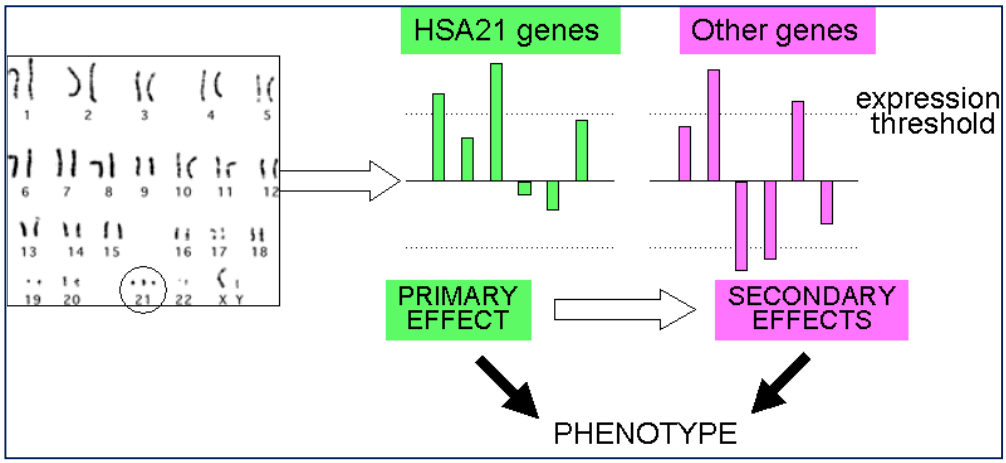

Figure 2. Primary and secondary effects of trisomy 21. Three copies of Hsa21 may cause a 50% increase in the expression of trisomic genes as primary dosage effect. The abnormal mRNA levels of Hsa21 genes may cause alteration of disomic gene expression as secondary effects. Both primary and secondary effects will finally result in developmental defects and phenotypic alterations.

A previous study performed in our laboratory on heart tissue [Conti et al. 2007] demonstrated that chromosome 21 genes were globally upregulated and that 441 genes, located on other chromosomes, were significantly dysregulated in trisomic heart samples. Downregulation of genes encoding mitochondrial enzymes and upregulation of genes encoding extracellular matrix (ECM) proteins appeared to be a hallmark of trisomy 21 in fetal heart samples. Other studies agree with these findings: in fact, data from functional studies suggest that multiple chromosome 21 genes affect protein processing, mitochondrial function and reactive oxygen species production, one-carbon metabolism and cell adhesion [Gardiner 2003].

2. Mitochondrial dysfunctions in DS

Trisomy of chromosome 21 has been associated to mitochondrial dysfunction, in several DS cell [Busciglio et al. 1995; Roat et al. 2007] and mouse models [Shuchman et al. 2000; Shukkur et al. 2006], suggesting that a mitochondrial dysfunction contributed to DS phenotype. It has been hypotesized that the pathogenetic mechanisms may be ascribed to oxidative stress caused by reactive oxygen species (ROS) formation, to altered intracellular calcium homeostasis and to apoptosis. No molecular studies have been performed yet to investigate the bases of mitochondrial dysfunction at transcriptional level.

Mitochondria: structure and function

Mitochondria are intracellular organelles present in the cytoplasm of all eukaryotic cells. The overall volume of mitochondria is high (thousands per cell) in tissues and organs with high metabolic activity such as brain, retina, skeletal muscle, heart, kidney, and endocrine glands. The overall volume of mitochondria further increases in cells with enhanced energy demands, as in hyperactive skeletal muscle or in cardiac myocyte hypertrophy.

Mitochondria are variable in size, with a diameter of about 1 μm-close to that of a bacterial cell. The shape and number of these organelles are regulated by fission and fusion processes which vary depending on the function of the cell and tissue. Mitochondria are surrounded by outer and inner membranes that are consistent with their symbiontic origin. The outer membrane is smooth and permeable, whereas the inner envelope is highly folded and structured in cristae and offers the major permeability barrier to ions and molecules that traverse to the inner mitochondrial compartment by active transport. The two envelopes enclose an intermembrane space and an area inside the inner membrane, called matrix, where the basic mitochondrial macromolecular syntheses (DNA replication, transcription, and translation) take place (**Fig. 3**).

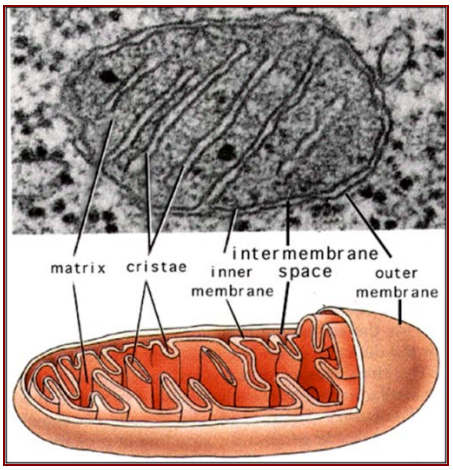

Figure 3. The mitochondrion. Electron microscope and simplified images of mitochondria, showing structural organization of outer and inner membranes, intermembrane space, cristae and matrix.

The function of the mitochondria is identical in all eukaryotic cells and is essentially devoted to energy production by oxidative phophorylation (OXPHOS) process. The energy produced in the mitochondrion is transferred to the whole cell, where it is essential for all biochemical processes. The OXPHOS system is embedded in the lipid bilayer of the mitochondrial inner membrane and is composed by five multiprotein enzyme complexes (I–V) and two electron carriers – coenzyme Q and cytochrome c (**Fig. 4**). Mitochondrial OXPHOS constitutes the major cellular ATP-producing mechanism under aerobic conditions.

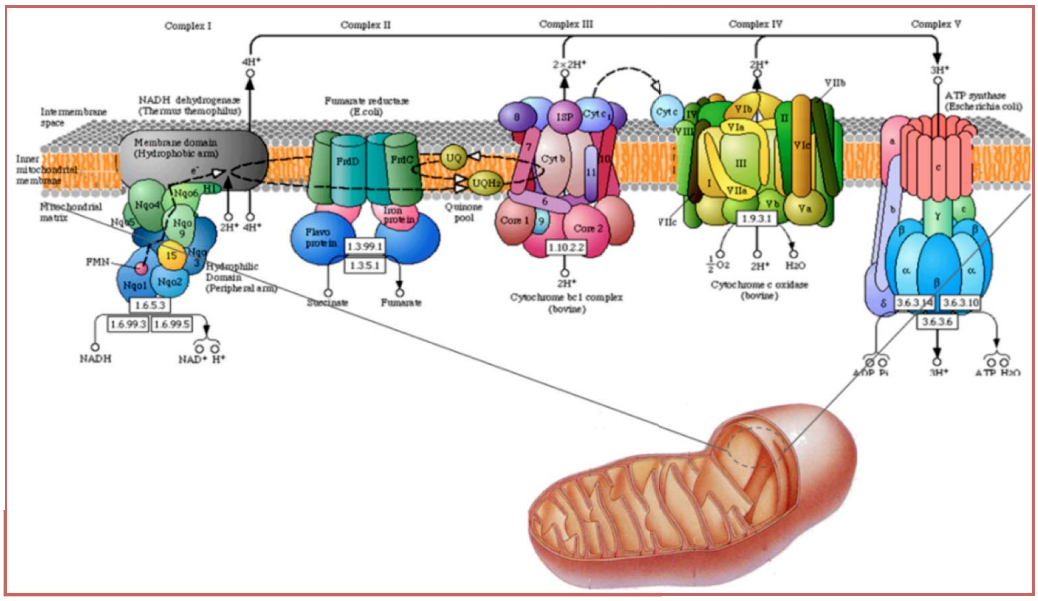

Figure 4. OXPHOS system in mammalian mitochondria. Schematic illustration of respiratory chain complexes, constisting of multiple subunits, in the mitochondrial inner membrane.

The multi-component structure of the OXPHOS network poses the question as to which step(s) is (are) critical in controlling the efficiency of the overall process. An understanding of this specific point, besides its interest in basic research, is also important for elucidating the aetiopathogenesis of a number of human diseases characterized by impairment in OXPHOS efficiency. Defects in oxidative phosphorylation are generally studied by the measurement of mitochondrial oxygen consumption (respirometric OXPHOS analysis) using the polarographic oxygen sensor [Gnaiger and Forstner 1983]. This analysis provides a screening approach that reflects not only derangement of membrane structure, but also defects of enzyme systems in membrane transport, dehydrogenases, electron transport, and coupled ADP phosphorylation [Gnaiger 2008].

A consequence of mitochondrial activity is the production of reactive oxygen species (ROS) that refers to a group of oxygen containing compounds with the

ability to react with reduced compounds. They comprise superoxide (O^{2-}•), hydrogen peroxide (H_2O_2), and the highly reactive hydroxyl radical (•OH), although minor amounts of singlet oxygen can also be formed by cells. The initial product of the electron transport chain is O^{2-}•, which is quickly transformed into H_2O_2 by the enzyme superoxide dismutase (SOD). H_2O_2 can be reduced to water by catalase or glutathione peroxidase or can be converted into •OH in presence of reduced transition metals (reduced copper or iron).
The main source of O^{2-}• are respiratory complexes I and III located at the inner mitochondrial membrane. These complexes generate a small amount of O^{2-}• as a side product of electron transport during oxidative phosphorylation. O^{2-}• is released into the matrix in the case of complex I and to both the matrix and the intermembranous space by complex III [Chen et al. 2003; Camello-Almaraz et al. 2006]. The relative importance of these sites in O^{2-}• mitochondrial output depends on tissue and mitochondria respiratory status.

Nuclear genes in mitochondrial biogenesis and morphology

With only 13 OXPHOS polypeptides encoded by mtDNA, most of the OXPHOS subunits (at least 70) are encoded by the nuclear genome. There are also several nuclear gene products that regulate mitochondrial gene expression. Different authors have provided important insight into the regulatory mechanisms that are involved in the transcriptional control of OXPHOS genes. The transcriptional regulatory network controlling the expression of nuclear and mitochondrial genes includes nuclear respiratory factor NRF-1 and NRF-2 and mitochondrial transcription factor A (mtTFA). NRF1, first characterized as an activator of cytochrome c expression, acts not only on the genes that encode OXPHOS subunits but also on the rate-limiting heme biosynthetic enzyme, and on mtDNA transcription and replication factors. NRF1 is itself a binding partner for the transcriptional co-activator PGC1α (peroxisome proliferator-activated receptor co-activator 1α). PGC-1α is a transcriptional coactivator that lacks DNA-binding activity but interacts with and coactivates numerous transcription factors, including nuclear receptors such as PPARγ and PPARα, estrogen receptor α, thyroid hormone, retinoid receptors, and hepatocyte nuclear factor-4α. PGC-1α also coactivates nonnuclear receptor transcription factors, such as NRF-1, to activate the expression of known target genes, including mtTFA, a factor that is critical for the initiation of mitochondrial DNA replication [Russel et al. 2004; Smeitink et al. 2001; Wu et al. 1999].
The functional versatility of mitochondria is paralleled by their morphological complexity. In certain cell types mitochondria are organized in networks of interconnected organelles. The ultrastructural changes in the architecture of mitochondria are due to differences that are established in the amount and form of the cristae, which result from folding of the inner membrane and can be either laminated or tubular, depending on the metabolic states of organelle.
The ultrastructure and the reticular organization of the organelle are determined by mitochondria-shaping proteins that affect the equilibrium between fusion and fission processes. The two dynamin-like GTPase, MFN1 and MFN2 are

the main regulators of the mammalian mitochondrial outer membrane fusion [Santel and Fuller 2001]; OPA1, another GTPase, is a protein that promotes fusion and, as well as other proteins involved in the modification of mitochondrial morphology, is closely regulated by complex post-transcriptional mechanisms that include proteolytic degradation [Liesa et al. 2009]. OPA1 has also an interesting role in apoptosis in particular it is involved in changes affecting the cristae (cristae remodeling) in order to promote the mobilization of cytochrome c from intermembrane space to the cristae and possibly to the cytosol [Scorrano et al. 2002]; the size of tubular connections between the cristae (cristae junctions) is controlled also by a complex consisting of two isoforms of OPA1, one of which is generated by protease PARL [Frezza et al. 2006]. Another protein implicated in these mechanisms is the mitofilin (encoded by the gene IMMT), a transmembrane protein localized at the base of the cristae, whose down-regulation results in a drastic change in the organization of the inner membrane that appears as densely packaged concentric layers and free of tubular connections [John et al. 2005]

Calcium signaling

The mitochondria are actively involved in the regulation of calcium signaling through its accumulation and release, as a result of physiologic stimuli. These organelles behave as a high-capacity, low-affinity transient calcium store. An important role in calcium signaling is covered by calcineurin/NFAT signaling pathway. NFAT is a Ca^{2+}/calcineurin (CaN)-dependent transcription factor that has been implicated in the development and function of various organ systems, including the immune, endocrine, and cardiovascular systems [Crabtree and Olson 2002]. NFAT is exquisitely sensitive to the duration of the Ca^{2+} signal, which is explained by its activation mechanisms.

In resting cells, phosphorylated NFAT resides in the cytosol. It is dephosphorylated by CaN in response to an increase in $[Ca^{2+}]_i$, resulting in unmasking of its nuclear localization signal (NLS) and its import into the nucleus. There, NFAT cooperates with other transcription factors to initiate transcription. Once $[Ca^{2+}]_i$ returns to basal levels, glycogen synthase kinase-3β (GSK3β) and several other protein kinases, as DYRK1A (a gene mapping to Hsa21 and upregulated in fetal DS hearts), rephosphorylate NFAT, which promotes NFAT export from the nucleus (**Fig. 5**) [Kim and Usachev 2009]. Thus, NFAT-mediated transcriptional responses depend on the balance between the activities of CaN and NFAT kinases. Consequently, retaining NFAT in the nucleus requires continuous CaN activity and persistent $[Ca^{2+}]_i$ elevation.

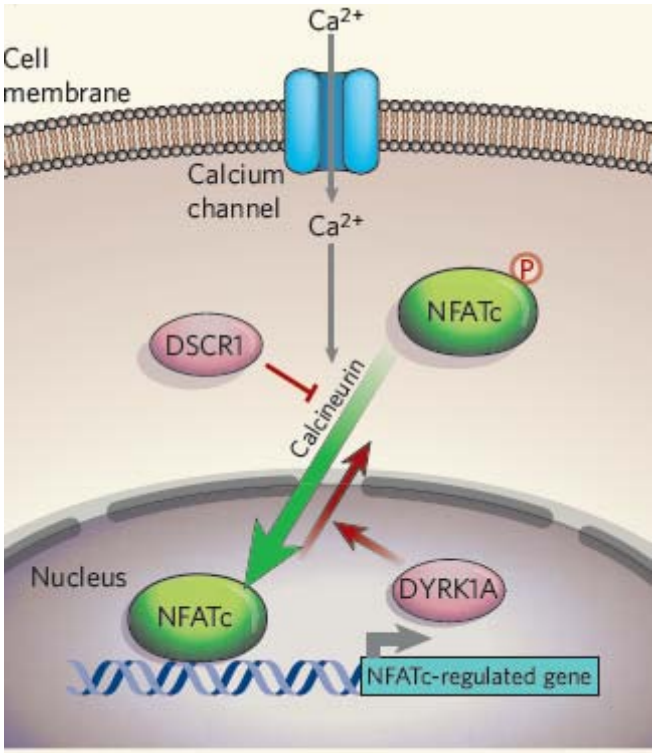

Figure 5. Calcineurin/NFAT signaling. The entry of calcium ions into the cell activates the enzyme calcineurin to remove phosphate groups (P) from NFATc factors in the cytoplasm, allowing NFATc to enter the nucleus and activate its target genes. However, once in the nucleus, the NFATc can be phosphorylated, and so returns to the cytoplasm. Arron et al. and Gwack et al. (2006) implicate the DSCR1 and DYRK1A proteins in regulating the levels of NFATc phosphorylation.

3. Choice of a model for trisomy 21: stem cells

Even though information about the function of chromosome 21 genes is going to increase rapidly, the molecular alterations that cause the Down syndrome (DS) phenotype are largely unknown. The investigation of the molecular mechanisms by which trisomy 21 causes the phenotype is hampered by the lack of specific models. Transgenic mice have proved to be an imperfect model and human tissues at proper developmental stages are difficult to obtain. New models are needed to bypass these inconveniences and stem cells might represent an adequate opportunity. Stem cells can be derived from individuals affected by a specific genetic disorder, like trisomy of Hsa21, and can be induced to differentiate into cell types that represent a target of the disease, mimicking the specific developmental changes that occur in vivo and that contribute to the phenotype.

As a matter of fact stem cell models have already been proposed to study the alterations in neuron development that occur in DS. This has been done through the formation of aggregates of stem and progenitor cells, isolated from neural tissue, the neurospheres, that represent a relatively pure population of dividing cells at a specific stage of development [Bhattacharyya and Svendsen 2003].
The model we have choosen is based upon the availability of non embryonic pluripotent stem cell lines that can be studied at various stages of differentiation. It has been recently demonstrated that human pluripotent stem cells can be conveniently obtained from amniocyte cell cultures (hAFSC) and can be differentiated into many cell types, including cardiomyocytes, muscle cells and neurons [De Coppi et al. 2007]. The choice of hAFSC is also due to the fact that we have access to a large collection of frozen amniocyte cells from euploid fetuses as well as from trisomy 21 fetuses and from many other pathologic conditions (Bank of Fetal Biological Samples, University of Naples Federico II).
The hAFSCs show characteristics of mesenchimal stem cells and, as such, they are able to differentiate along adipogenic, osteogenic, myogenic, endothelial, neurogenic and hepatic pathways [Siddiqui and Atala 2004]. Thus they are a broad-spectrum multipotent stem cells. Approximately 1% of the cells in cultures of human amniocentesis specimens obtained for prenatal genetic diagnosis express the surface antigens such as c-Kit (CD117), the receptor for stem cell factor or the stage-specific embryonic antigen (SSEA)-4 [Miyake et al. 1983]; the presence of these antigens allows the immunoselection with magnetic microspheres using specific antibodies.

AIMS OF THE STUDY

The global downregulation of genes encoding mitochondrial enzymes and respiratory chain complex subunits, previously found in fetal hearts with chromosome 21 trisomy, have induced us to perform a molecular, functional and morphological study of mitochondria in primary lines of fetal fibroblasts, obtained from trisomic and euploid fetuses. The aim of this study was to analyze the mitochondrial defect associated with DS as consequence of the dysregulation of mitochondrial genes.

Gene expression profile has been determined in trisomic and euploid samples by microarray and qRT-PCR analysis, with particular attention to genes involved in mitochondrial biogenesis and function.

Functional study has been performed in collaboration with the Department of Biomedical Sciences of Foggia University. Measurements of oxygen consumption, OXPHOS complex activities, ROS production, membrane potential and mtDNA copy number were studied. Finally, in collaboration with the Centre for Electron Microscopy of Naples University, mitochondrial ultrastructure was analyzed on fibroblasts in order to define morphological changes. The results of these studies lead us to hypothesize possible pathophysiological mechanisms of mitochondrial dysfunction in DS.

The second step of this work was to set up an in vitro cell culture model that would enable us to detect the earliest changes in gene expression profile occurring during differentiation of trisomic cells. The rationale for this approach is the fact that the study of the mechanisms by which trisomy 21 causes the phenotype is hampered by the lack of appropriate models. We decided to take advantage of the fact that it has been recently demonstrated that stem cells can be obtained from amniocyte cell cultures (hAFSC). Thanks to collaboration with Prof. Paolo De Coppi at Padova University and Prof. Gabriella Rosi at Perugia University, we obtained hAFSCs from amniotic fluid of trisomic fetuses and from non-trisomic controls.

MATERIALS AND METHODS

Samples

Human heart tissues and primary lines of fetal fibroblasts were used for this study. All samples were explanted from fetuses after therapeutic abortion and were obtained from the Telethon Bank of Fetal Biological Samples at the University of Naples. According to protocols approved by our Institutional Ethics Committee heart tissues from fifteen human fetuses from 18- to 22-week-gestation with and without Hsa21 trisomy were analyzed by DNA microarray: ten were trisomic for Hsa21; 5 non trisomic fetuses served as controls. Fetal fibroblasts obtained from skin biopsies of 8 human fetuses (4 trisomic for Hsa21 and 4 non trisomic, **table 1**) were used for qRT-PCR evaluations and functional and morphological studies.

Table 1. Primary lines of fetal fibroblasts used in the study

EUPLOID SAMPLES (N)	TRISOMIC SAMPLES (DS)
BIO-21	BIO-22 (DC)
BIO-23	BIO-36 (DC)
BIO-27	BIO-37 (D)
BIO-29	BIO-48 (D)

N: control samples; DS: Down Syndrome samples; DC: samples derived from trisomic fetuses with cardiopathy; D: samples derived from trisomic fetuses without cardiopathy.

RNA extraction and Quantitative Real-time PCR

Total RNA from each sample was extracted using TRIzol reagent (Gibco/BRL Life Technologies, Inc., Gaithersburg, MD) and was reverse-transcribed using iScript cDNA Synthesis kit (Biorad). Real-time PCR was performed using iQ Supermix SYBR Green 2X on the Bio-Rad iCycler (www.bio-rad.com) according to the manufacturer's protocols. PCR reactions were performed in triplicate. The primers (MWG Biotech, Ebersberg, Germany) used for amplification are listed in **table 2**. Primer pairs were designed using the Primer 3 software (http://frodo.wi.mit.edu/cgi-bin/primer3/primer3_www.cgi/) to obtain amplicons ranging from 100 to 150 base pairs. In order to test primer efficiency, serial dilutions of cDNAs generated from selected samples, that expressed target genes at a suitable level, were used to generate standard curves for each gene. GAPDH housekeeping gene was chosen as reference gene.

Table 2. **Primer sequences of genes analyzed by qRT-PCR.**

GENE NAME	PRIMER SEQUENCES
NRF1	**LEFT**: AAACGGAAACGGCCTCAT **RIGHT**: CTTGCTGTCCCACACGAGTA
TFAM	**LEFT**: GCTCAGAACCCAGATGCAA **RIGHT**: TGCCACTCCGCCCTATAA
PPRC1	**LEFT:** ATTGAGGCATCGGACCTGT **RIGHT**: GAGGAGGACACTCCTTTTTGG
SLC25A4	**LEFT**: GGGTTTCAACGTCTCTGTCC **RIGHT**: TCCAGCTCACAAAAATGTGC
IMMT	**LEFT**: AGTTTGTCCTCCGTCCATTG **RIGHT**: CCACCAATACCTCCACCAAC
NDUFA13	**LEFT**: TCGACTACAAACGGAACTTGC **RIGHT**: ATTATGCTCCAGTGCCCGTA
OPA1	**LEFT**: CATTGTGTGGGAAATTGATGAG **RIGHT**: GGTGCTAACTTTACAAGGTCTTCTG
PARL	**LEFT**: TGGGATTAACAAGTGGTGGAATA **RIGHT**: TCTCCATAAACAGAATACAAGGACAT
ITSN1	**LEFT**: GTGAGCGGCACTGATTTGT **RIGHT**: GATCATGCTTCGCTCTTTCC
BTG3	**LEFT**: GAGGCAGTTGAGAGGTTTGC **RIGHT**: GAGTGAGCTCCTTTGGCAAG
DYRK1A	**LEFT**: GATATCATATGGGTCAGGTCATTTT **RIGHT**: CTGGACTGTAACATAACACAGTATGC
NDUFB8	**LEFT**: GCCAAGAAGTATAATATGCGTGTG **RIGHT**: GTCAGGGAGCTTCGGGTAG
NDUFS3	**LEFT**: GATTATGGCTTCGAGGGACA **RIGHT**: ACCCGCTTCACTTCATCATC
COX5A	**LEFT**: AACTGGGCCTTGACAAAGTG **RIGHT**: GGTAACTGTTCACACTCAAGTAGC
COX10	**LEFT**: CTTTTGACTGGCCCTGTTTC **RIGHT**: ACCAGCGGTCTGTTCTTTGT
UQCRC1	**LEFT:** CCGAGCAGTCCTCTCAGC **RIGHT**: TGTTCCCTTGAAAGCCAGAT
SOD1	**LEFT:** GGCCGATGTGTCTATTGAAGA **RIGHT:** TTCCAGCGTTTCCTGTCTTT

Measurement of the respiratory activity in intact cells

Cultured cells were gently detached from the dish by tripsinization, washed in PBS, harvested by centrifugation at 500g for 5 min and immediately assessed for O_2 consumption with a high resolution oxymeter (Oxygraph-2k, Oroboros Instruments). About $5x10^6$ viable cells/ml were assayed in 50 mM KPi, 10 mM

Hepes, 1 mM EDTA, pH 7.4 at 37°C; after attainment of a stationary endogenous substrate-sustained respiratory rate, 2 μg/ml of oligomycin was added. The rates of oxygen consumption were corrected for 2 mM KCN-insensitive respiration. The respiratory control ratio (RCR) was obtained dividing the rates of oxygen consumption achieved before and after the addition of oligomycin [Piccoli et al. 2007].

Measurement of the mitochondrial respiratory chain complexes activity

The specific activities of NADH: ubiquinone oxidoreductase (complex I) and cytochrome c oxidase (complex IV) were assayed spectrophotometrically on frozen–thawn and ultrasound-treated cells in 10 mM Tris, 1 mg/ml serum albumin, pH 8.0. Complex I was assayed (in the presence of 1 μg/ml of antymicin A plus 2 mM KCN) by following the initial 2 μg/ml rotenone-sensitive rate of 50 μM NADH oxidation (ε340nm = 6.22 mM^{-1} cm^{-1}) in the presence of 200 μM decylubiquinone (dUQ) as electron acceptor; the NADH-ferricyanide reductase activity of complex I was measured in the presence of rotenone, antimycin A and KCN with 200 μM potassium ferricyanide from the oxidation of NADH. Complex IV was assayed by following (in the presence of antymicin A) the initial 2 mM KCN-sensitive rate of 20 μM ferro-cytochrome c oxidation under aerobic conditions. The activities were normalized to the initial cell number and to cellular protein content [Cela et al. 2010].

Citrate synthase catalyzes the reaction between acetyl coenzyme A (acetyl CoA) and oxaloacetic acid (OAA) to form citric acid. Citrate synthase activity was assayed spectrophotometrically measuring the reaction between CoA-SH (CoA with a thiol group) and DTNB (5,5′-dithiobis(2-nitrobenzoic acid)) to form 5-thio-2-nitrobenzoic acid (TNB) that absorbs at 412 nm.

Laser scanning confocal microscopy imaging of mitochondrial membrane potential and ROS in live cells

Cells cultured on fibronectin-coated 35mm glass-bottom dishes were incubated for 10 min at 37°C with the following probes: 2 μM tetramethylrhodamine, ethyl ester (TMRE), to monitor mitochondrial membrane potential (mtΔΨ) or 10 μM 2',7'-dichlorodihydrofluorescein diacetate (H_2DCF-DA) for detection of H_2O_2. Both probes were from Molecular Probes (Eugene, OR). Stained cells were washed with PBS and examined by a Nikon TE 2000 microscope (images collected using a 60X objective (1.4 NA)) coupled to a Radiance 2100 dual laser (four-lines Argon-Krypton, single-line Helium–Neon) confocal laser scanning microscopy system (Biorad). TMRE is a fluorescent lypophilic cations that accumulates electrophoretically in mitochondria. The red fluorescence of TMRE was analysed by exciting the sample with the He–Ne laser beam (λ_{ex} = 543 nm). DCF-DA is a membrane permeant probe which is hydrolysed by intracellular esterases and converted to the ROS (mainly H_2O_2)-reacting product dichlorofluorescein (DCF). The green fluorescence of oxidised DCF was analysed by exciting the sample with the Ar–Kr laser beam (λ_{ex} = 488 nm). Confocal planes (18–20) of 0.2 μm in thickness were examined

along the z-axes, going from the top to the bottom of the cells. Acquisition, storage and analysis of data were made by using LaserSharp and LaserPix software from Biorad or ImageJ (NIH, USA-http://rsb.info.nih.gov/ij/). Correction was made for minimal background by repeating the procedure in a cell-free field. At least 20 cells were randomly selected from 8 to 10 different fields for each cell samples under the indicated conditions and statistically analysed [Cela et al. 2010].

Morphological analysis

Fibroblasts from trisomic and euploid fetuses were fixed and embedded for the electron microscope, using agarose as an intermediate embedding medium [Hayat 1981; Kerstens et al. 2000]. In the petri dishes the cells were fixed with 4% paraformaldehyde and 5% glutaraldehyde in PBS buffer (0.1M, pH7,3) for 30' at room temperature, then washed in buffer, scraped from culture plates and pelleted by centrifugation for 10 min at 2000g; the supernatant was discarded and the cells were resuspended in 1 ml of 2% liquid agarose at 65°C. Again, the reaction tube was centrifuged for 5 min at 1000g to concentrate the cells in agarose. The agarose-cell pellet was solidified in ice for 30 min, then the agarose cone was carefully taken out of the reaction tube and divided in small pieces (1 mm^3). The agarose-cell blocks was post-fixed in osmium tetroxide (1% in PBS buffer) for 1 h at 4°C, dehydrated and transferred first in propylene oxide, then in a mixture of propylene oxide-Epon 1:1 and finally embedded in Epon resin. The Epon blocks were polymerized for two days at 60°C and then sectioned with a diamond knife to give thin sections, 70-80 nm each; the sections were picked up on 200 mesh copper grids, stained with uranyl acetate (5% in 50% methanol) and Reynolds lead citrate [Reynolds 1963] and observed by transmission electron microscope Philips 208S. Micrographs were acquired with a Mega View II Soft Imaging System camera.

Stereological investigations

Three N and three DS samples were analyzed for this study (BIO-21, BIO-23, BIO-27 and BIO-36, BIO-37, BIO-48, respectively). We used a stereological estimator, the "fractionator" method, to obtain a systematic and uniformly random sampling, which ensures that even for relatively small samples the error is so small that it may safely be ignored [Gundersen 2002].

Stereology is a method for translating images 2-D data into 3-D quantitative morphological information (volumes, surface-area-length, numbers) [Weibel et al. 1966; Mayhew 1991; Mandarim-De-Lacerda 2003].

Fifty cells per sample were analyzed and for each cell the percentages of broken and branched mitochondria and mitochondria with concentric or longitudinal cristae were determined. Furthermore, for each sample 25 micrographs were collected to evaluate the mitochondrial volume density (Vmt, relative volume of mitochondria on cell volume) and mitochondrial cristae volume density (Vmc, relative volume of mitochondrial cristae on mitochondria volume) [Weibel et al. 1966]. To this end, a regular point lattice

was placed random on each micrograph, by using ImageJ 1.43 software: the Vmt is obtained by differential counting of the points lying on mitochondrial surface and the total points lying on the micrograph; Vmc is obtained by differential counting of the points lying on mitochondrial cristae surface and the total points lying on the mitochondria surface.

Isolation and culture of human amniotic fluid stem cells (hAFSC)

Amniotic fluid samples were obtained from Department of Obstetrics and Gynecology of University of Naples Federico II. Four milliliter of amniotic fluid were cultured in Chang B/C medium (Irvine Scientific), 1% penicillin/streptomycin (5000 units/ml and 5000 mg/ml) and 1ml glutamine 200mM (Gibco) in 35mm plates (BD Falcon). After 10 days, cells were harvested by trypsinization and incubated with a mouse monoclonal antibody (1µl/10^6 cells) to CD117 (c-Kit) or SSEA-4 (Santa Cruz Biotechnology). The positive cells were purified by incubation with magnetic Goat anti−mouse IgG Dynabeads (Dynal, Invitrogen), using a magnetic column (Dynal). Isolated hAFSCs were cultured in αMEM medium (Gibco, Invitrogen) containing 15% FBS, 1% glutamine and 1% penicillin/streptomycin (Gibco), supplemented with 18% Chang B and 2% Chang C at 37°C with 5% CO_2 atmosphere. After 6−7 days, clones of c-kit or SSEA-4 positive cells were visible. hAFSCs were subcultured and not permitted to expand beyond 70% of confluence. Cloned hAFSC cell lines were generated by the limiting dilution method in 96−well plates.

Immunofluorescence and confocal microscopy

Cells were fixed in 4% paraformaldehyde in PBS for 20 min, washed twice for 5 min each time, with 50mM NH_4Cl in PBS. The cells were then blocked in 5% goat serum in PBS for 1 h and washed twice in PBS. Mouse monoclonal primary antibody anti-SSEA-4 (Santa Cruz Biotechnology) diluted 1 : 100 in PBS 1% goat serum for 1 h in a humidified atmosphere was used.The cells were then extensively washed in PBS before staining with secondary goat anti-mouse Alexa Fluor 546 (Molecular Probe, Invitrogen Corporation, Carlsbad, CA, USA). Nuclei were counterstained with Hoechst 33258 (0.5 mg/ml in PBS) (Sigma Aldrich) for 10 min. Finally, the cells were washed in PBS and mounted on glass slides with PBS containing 50% glycerol.

Immunofluorescence analysis was performed at a confocal laser scanner microscope (LSM 510; Zeiss, Göttingen, Germany). The lambda of HeNe laser was set at 543 nm. Fluorescence emission was revealed by BP 560–615 band pass filter for Alexa Fluor 546. Nuclei stained with Hoechst 33258 were acquired as non confocal images by mean of a light detector and 352/461 nm filter (UV light). Images were acquired at a resolution of 1024x1024 pixels.

Flow cytometry

Assays were performed using CY−N (DAKO) according to the manufacturer protocols. The cells ($7x10^6$) were detached from culture dishes by incubation

with Accutase (Invitrogen) and incubated with the following antibodies: CD29-FITC, CD44-FITC, CD45-PE, CD117-PE (Immunotech, Beckman Coulter, Marseille, France); CD73 (BD Biosciences Pharmingen, Europe), CD105 (Abcam), and SSEA-4 (Santa Cruz Biotechnology). Secondary antibodies were AlexaFluor546−goat anti−mouse IgG or AlexaFluor488−goat anti−mouse IgG (Molecular Probes / Invitrogen, Eugene, OR). To determine cellular viability, 7-Amino-actinomycin D (AAD) (Immunotech, Beckman Coulter, Marseille, France) was used. 7-AAD intercalates into double-stranded nucleic acids and is excluded by viable cells but can penetrate cell membranes of dying or dead cells.

Statistics

The Student's t-test was applied to evaluate the statistical significance of differences measured throughout the data-sets presented.

Concerning stereological investigations, the data obtained from each samples were averaged per group (DS and N) and statistical evaluation was performed by two non-parametric statistical tests, the Kolmogorov-Smirnov and the Kruskal-Wallis tests.

The threshold for statistical significance (p-value) was set to 0.05.

RESULTS

1. Differential gene expression in DS hearts and in cultured fibroblasts

By comparing the gene expression profile of 10 human hearts from trisomic fetuses (DSH) to 5 fetal hearts of non-trisomic controls (NH), we previously demonstrated a global upregulation of Hsa21 genes and a dysregulation of about 400 genes localized on other chromosomes [Conti et al. 2007]. Functional analysis of the genes differentially expressed between trisomic and control samples showed global downregulation of genes encoding mitochondrial proteins, especially enzymes involved in the oxidative phosphorylation pathway [Conti et al. 2007].

Based on these results we focused our attention on mitochondrial genes as potential candidates to favor or promote the cardiac phenotype observed in the DS. In particular we considered genes encoding transcription factors involved in mitochondrial gene regulation (NRF1, TFAM, and PPRC1), genes involved in oxidative phosphorylation processes (NDUFA13 and SLC25A4) and genes important for maintenance of mitochondrial shape and morphology (IMMT, OPA1 and PARL). Quantitative Real-Time PCR (qRT-PCR) experiments validated microarray analysis demonstrating the downregulation of NRF1, PPRC1, IMMT, NDUFA13 and SLC25A4 in DSH versus NH samples (**Fig. 6**), while OPA1, PARL and TFAM were normoregulated. Analyzed genes and their expression ratios, obtained by microarray and by qRT-PCR, are listed in **table 3**.

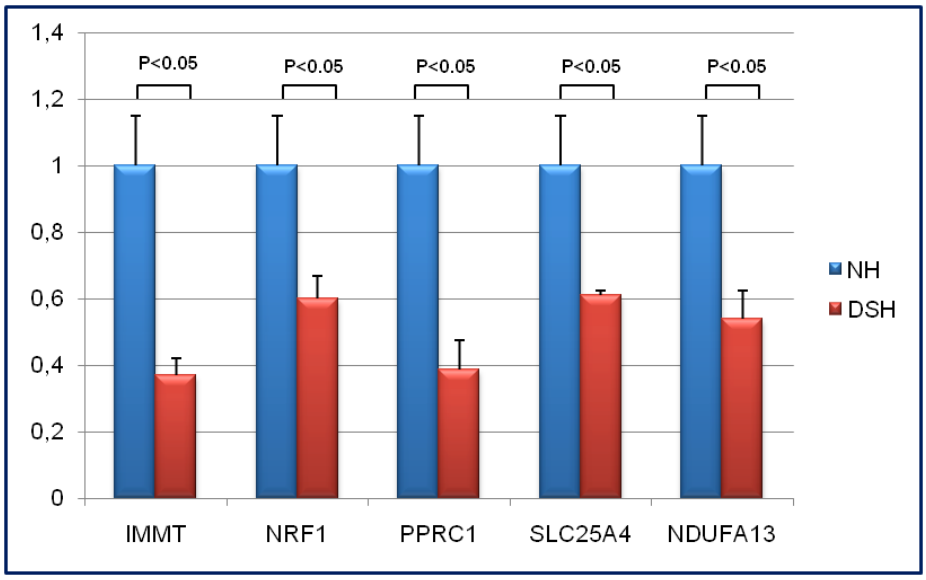

Figure 6. Expression of mitochondrial genes in DS hearts by qRT-PCR. Gene expression level of IMMT, NRF1, PPRC1, SLC25A4 and NDUFA13 was determined by qRT-PCR in trisomic hearts (DSH, red bars) versus euploid hearts (NH, blue bars). Five hearts per group were analyzed. All genes were significantly downregulated in DS samples ($p<0.05$).

Table 3. Expression ratios of mitochondrial dysregulated genes in trisomic vs euploid samples

Gene Name	Probe set ID	Fold Change by microarray	qRT-PCR ratio
NRF1	204652_s_at	0,663	0,60
PPRC1	203737_s_at	0,587	0,39
NDUFA13	220864_s_at	0,746	0,54
IMMT	200955_at	0,774	0,37
SLC25A4	202825_at	0,645	0,61

Gene name, probe set ID, Fold Change and qRT-PCR ratio are listed.

Overall the microarray analysis indicated the downregulation of genes encoding all five complex subunits of OXPHOS process and of other genes implicated in mitochondrial biogenesis. This widespread dysregulation of mitochondrial genes suggested that the mitochondrial function could be also impaired. To investigate the presence of a mitochondrial dysfunction associated with DS, 8 primary lines of fetal fibroblasts derived from trisomic and euploid fetuses were chosen as cell model (**table 1** in methods). It was ascertained that no changes in chromosome number and structure had occurred in the fibroblasts after thawing and culture passages: in fact, all trisomic fibroblasts showed three copies of Hsa21 as the only cytogenetic alteration (**Fig. 7**).

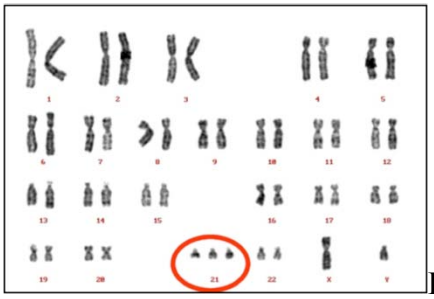

Figure 7. Karyotype of DS fetal fibroblasts

To confirm the upregulation of Hsa21 genes in DS versus control fibroblasts, the expression of Hsa21 genes was determined by qRT-PCR. In particular, Hsa21 genes BTG3, SOD1, ITSN1 and DYRK1A, were upregulated in trisomic fibroblast samples when compared to control samples (**Fig. 8**).

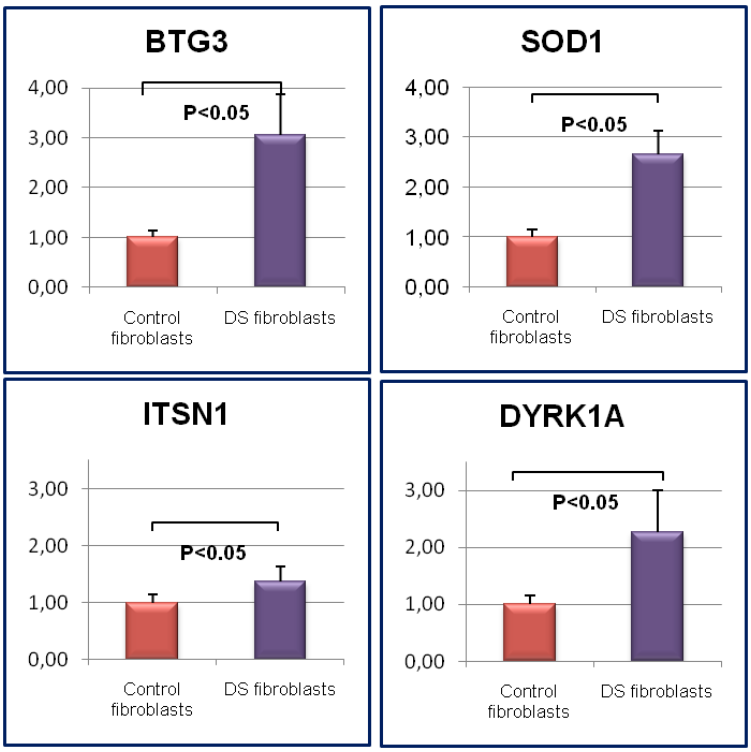

Figure 8. Expression of Hsa21 genes in fibroblasts by qRT-PCR. Gene expression level of Hsa21 genes in trisomic samples (DS fibroblasts, purple bar) versus euploid samples (Control fibroblasts, red bar). All analyzed genes were significantly upregulated in DS samples ($p<0.05$).

The dysregulation of genes involved in mitochondrial function was then determined in fetal trisomic fibroblasts versus euploid samples, by qRT-PCR (**Fig. 9**). The results confirmed the downregulation of IMMT and NRF1, as observed in fetal hearts, while NDUFS3, UQCRC1, COX10 and PPRC1 were normoregulated and NDUFB8 and COX5A turned out to be upregulated in DS fetal fibroblasts versus controls.
These results only partially confirm the overall dysregulation of genes encoding for mitochondrial proteins, as it was previously determined in human fetal hearts, indicating that different tissues or cells may undergo different mechanisms of transcription regulation.

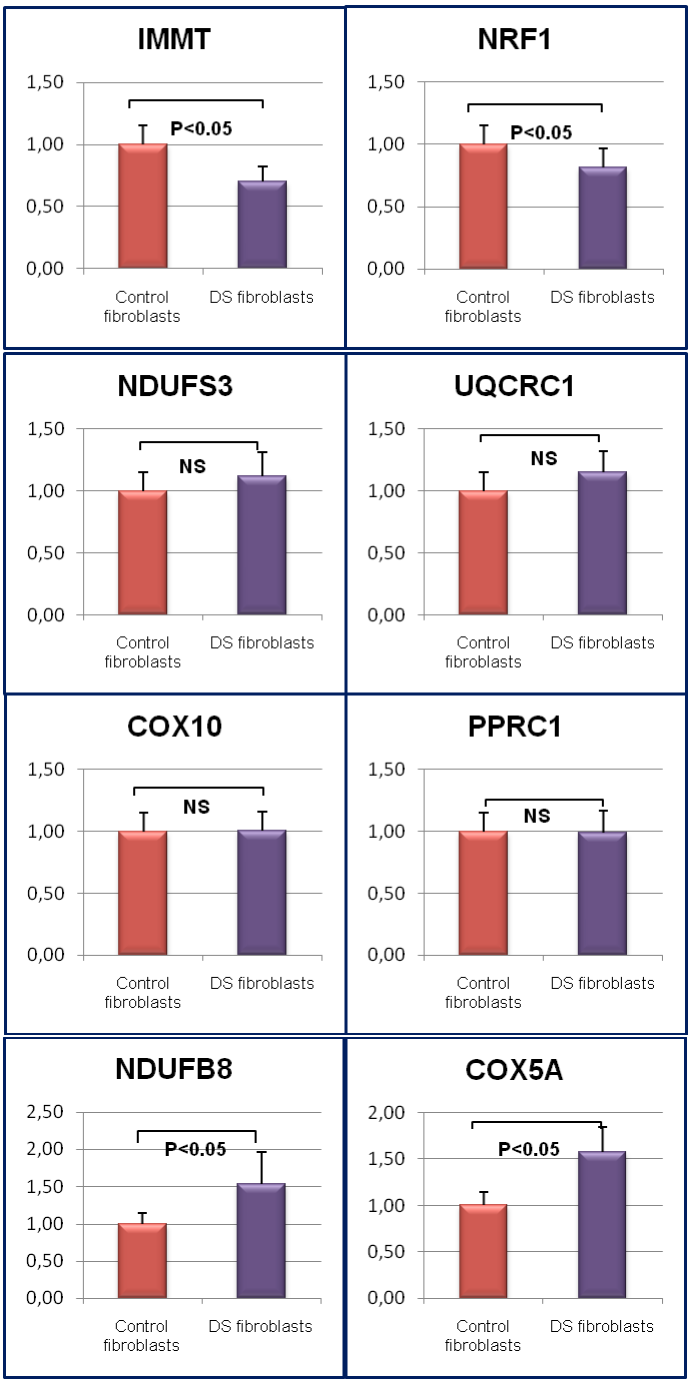

Figure 9. Expression of mitochondrial genes in fibroblasts by qRT-PCR. Gene expression level of mitochondrial genes in trisomic samples (DS fibroblasts, purple bar) versus euploid samples (Control fibroblasts, red bar) showed that only IMMT, NRF1, NDUFB8 and COX5A were significantly dysregulated ($p<0.05$), while NDUFS3, UQCRC1, COX10 and PPRC1 were not significantly altered (NS).

It has been demonstrated that the calcineurin(CaN)/NFAT signaling pathway has a critical role during heart development; for this reason we have previously evaluated the expression of the NFATc transcription factor family and of the catalytic subunits of CaN (PPP3CA, PPP3CB and PPP3CC) by microarray and qRT-PCR experiments on fetal hearts (**Fig. 10**). We found a significative downregulation of these genes in trisomic hearts [Conti et al. 2007]. Quantitative RT-PCR experiments have demonstrated that the NFATc expression was perturbated also in trisomic fetal fibroblasts. In particular NFATc2, NFATc3, NFATc4, were significantly ($p<0.05$) downregulated in trisomic fibroblast samples if compared to the control samples (**Fig. 11**).

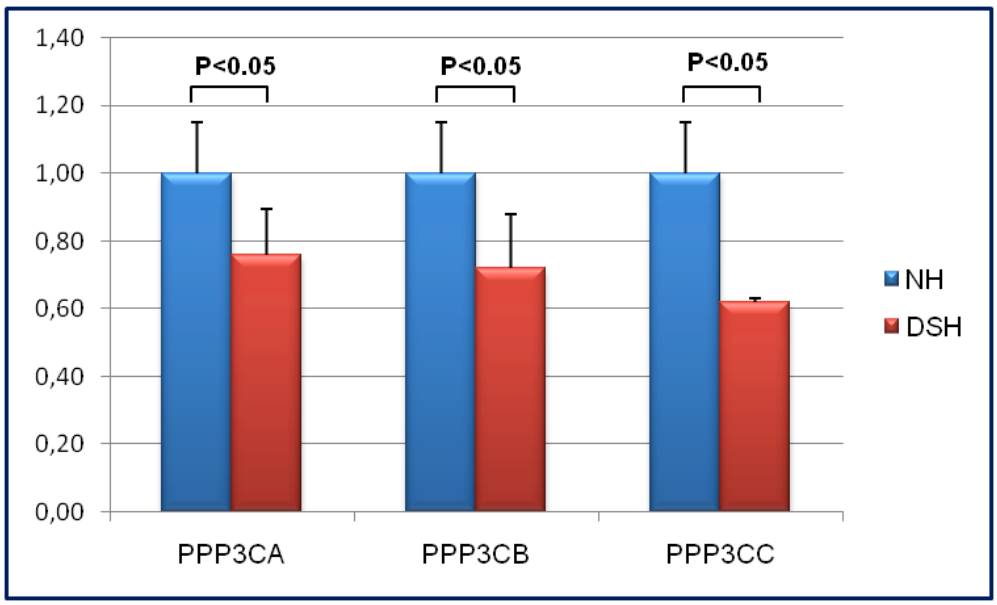

Figure 10. Expression of catalytic subunits of CaN in DS hearts by qRT-PCR.
Gene expression level of PPP3CA, PPP3CB and PPP3CC was determined by qRT-PCR in trisomic hearts (DSH, red bars) versus euploid hearts (NH, blue bars), showing a significative downregulation in DS samples ($p<0.05$).

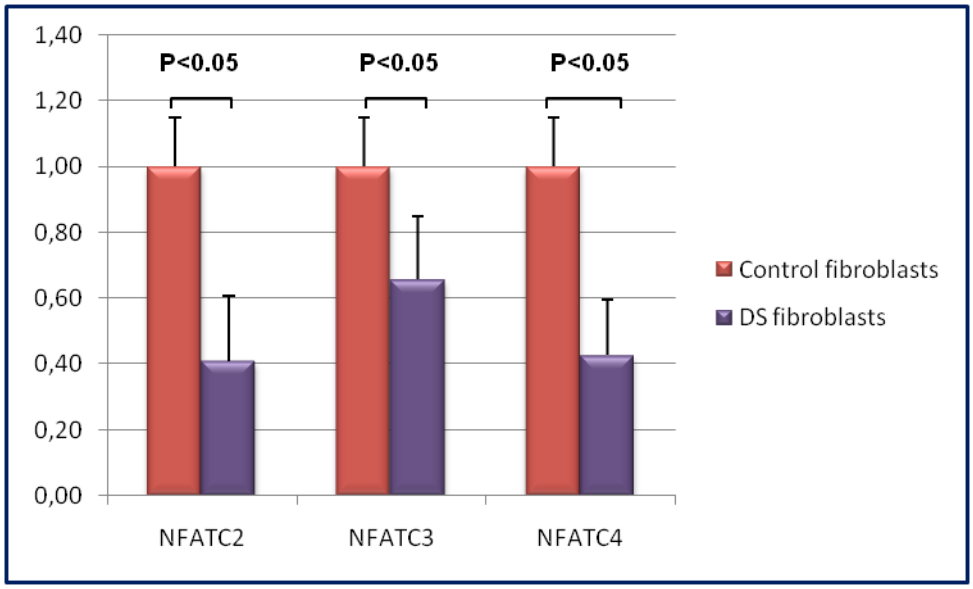

Figure 11. Expression of NFATc transcription factors in fibroblasts by qRT-PCR.

Gene expression level of NFATc2, NFATc3 and NFATc4 in trisomic samples (DS fibroblasts, purple bar) versus euploid samples (Control fibroblasts, red bar). All NFATc genes were significantly downregulated in DS fibroblasts ($p<0.05$).

2. Functional analysis of mitochondria in DS fibroblasts

To verify the hypothesis that the mitochondrial transcriptome dysregulation caused by Hsa21 trisomy might be responsible for mitochondrial dysfunction, a mitochondrial functional analysis in DS fibroblasts was carried out through several approaches: 1) measurement of endogenous respiration; 2) measurement of mitochondrial respiratory chain complexes activity; 3) production of Reactive Oxygen Species; 4) measurement of mitochondrial transmembrane potential ($\Delta\Psi m$); 5) determination of copy number of mitochondrial DNA (mtDNA).

Measurement of endogenous respiration

A typical output of respirometric measurements for oxygen consumption was first carried out on normal intact cells (**Fig. 12**). The respiratory rate was substained by endogenous substrates and relied almost completely on the mitochondrial contribution, as it was fully inhibited by KCN.

The amount of the endogenous oxidizable substrates was apparently never limiting, since oxygen consumption was linear up to the instrumental detection limit (<5% oxygen saturation). By comparing the mean value of oxygen consumption (nmol/min/10^6 cells) of euploid versus trisomic samples, it was observed a 25% reduction ($p<0.05$) of respiratory activity in trisomic cells (**Fig. 13A**).

Addition of the ATP synthase inhibitor oligomycin resulted in a marked decrease of the oxygen consumption rate, indicating an active phosphorylating State III for the endogenous respiration, but the differences between two groups were not significative (**Fig. 13B**).

The final step was the addition of an uncoupler of the OXPHOS, FCCP (*p-trifluoromethoxy carbonyl cyanide phenyl hydrazone*), a potent reversible inhibitor of mitochondrial oxidative phosphorylation able to depolarize mitochondrial membrane potential. In this condition, oxygen consumption rate was different ($p<0.05$) between DS and normal cells, with a reduction of about 25-30% in trisomic samples, and the difference was statistically significant (**Fig. 13C**).

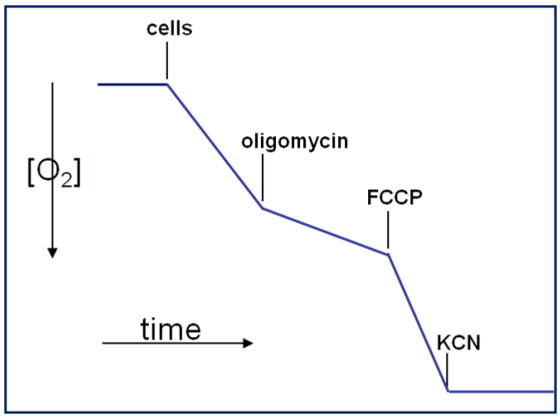

Figure 12. Schematic representation of polarographic assay.

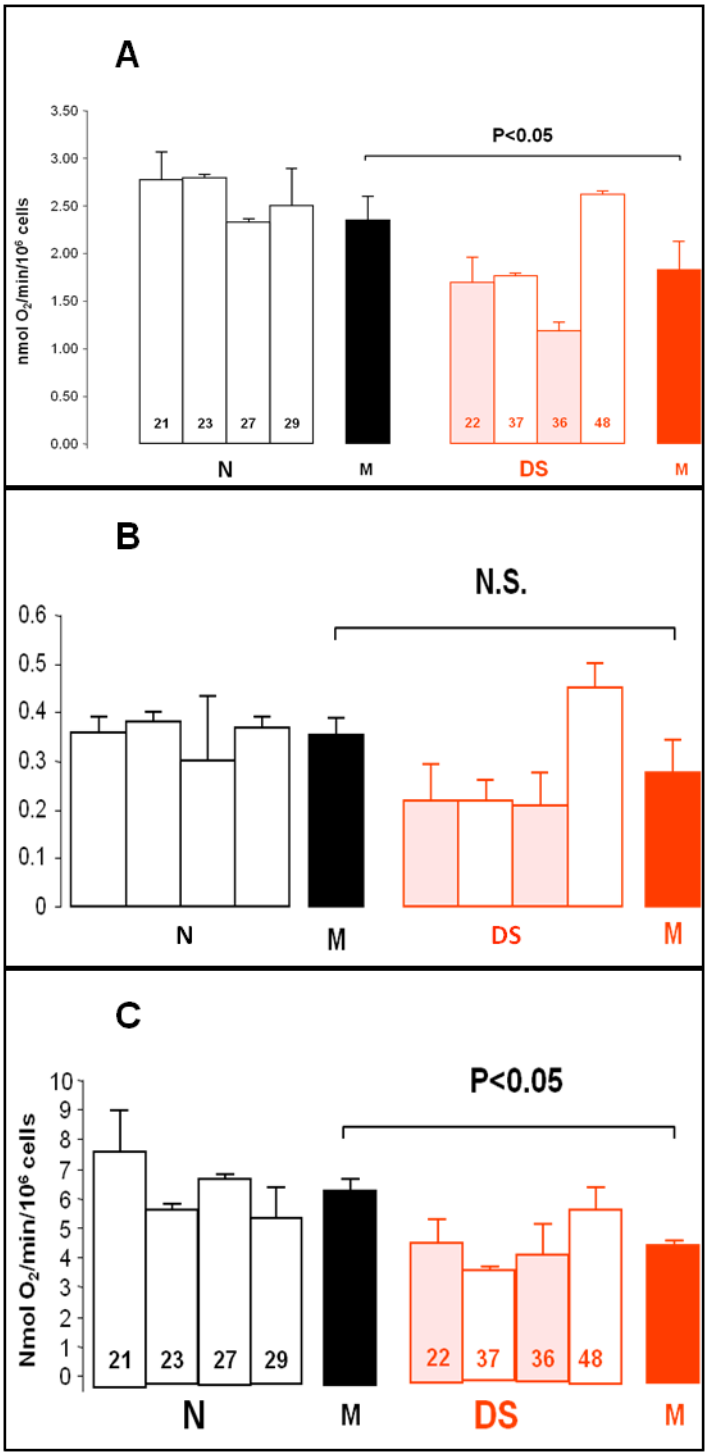

Figure 13. Oxygen consumption in intact cells. Measurements of oxygen consumption rate in endogenous respiration condition (**A**), with the addition of oligomycin (**B**) and of FCCP (**C**). N: normal samples. DS: Down Syndrome samples. M: mean value. The differences in A and C conditions were statistically significant ($p<0.05$). NS: not significant.

Mitochondrial respiratory chain complexes activity

Spectrophotometric measurement of the activity of the mitochondrial proton pump respiratory complexes on solubilized cells revealed significative reduction (30-35%; $p<0.05$) of complex I in trisomic cells (**Fig. 14A**); conversely, the activity of complex IV was not significantly reduced (**Fig. 14B**). For complex I and IV respectively, nmol of both NAD+ and reduced cytochrome c were measured. The citrate synthase activity was evaluated as internal reference of mitochondrial activity and cellular content. There was no statistical difference in citrate synthase activity between trisomic versus euploid samples (**Fig. 14C**). Normalization of individual complex activity on citrate synthase activity confirmed a significative reduction of complex I activity (**Fig. 14D**).

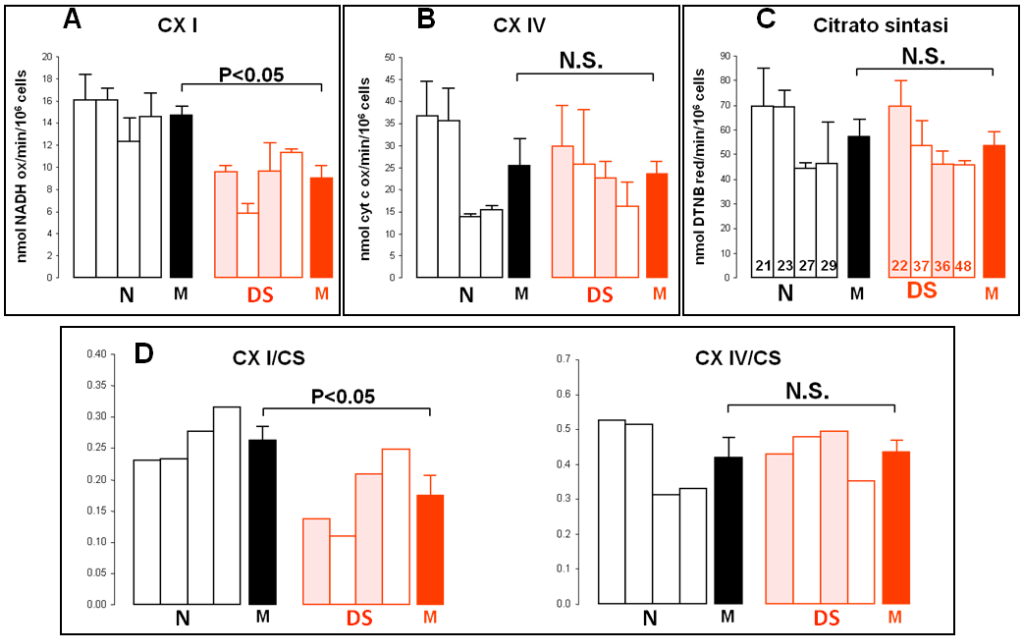

Figure 14. Measurements of mitochondrial respiratory complex activity. Mitochondrial respiratory chain complex I (**A**) and IV (**B**) were measured in control (N) and Down Syndrome (DS) samples. Citrate synthase activity and normalization are shown in **C** and **D** respectively. The mean activity value of the two groups, DS versus N fibroblasts, was compared and only complex I activity was significantly different ($p<0.05$). M: mean value

Results were also normalized on cellular protein content (mg/10^6 cells). Cellular protein content was measured in trisomic and euploid cells (**Fig. 15A**) showing a 15-20% increase in DS samples. The normalized data demonstrated:
- a 20% reduction of citrate synthase (**Fig. 15B**) and complex IV activities (**Fig. 15C**) in trisomic cells, although not significative;
- a 50% reduction ($p<0.01$) of complex I activity in trisomic cells (**Fig. 15D**);

- a 40-45% reduction of oxygen consumption in trisomic cells in 3 different conditions: endogenous activity ($p<0.01$), plus olygomicin ($p<0.05$) and plus FCCP ($p<0.01$) (**Fig. 15E, F, G**).

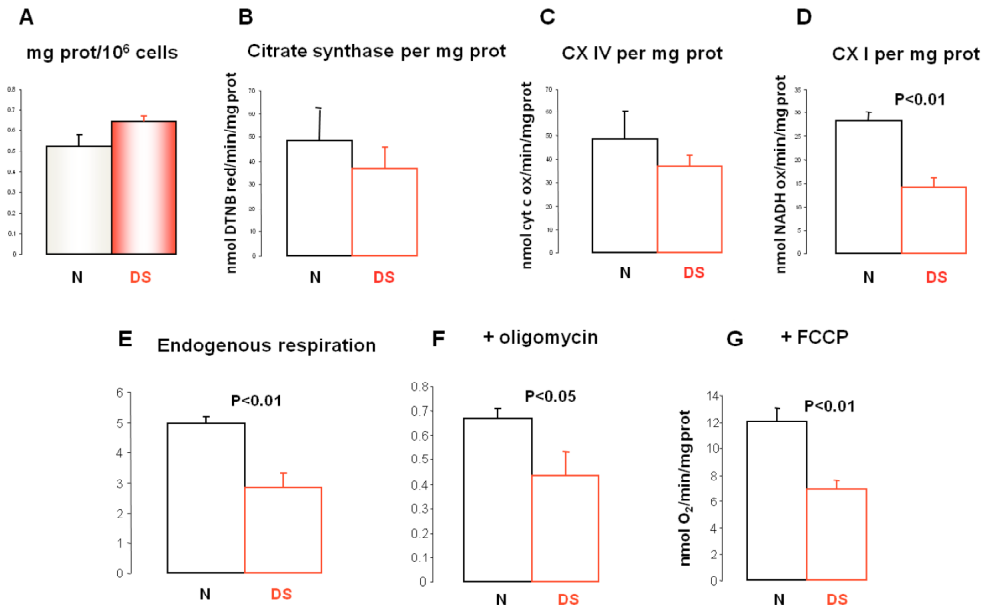

Figure 15. Normalization of measurements by protein content. Protein content was measured in euploid and trisomic cells (**A**); citrate synthase (**B**) and respiratory chain complex (**C**, **D**) activities and oxygen consumption (**E**, **F**, **and G**) were normalized by cellular protein content. Mean values are shown. Differences in D, E, F and G were statistically significant ($p<0.01$ and $p<0.05$). N: control samples; DS: Down Syndrome samples.

In conclusion, all these results suggest that in trisomic fibroblasts there is a respiratory failure, probably due to complex I deficiency that plays a critical role in controlling mitochondrial respiration.

Production of Reactive Oxygen Species

Since the mitochondrial respiratory chain is known to be the major source of reactive oxygen species (ROS) within the cell, and complex I is considered one of the sites of generation of superoxide radicals [Kussmaul and Hirst, 2006; Li and Trush, 1998], the intracellular redox state was assessed by confocal microscopy using the fluorescent H_2O_2-sensitive probe dichlorofluorescein (DCF). Trisomic cells displayed in general a dotted green signal with higher intensity than euploid cells (**Fig. 16A**), indicating a more pronounced production of hydrogen peroxide. The dotted distribution of fluorescent signal clearly resembled the mitochondrial localization. Furthermore, a considerable increase of ROS production was observed in 2 out of 4 trisomic samples. These were the BIO22-DC and BIO36-DC samples that were derived from fetuses with cardiopathy. Measurements of mean fluorescence per cell of two sample

groups and the differences between averages, showed a ~3-fold increase of ROS production in DS versus N cells (**Fig. 16B**).

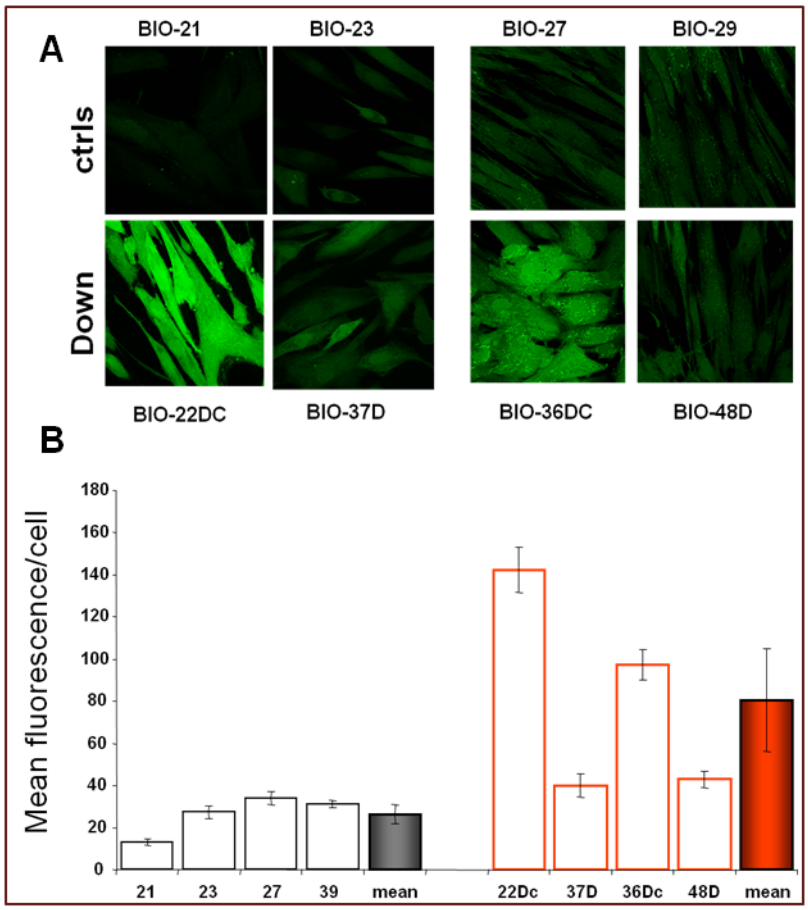

Figure 16. ROS production by DS and control fibroblasts. A. Confocal microscopy images of DCF-H_2O_2 indicating mitochondrial localization of superoxide radicals (green signals). **B**. Mean fluorescence of DCF-H_2O_2 signal in euploid (gray bars) and trisomic samples (red bars).

Measurement of mitochondrial transmembrane potential

hŒ involvement of the membrane potential (ΔΨm) in the control of mitochondrial respiration in intact cells was directly assessed by laser-scanning confocal microscopy using the probe TMRE (Tetramethylrhodamine, ethyl ester). Depending on the extent of the transmembrane electrical potential, the dye accumulates in mitochondria and emits a red-orange fluorescence. The fluorescence signal due to accumulation of the probe in response to membrane potential was not significantly different between trisomic and euploid cells (**Fig. 17A**). The same result was obtained comparing the mean fluorescence per cell of the two sample groups (**Fig. 17B**).

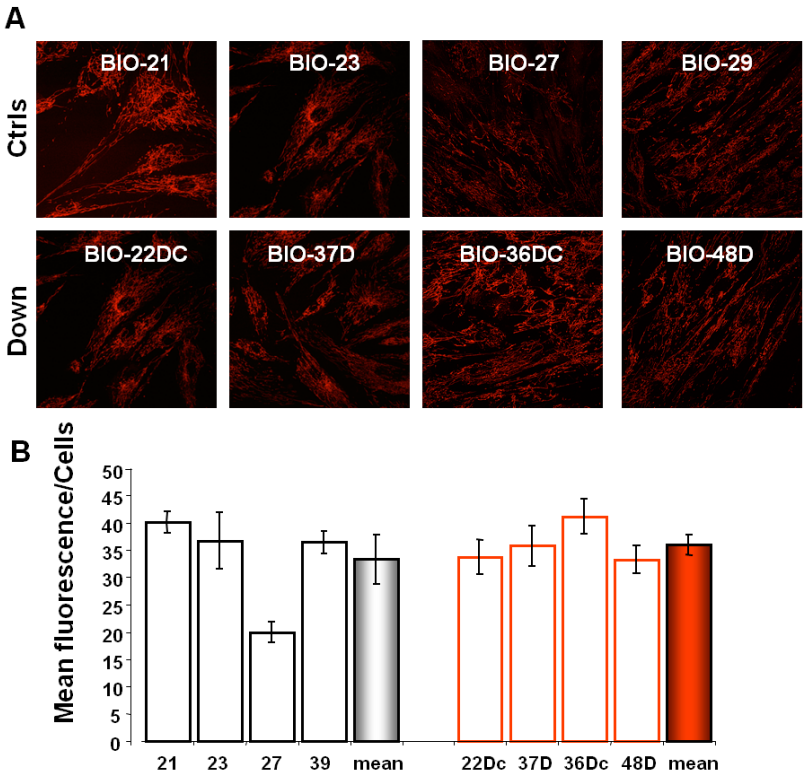

Figure 17. Mitochondrial transmembrane potential determination. Confocal microscope images (**A**) and mean fluorescence values (**B**) of TMRE accumulation in mitochondria of trisomic (red bars) and euploid (gray bars) cells.

Assessment of mtDNA copy number

The assessment of mtDNA copy number is a further method to evaluate mitochondrial properties and it is usually proportional to mitochondria cellular content. By qRT-PCR, it has been demonstrated that in trisomic cells, mtDNA copy number, calculated against nuclear DNA (nDNA) copy number, was as mean reduced of about 40%, if compared to euploid controls (**Fig. 18**).

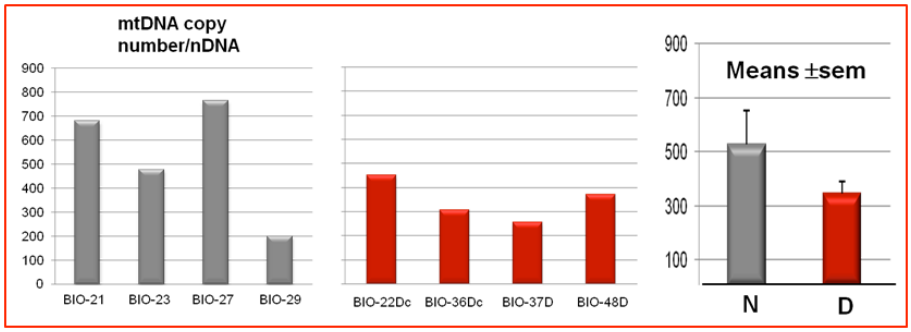

Figure 18. mtDNA copy number determination: mtDNA copy number of single sample and as mean are shown. N: normal samples; D: Down Syndrome samples.

3. Morphological and stereological analysis of mitochondria in DS fibroblasts

Electron microscopy of trisomic fibroblasts revealed that a large number of mitochondria showed an abnormal morphology, an increase in size, irregular shape and evident breaks of both inner and outer membranes. In addition, mitochondria of DS samples showed an altered pattern of cristae, that presented broadened and arranged concentrically or oriented in parallel to the long axis of the organelle (longitudinal cristae) (**Fig. 19**).

The percentage of mitochondria with morphological abnormalities (breakage of the outer, inner or both membranes, branched mitochondria and with concentric or longitudinal cristae) has been evaluated in three DS and three euploid samples. Broken mitochondria and mitochondria with concentric and longitudinal cristae are significantly more abundant in trisomic samples than in the euploid samples. The difference was not significant for branched mitochondria (**Fig. 20**).

Stereological analysis to determine the volume density of mitochondrial compartment, expressed as percentage of cellular volume, and of the cristae, expressed as percentage of mitochondrial volume, demonstrated that the mitochondrial volume density was comparable between trisomic and euploid samples (**Fig. 21**) while the cristae volume density in DS fibroblasts was significantly lower with respect to euploid controls (**Fig. 22**).

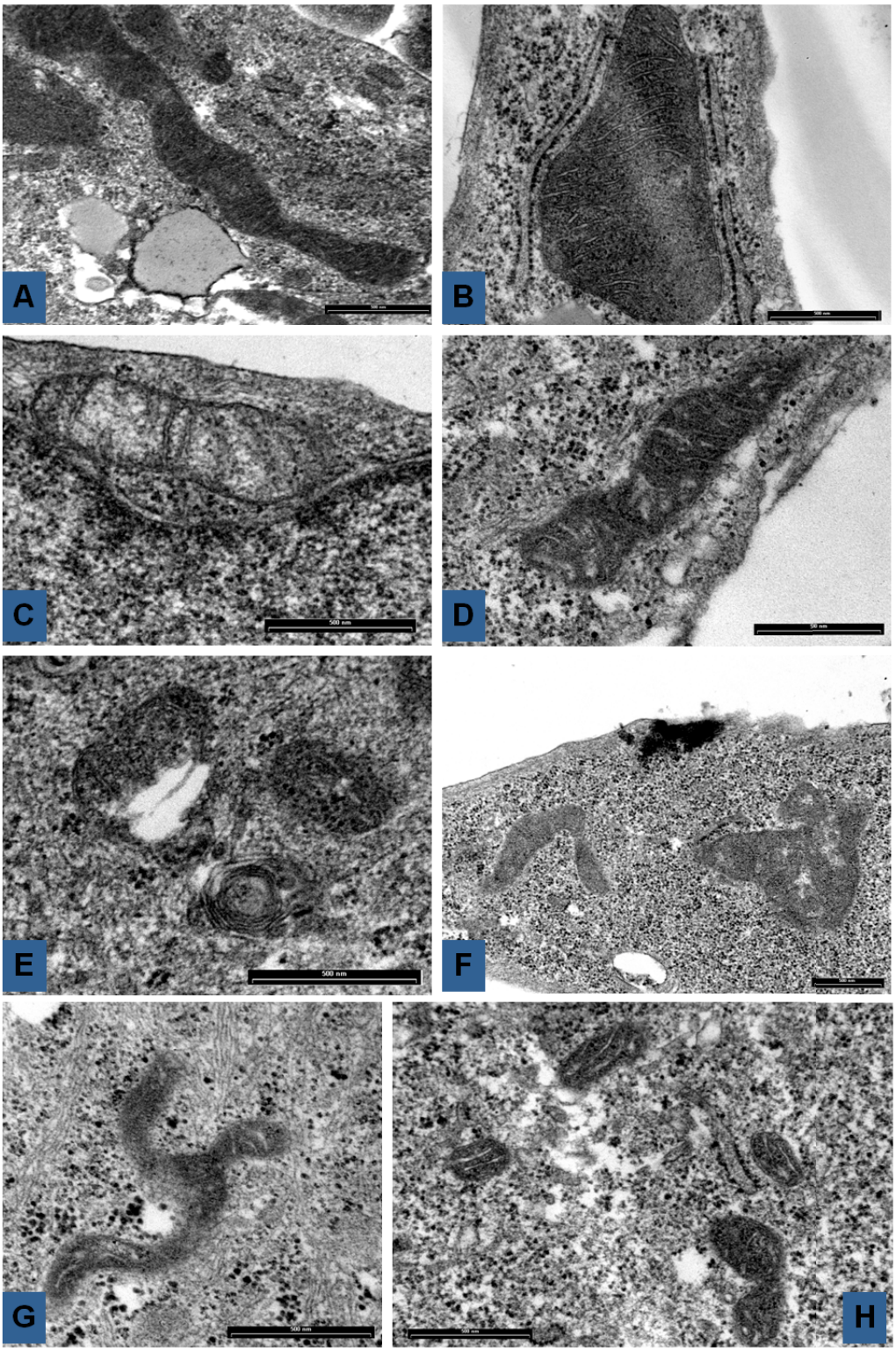
A
B
C
D
E
F
G
H

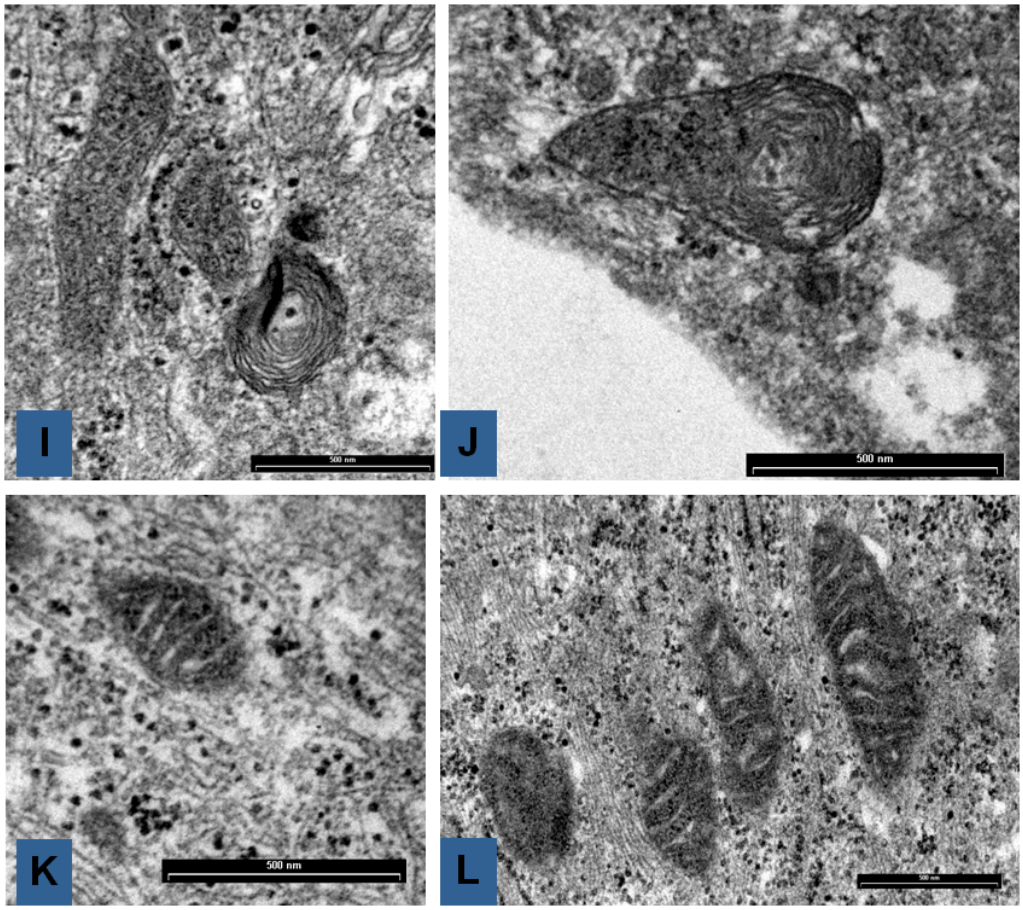

Figure 19. Electron micrographs of morphologically abnormal mitochondria in DS fibroblasts (A-J) and normal mitochondria in N fibroblasts (K, L).

A and **B**: giant mitochondria; **C** and **D**: mitochondria with few and dilated cristae; **E-G**: broken and branched mitochondria; **H**: longitudinal cristae; **I** and **J**: concentric cristae; **K** and **L**: normal mitochondria in control fibroblasts.

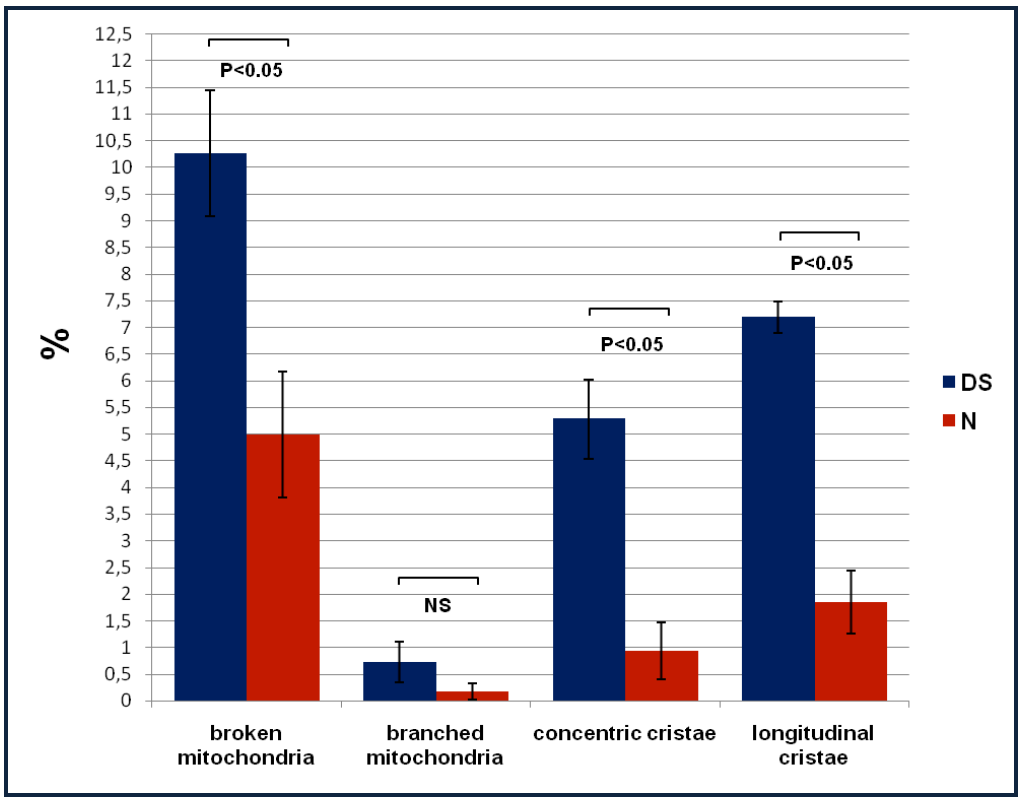

	Broken mitochondria	Branched mitochondria	Concentric cristae	Longitudinal cristae
DS fibroblasts	10,26 ± 1,17%	0,72 ± 0,38 %	5,28 ± 0,75 %	7,19 ± 0,29 %
Control fibroblasts	4,99 ± 1,17 %	0,18 ± 0,15 %	0,93 ± 0,53 %	1,85 ± 0,58 %

Figure 20. Percentages of mitochondria with abnormal morphology in fibroblasts.

The percentage of mitochondria that are broken or with concentric or longitudinal cristae is significantly higher in trisomic samples (DS) compared with euploid samples (N). No significant difference in the percentage of branched mitochondria. (Kolmogorov-Smirnov and Kruskall-Wallis test, p significant cut off <0.05). Mean values for DS and N samples ± standard error of the mean (SEM) are shown.

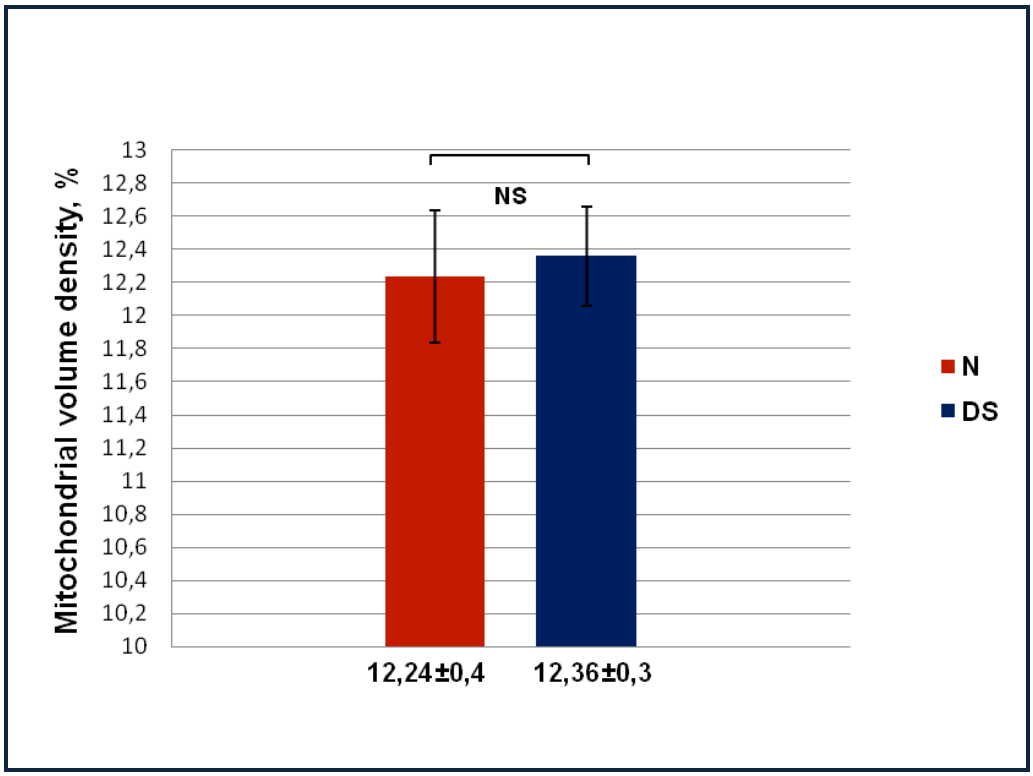

Figure 21. Mitochondrial volume density (%) relative to cell volume.
The mitochondrial volume density is not significantly different between trisomic and euploid fibroblasts. In graph the mean values of mitochondrial volume density for DS and N samples ± SEM are shown. NS: not significant.

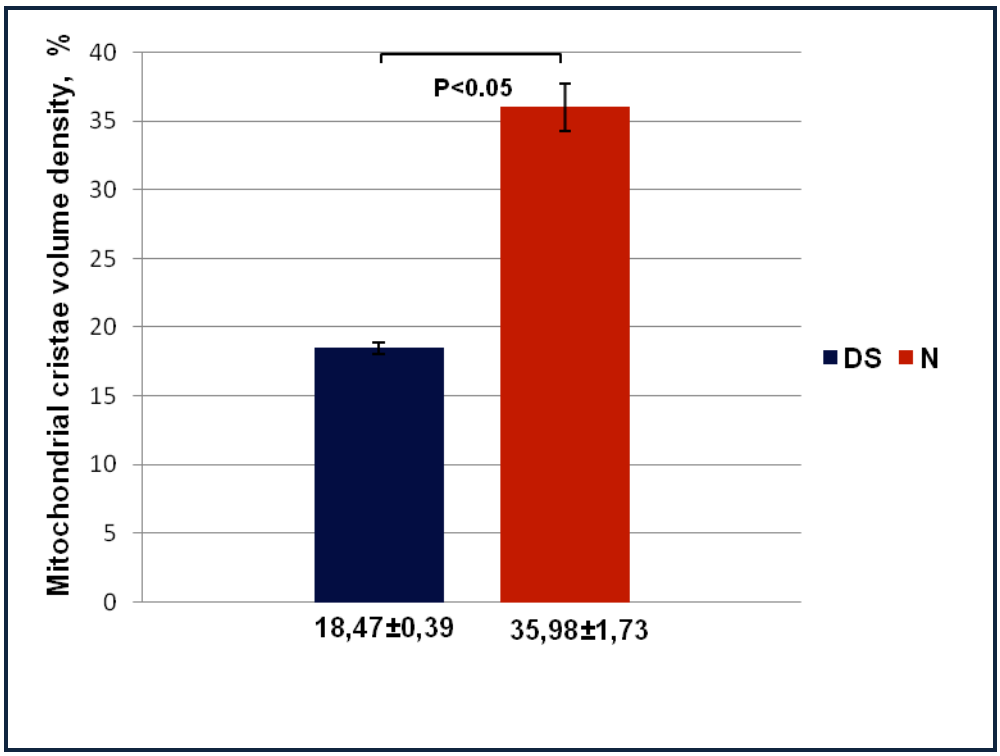

Figure 22. Mitochondrial cristae volume density (%) relative to mitochondrial volume.

The mitochondrial cristae volume density value of trisomic fibroblasts is almost 50% of the value calculated in the euploid samples. In graph the mean values of mitochondrial cristae volume density for DS and N samples ± SEM are shown. (Kolmogorov-Smirnov and Kruskall-Wallis test, p significant cut off <0.05)

4. Isolation and characterization of hAFSC

Selection of c-kit-positive AF cells

To generate a cell culture model from fetuses with trisomy of chromosome 21, stem cells isolation from amniotic fluid was performed in collaboration with Dr. Paolo de Coppi at the Venetian Institute of Molecular Medicine (VIMM) of Padova. Twenty cultures of amniotic fluid cells were subjected to immunoselection with magnetic microspheres to isolate c-kit (CD117)-positive population (**Fig. 23**).

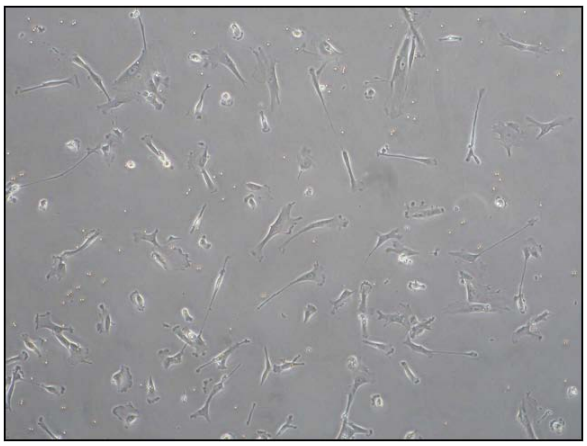

Figure 23. C-kit-positive isolated hAFC. Phase contrast image of hAFC after immunomagnetic selection of c-kit positive cells.

Isolated cells were cultured to confluency not greater than 70% and grown to verify their proliferative potential. Immunophenotypic characterization was performed at passage 4 in non-tissue culture petri dish.
Only 7 hAFC selections were able to reach passage 4 and the expression of appropriate markers, listed in **table 4**, was assessed by immunofluorescence and flow cytometry.

Table 4. Surface markers assessed in selected hAFC

Marker	Description
SSEA4	Stage-specific embryonic antigen 4
CD29	B_1-integrin
CD44	Hyaluronan receptor
CD45	Leukocyte Common Antigen
CD73	Glycoprotein present on subsets of T and B lymphocytes, follicular dendritic cells, endothelial cells and marrow stromal cells
CD105	Also known as endoglin, it is a proliferation-associated and hypoxia-inducible protein, abundantly expressed in angiogenic endothelial cells.
CD117	Stem cell factor (SCF) receptor

All the selections tested showed the enrichment of the stage-specific embryonic antigen SSEA4. C-kit-selected populations showed on average a 70% positivity to SSEA4 (**Fig. 24**) while the presence of c-kit on cellular membrane was never demonstrated.

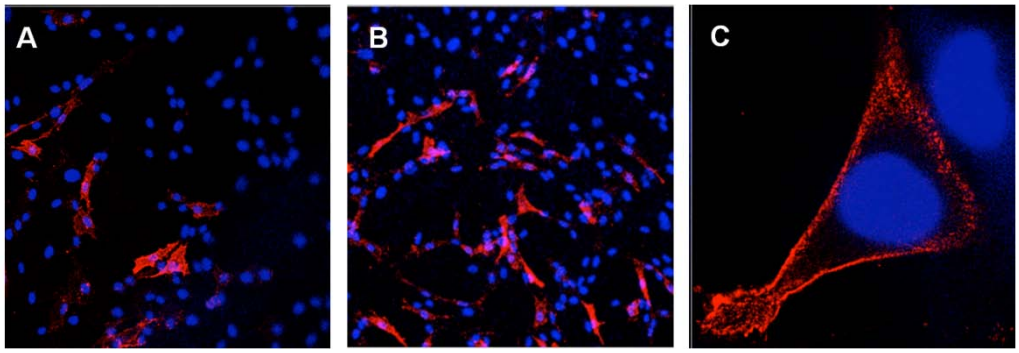

Figure 24. SSEA4 immunofluorescence of c-kit-positive hAFC. A: SSEA4 positive cells in amniotic fluid culture; **B**: SSEA4 positive cells in c-kit-selected hAFC; **C**: Enlargement of a single SSEA4 positive cell. Blue staining: Hoechst; red staining: mouse monoclonal antibody against SSEA4.

Flow cytometry experiments using antibodies against several antigens demonstrated that selected hAFC showed, as mean, a marked positivity for SSEA4, CD105, CD29, CD73 and CD44; they were slightly positive for CD117 and negative for CD45. Percentages of positivity for each antigen are shown in **Fig. 25**.
On the basis of these results, we concluded that it is possible to isolate c-kit-positive cells by immunomagnetic selection and that these cells express several markers of stem cells [De Coppi et al. 2007]. C-kit antigen however is detectable neither by immunofluorescence nor by flow cytometry assays.

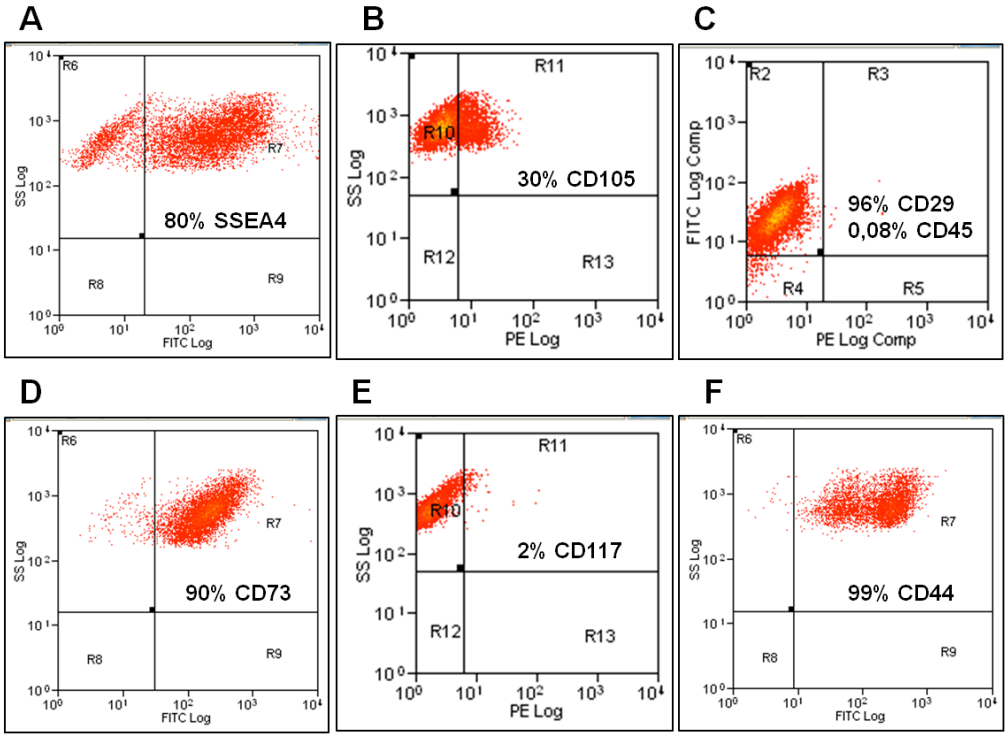

Figure 25. Surface marker expression of c-kit-selected hAFC by flow cytometry. Expression of surface antigens of cells labeled with specific antibodies: SSEA4-FITC (**A**), CD105-PE (**B**), CD29-FITC/CD45-PE (**C**), CD73-FITC (**D**), CD117-PE (**E**) and CD44-FITC (**F**).

Selection of SSEA4-positive AF cells

As an alternative approach, hAFC were selected on the basis of the surface expression of SSEA4 antigen. Ten to twenty percent of amniotic fluid cells were positive for SSEA4 surface antigen. We tried to isolate these cells from amniotic fluid using a primary antibody against SSEA4. Twenty amniotic fluid cultures were subjected to immunomagnetic selection to obtain a SSEA4 enriched cell population. The proliferative capacity in the selected SSEA4 positive cultures was higher than that of the cells selected on the basis of the c-kit positivity, as it has been possible to expand and characterize 10 of them. Flow cytometry assays demonstrated that SSEA4-selected cells showed generally high positivity for SSEA4, CD29, CD105 and CD73, while CD117 was always undetectable (**Fig. 26**).

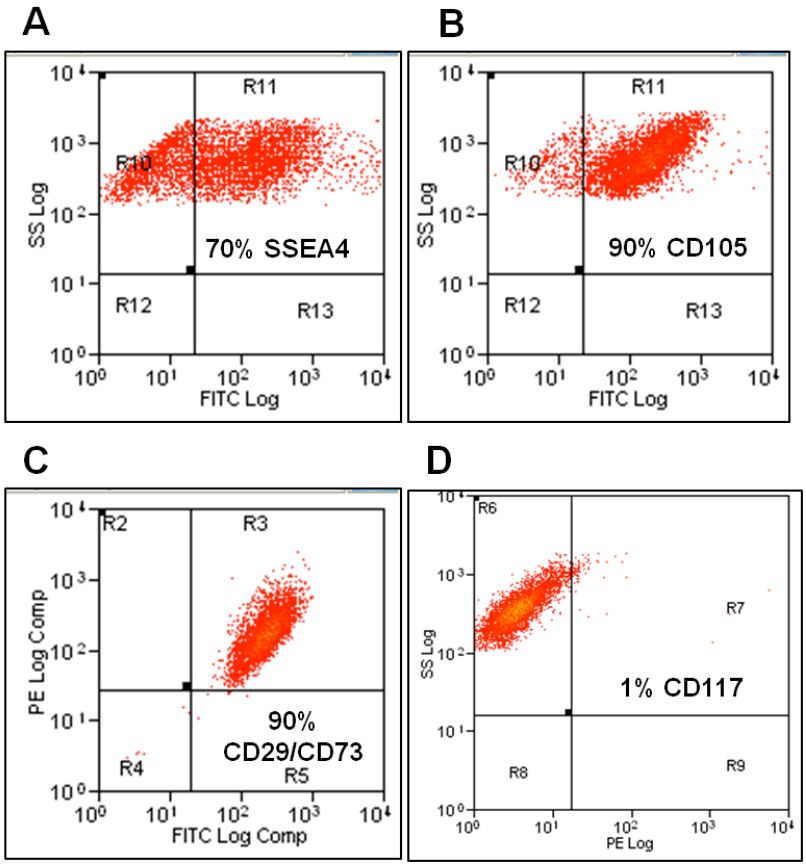

Figure 26. Surface marker expression of SSEA4-selected hAFC by flow cytometry. Expression of surface antigens of cells labeled with specific antibodies: SSEA4-FITC (**A**), CD105-FITC (**B**), CD29-FITC/CD73-PE (**C**), CD117-PE (**D**).

To obtain a pure stem cell population, cloning of SSEA4-positive hAFC was performed by limiting dilution in 96-well plates. Most of the selected cells were unable to overpass 8 culture passages and rapidly lost their proliferating capacity, while continuing to express stem cell surface markers.
The presence of c-kit mRNA was assessed by qualitative PCR. RNA was extracted from c-kit- and SSEA4-selected hAFC cultures and from an amniotic fluid culture not subjected to immunoselection. PCR demonstrated that the c-kit transcript was indeed present (**Fig. 27**). Since the surface protein was undetectable by immunofluorescence and flow cytometry assays, it is likely that the protein either is unstable or does not reach the cell plasma membrane.

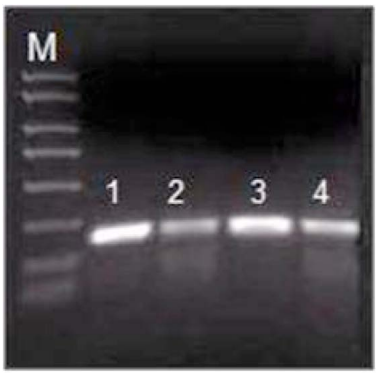

Figure 27. PCR analysis of c-kit mRNA. Lane 1: c-kit selected hAFC; lane 2 and 4: control unselected cells; lane 3: SSEA4 selected hAFC. M: Molecular weight marker

In conclusion these stem cells, obtained through immunomagnetic selection of c-kit and SSEA4 positive cells in amniotic fluid culture, were relatively simple to obtain but the following problems were noticed: 1-these cells were slow proliferating over 8 culture passages; 2-the immunophenotype was variable from one passage to another; 3-their cloning was difficult to obtain.

Adhesion based hAFSC selection

An alternative approach to obtain hAFSC, based upon differential adhesion and an appropriate culture medium, has been successfully used by the Prof. Rosi's group at the University of Perugia [Romani R. and Rosi G. personal communication].

These cells appeared as a homogeneous population, with a high proliferative potential and no karyotype anomalies or in vitro transformations even after 10 culture passages. The immunophenotypic and molecular characterization by flow cytometry and RT-PCR respectively is shown in **table 5**.

Profiling of surface markers and proliferation potential suggested that these cells could be used as model to investigate the molecular mechanisms by which trisomy 21 causes the phenotype. Two trisomic and 4 euploid cell lines have been obtained from fresh amniocyte cultures.

Table 5. Characterization of hAFSC obtained from adhesion based selection

Marker assessed by flow cytometry	Expression	Marker assessed by RT-PCR	Expression
HLA-ABC	+	Oct4	+
CD29	+	Nanog	+
CD44	+	Sox2	+
CD73	+	FGF4	+
CD105	+	FGF5	+
HLA-DR	-	c-Myc	+
CD10	-	Klf4	+
CD11b	-	Alkaline Phosphatase	+
CD14	-		
CD34	-		
CD38	-		
CD49b	-		

The possibility to obtain hAFSC from frozen amniocytes was also tested since many frozen samples of amniocytes with different chromosomal disorders are available at the Bank of Fetal Biological samples (University of Naples, Dpt of Biology and Pathology, Cellular and Molecular). Nine frozen amniocytes from trisomic fetuses were used and from 3 of them hAFSCs were obtained with properties similar to the ones selected from fresh cultures.

DISCUSSION

A preliminary study performed in our laboratory, comparing DS fetal heart tissues to control heart tissues [Conti et al. 2007], demonstrated that chromosome 21 genes were globally upregulated and that 441 genes, located on other chromosomes, were significantly dysregulated in trisomic heart samples, supporting the hypothesis that genes outside Hsa21 play a role in determining DS features.

Functional analysis of the genes differentially expressed between trisomic and control samples showed global downregulation of nuclear genes encoding mitochondrial proteins, especially enzymes involved in the oxidative phosphorylation pathway. Genes from all five complexes were downregulated suggesting that the corresponding proteins and enzymatic activities might be reduced, and that the mitochondrial function might be consequently impaired. For this reason we have conducted a molecular, functional and morphological analysis in primary cell lines of fetal fibroblasts, obtained from trisomic and euploid fetuses at about 20 weeks of gestation.

Mitochondrial function and reactive oxygen pathways have been investigated by other authors with respect to neurodegeneration. Protein levels of mitochondrial complex I, III and V were found to be decreased in cerebellar and brain regions of DS subjects [Kim et al. 2001], and a reduction of mitochondrial enzyme activity has been reported in platelets from DS patients [Prince et al. 1994]. Moreover, impaired mitochondrial function, indicated by reduced mitochondrial redox activity and membrane potential, has been observed in DS astrocytes and in primary cultures of DS fibroblasts [Arbuzova et al. 2002, Busciglio et al. 2002]. More recently it has been also reported that the brain of the DS mouse model Ts1Cje shows decreased mitochondrial membrane potential and ATP production [Shukkur et al. 2006]. These results are indicative of widespread mitochondrial dysfunction in DS.

Dysregulation of mitochondrial genes

Microarray data analysis performed in our study demonstrated that several genes involved in mitochondrial biogenesis and function were downregulated in trisomic fetal hearts at 18-22 weeks of gestation when compared to euploid hearts. We focused our attention on some of these genes, namely: NRF1, IMMT, PPRC1, NDUFA13 (GRIM19) and SLC25A4 (ANT1), and confirmed their downregulation in fetal heart tissue by qRT-PCR. Quantitative RT-PCR experiments confirmed the downregulation of NRF1 and IMMT genes also in fetal fibroblasts. SLC25A4 was not evaluated in fibroblasts because this is a cardiac-specific isoform of adenine nucleotide translocator.

NRF-1 is involved in the transcriptional control of mitochondrial biogenesis during adaptive thermogenesis through its interaction with the cold-inducible coactivator PGC-1. The targeted disruption of the NRF-1 gene in mice established that NRF-1 is essential for early embryogenesis in mammals, and its loss of function resulted in a peri-implantation lethal phenotype. In addition,

loss of NRF-1 determined a dramatic decrease in the amount of mtDNA in the blastocyst, thus providing the first evidence that NRF-1 is required for mitochondrial maintenance of the respiratory apparatus [Huo et al. 2001]. NRF1 downregulation both in DS hearts and fibroblasts might be responsible for about 40% mtDNA copy number decrease.

IMMT is a critical protein for maintenance of mitochondrial cristae ultrastructure and is involved in the stability of the whole mitochondria structure; its downregulation is responsible for abnormalities of the inner membrane and it has been speculated that these structural alterations may precede abnormal function, such as the hyperpolarization of the inner membrane and ROS iperproduction [John 2005].

PPRC1 or PRC is a member of the PGC-1 gene family that is expressed in organs with a high energy demand, especially in actively proliferating cells. It is a key trascriptional regulator of the fatty acid β-oxidation (FAO) pathway which is the principal source of mitochondrial ATP in the heart. PGC-1 plays a role in determining the metabolic phenotype of mitochondria among specialized cell types. It is possible that the availability of PGC-1 partners in a given tissue, such as NRF-1, PPARα, PPARγ, and other not yet identified, transcription factors dictate the level of expression of enzymes and proteins in specific mitochondrial pathways. This notion is supported by the observation that PGC-1 is capable of inducing either uncoupled or coupled respiration in a cell type–specific manner. Taken together, these findings suggest that PGC-1 controls mitochondrial functional capacity in a tissue-specific manner [Wu et al. 1999; Lehman et al. 2000].

GRIM-19 (Genes associated with Retinoid–IFN-induced Mortality-19) was originally identified as an interferon (IFN)-β and retinoic acid (RA)-inducible gene with apoptotic effects in human cancer cell lines [Angell et al. 2000]. However, it was subsequently found to copurify with mitochondrial NADH:ubiquinone oxidoreductase (complex I) in bovine heart [Fearnley et al. 2001]. By gene targeting in mice, it was further demonstrated that GRIM-19 is localized in complex I and it is essential for complex I assembly and electron transfer activity [Huang et al. 2004]. Various biological functions of GRIM-19 have been revealed. Knockout of GRIM-19 in mice caused early embryonic lethality, indicating its essential role in the embryonic development [Huang et al. 2004]. Further studies in Xenopus demonstrated that GRIM-19 is necessary for early heart development by regulating $Ca2^{+}$ homeostasis and the Ca^{2+}-dependent NFAT signaling pathway [Chen et al. 2007]. Furthermore, Lu et al. (2008) demonstrated that GRIM-19 has a unique role in the maintenance of $\Delta\Psi m$, that overlaps its electron transfer activity.

SLC25A4 or ANT1 encodes the adenine nucleotide translocator-1, playing an important role in the regulation of the intracellular energetic balance, and facilitates the exchange of extramitochondrial adenosine diphosphate (ADP) and intramitochondrial adenosine triphosphate (ATP). ANT1 is primarily espressed in heart and in skeletal muscle. Mutations and dysfunction of the ANT1 isoform result in severe cardiac and muscular disorder, impressively

shown in the knockout mice generated by Graham et al. (1997). Hearts from ANT1 null mutants revealed cardiac hypertrophy and developed pronounced characteristics of mitochondrial myopathy and cardiomyopathy with restricted oxidative phosphorylation, massive mitochondrial proliferation, and disarrangement of myofibers. In addition, knockout of ANT1 was associated with increased mitochondrial oxidative stress shown by elevated H_2O_2 production, increased mitochondrial DNA mutations, and an activated detoxification enzyme system [Esposito et al. 1999].
In conclusion, the downregulation of NRF1, IMMT, PPRC1, GRIM19 and ANT1 in DS fetal heart tissues and the downregulation of NRF1 and IMMT genes in DS fetal fibroblasts might account for mitochondrial dysfunctions, morphological changes and mtDNA copy number reduction as discussed in the next sections.

Mitochondrial dysfunction in trisomic fibroblasts

Oxidative stress is a phenotypic hallmark in several genetic disorders characterized by cancer predisposition and/or propensity to premature ageing. Mitochondria have a key role in oxygen metabolism and subsequently they are the major source of ROS formation. Studies on mitochondrial function have focused so far on neurological appearance, suggesting that neurological disorders, including mental retardation in DS, are associated to mitochondrial dysfunction [Kim et al. 2001; Prince et al. 1994; Busciglio et al. 2002; Shukkur et al. 2006].
Our study, in turn, focused on the cardiac phenotype of DS, showing a dysfunction in tissues other than brain and associating it with the expression profile of key genes.
Respirometry experiments conducted in this study demonstrated that oxygen consumption rate was significantly reduced both in basal respiration condition, and in uncoupled state. The analysis of individual complexes showed a strong reduction in the activity of complex I, and a decrease in activity of complex IV in DS fibroblasts. It was also found a strong decrease of mtDNA copy number.
It can be assumed, therefore, that in fibroblasts derived from trisomic fetuses there is a respiratory failure, possibly associated with a reduction of complex I activity which controls to the largest extent the respiratory activity. The two events, respiratory depression and deficit of complex I, do not show a direct correlation due to several compensatory mechanisms.
A complex I deficiency is characteristic of mitochondrial diseases, as an isolated defect or, in most of cases, as a part of multiple respiratory chain deficiencies. Isolated complex I deficiency has been associated with a wide spectrum of symptomatic phenotypes, varying from fatal infantile lactic acidosis to some cases of Leigh's disease, adult onset exercise intolerance, and some neurodegenerative diseases as Leber's hereditary optic neuropathy (LHON), focal dystonia, and Parkinson's disease. Experiments on cell lines and on isolated mitochondria have shown that inhibition of complex I with rotenone causes a reduction of cell growth, an increase in the ROS production

associated with an increased peroxidation of mitochondrial membrane and a reduction of membrane potential due to the reduction of the extrusion of protons in the intermembrane space [Barrientos et al. 1999]. The decrease in complex I was also found in mouse models with trisomy of chromosome 16 and results were similar to those obtained from models of Parkinson's disease, suggesting that different neurodegenerative diseases may be associated to the same mitochondrial dysfunction [Bambrick et al. 2008].
Redox imbalance demonstrated in DS cells might also be secondary to overexpression of copper-zinc superoxide dismutase (SOD1), as we found in trisomic fibroblasts by qRT-PCR. Neuronal death in DS has been linked to the triplicated expression of SOD1, which was suggested to be involved in the oxidative damage to neurons [Lee et al. 2001]. Furthermore it has been demonstrated that in fibroblasts from DS patients there was a defective repair of oxidative damage to mtDNA [Druzhyna et al. 2008] and that neurons of Ts16 mouse model had an increased $O^{2-\bullet}$ basal generation, possibly attributed to a complex I deficiency [Schuchmann and Heinemann 2000]. This last consideration might be another cause of mtDNA copy number reduction.
In this study we demonstrated not only that in fetal fibroblasts ROS production was ~3-fold increased in DS cells versus euploid controls, but that interestingly ROS were also significantly increased in fibroblasts from DS fetuses with cardiopathy if compared to controls.

Morphological abnormalities of mitochondria in trisomic cells

Morphological analysis of mitochondria that we have performed in fetal fibroblasts derived from trisomic and euploid fetuses demonstrated that ultrastructural changes occur in mitochondria of DS samples. In particular, we found an increase in size or giant mitochondria with irregular shape and evident breaks of both inner and outer membranes. In addition, mitochondria of DS samples showed an altered pattern of cristae, that presented broadened and arranged concentrically or longitudinally to the organelle. Broken mitochondria and mitochondria with concentric and longitudinal cristae were significantly more abundant in trisomic samples than in euploid samples, but the difference was not significant for branched mitochondria. Stereological evaluations of mitochondrial volume density and cristae volume density in the same samples demonstrated that cristae volume density was significantly reduced in trisomic fibroblasts while there was no significant difference in mitochondrial volume density between trisomic and euploid cells.
These results further expand evidences obtained mainly on brain tissues from other authors. Ultrastructural abnormalities like an unusual branched morphology of mitochondria in cultured cerebellar neurons from Ts16 mice were reported by Bersu et al. (1998). Shukkur et al. (2006) described an increased number of abnormal mitochondria, especially with broken cristae, in brain tissue of Ts1Cje mice.
Mitochondria undergo regulated fusion and division, which appear to play key roles in establishing and maintaining mitochondrial shape. In certain cell types

mitochondria are organized in networks of interconnected organelles, depending on the equilibrium between fusion and fission. These mechanisms are susceptible to cellular metabolic needs and they influence not only cristae pattern but also the number and structure of tubular connections between them (cristae junctions) and between cristae and periferic portion of inner membrane.
The molecular mechanisms governing the biogenesis and configuration of the inner membrane are largely unknown. John et al. (2005) demonstrated that the downregulation of mitofilin resulted in a drastic change in the organization of the inner membrane that formed concentric layers instead of organizing into tubular cristae. In this study we demonstrated that mitofilin (IMMT) is downregulated both in trisomic hearts and fibroblasts. Furthermore, electron microscope observations revealed that the inner membrane of trisomic fibroblast mitochondria formed concentric layers. Cristae formation is critical for achieving high surface-to-volume ratio of the inner membrane. Although the concentric layering increases the inner membrane surface area, the tightly packed membranous sheets and internal compartmentation might hinder exchange for ions and metabolites, possibly leading to altered membrane potential and ROS production as well as defective oxidative phosphorylation.
For the first time, an abnormal mitochondrial ultrastructure has been observed in DS samples associated to IMMT downregulation.

Calcineurin/NFATc signaling in trisomic samples

We demonstrated, both by microarray and by qRT-PCR, that the pathway of calcineurin/NFATc, a critical regulator of vertebrate development and organogenesis, was dysregulated in trisomic hearts and fibroblasts, being DYRK1A upregulated in DS samples while catalytic subunits of calcineurin (not yet evaluated in fibroblasts) and NFATc2, NFATc3 and NFATc4 were significantly downregulated. Moreover, NFAT gene regulation is deeply affected by the abundance of DSCR1/RCAN1, a gene mapping to Hsa21. Microarray data in DS heart tissues showed that DSCR1 expression is variable but it is always inversely correlated to NFAT gene expression. The expression variability of these genes might be ascribed to the evidence that calcineurin/NFATsignalling is only required for brief and sharply defined time windows during embryonic development.
It might be useful to assess the expression of both catalytic and regulatory subunits of calcineurin in trisomic fibroblasts and regulatory subunits in trisomic hearts.
It has been demonstrated that in Nfatc3-/-; Nfatc4-/- cardiomyocytes the enzymatic activity of complex II and IV of the respiratory chain and mitochondrial oxidative activity were reduced and mitochondria were swollen, with an abnormal cristae pattern [Bushdid et al. 2003], suggesting that the calcineurin/NFAT pathway affects mitochondrial activity and morphology during heart development.

A key issue of DS pathogenesis is to understand how upregulation of Hsa21 genes dysregulates genes on different chromosomes, in this case genes encoding mitochondrial enzymes.
Recent data suggest that perturbation of NFATc genetic regulatory circuit by an increased dosage of DSCR1 and/or DYRK1A, both mapping to Hsa21, may explain many of the developmental phenotype in Down Syndrome, especially cardiac defects. Nfatc2-/-; Nfatc3-/-; Nfatc4-/- triple-knockout mice showed, in presence of Dyrk1a and Dscr1 overexpression, phenotypic anomalies that resembled those observed in human DS and 65% of Nfatc1-4 and Cnb1(ortholog gene of calcineurin regulatory subunit PPP3R1) -null mice had endocardial cushion defects [Arron et al. 2006]. According to our results, we propose that upregulation of DYRK1A and/or DSCR1 in DS might affect the expression of mitochondrial proteins, and therefore mitochondrial function in trisomic hearts and fibroblasts, through the calcineurin/NFAT pathway.

Establishment of a new model to study molecular bases of DS feature

An aim of this study was to isolate stem cells from amniocytes of euploid and of trisomy 21 fetuses, either from fresh amniotic fluid either from frozen culture samples. Indeed, there is the evidence that most of phenotypic features of DS are determined very early during organ differentiation. Neuronal precursors, for instance, show a reduced capability to generate normal differentiated neurons [Mensah et al. 2010] both in DS subjects and mouse models. The analysis of human hearts from DS embryos at 10 gestation weeks revealed a retardation of development in all hearts even though heart defects are detectable at birth in only 40-50% of DS subjects [Gittenberger-de Groot et al. 2003].
One methodology to isolate stem cells is based on the fact that stem cells in primary cultures of amniotic fluid express several specific antigens on their plasma membrane. We performed immunoselection of amniotic fluid stem cells (hAFSc) with magnetic microspheres using antibodies against membrane antigens, such as c-Kit (CD117) and SSEA-4. SSEA-4 is a stage-specific embryonic antigen that is a expressed by ES cells but generally not by adult stem cells, and is expressed in human amniotic fluid stem cells. C-Kit selection has already demonstrated to allow the isolation of clonal multipotent stem cell lines, positive for mesenchymal markers and negative for hematopoietic markers [De Coppi et al. 2007].
Both immunoselections proved to be effective and cells enriched in mesenchimal and/or neural stem cell markers, such as SSEA4, CD105, CD29, CD73 and CD44, were obtained. However, cells immunoselected for either marker (CD117 or SSEA-4) turned out to be negative for CD117, either by flow cytometry either by immunofluorescence analysis. It has been puzzling to us for some time the fact that cells immunoselected for CD117 were then negative for the expression of that same marker. It turned out that mRNA for CD117 was indeed expressed by selected cells, suggesting that the CD117 protein might be expressed on the plasma membrane only in a limited window

of time, in the cell life span. It is interesting to note that although both CD117 and SSEA-4 marker immunoselection yielded cells that expressed the same markers, there was variability in the level of expression of each of them. This result might be in agreement with the fact that different types of mesenchimal stem cells were suggested to be present in the amniotic fluid [Siegel et al. 2007].

A major question that arises from this study is whether the cells enriched by either immunoselection were bona fide stem cells. By definition a stem cell should be able to keep a high proliferative potential in the undifferentiated state and should be able to differentiate in one or more differentiated cell type(s) upon appropriate induction. On the other side a characteristic of stem cells is the expression of a specific panel of membrane antigens. The cells that we obtained by CD117 or SSEA-4 immunoselection manifested this last property but we have not been able to prove a high proliferative rate for any of the cultures that were prepared. We neither managed to clone any of them, which might be needed for our studies, since human amniotic fluid might contain more than one stem cell type [Siegel et al. 2007]. Of course this failure might be due to inappropriate culture conditions, such as inappropriate substrate or culture medium.

Cells with stem cell properties, with respect to the expression of membrane markers (see table 5**)** and with long life span, were made available to us. It was also possible to obtain these stem cells from trisomic samples. This was relevant since stem cells have not yet been isolated from trisomy 21 amniotic fluid samples, though a preliminary study demonstrated that cells from those samples normally expressed stem cell markers [Prusa et al. 2003]. Stem cells were also obtained from frozen amniocytes derived from trisomic fetuses. This represents an important progress since we were able to use samples stored in the Bank of Fetal Biological Samples, which has been set up, over the years, in our own Department. Amniocyte samples from fetuses affected by other diseases are stored in the Bank unveiling the possibility to set up more cell models of human pathologies. What can be done with these cell models? They may provide a new source for the development of new approaches for stem cell therapies and tissue engineering, such as the surgical repair of congenital anomalies in the perinatal period and pathologies that might occur in the adult life. But, of course, they can be used for basic research on human genetic diseases and to design new therapeutic approaches in the near future [Siegel et al. 2007].

With regard to our trisomy 21 cell model, there is of course a need for further characterization of the cell cultures, cloning if possible and monitoring the karyotype and the telomere length, to verify that cells are not altered after several passages in culture. In order to systematically evaluate primary dysregulations already occurring at the stage of stem cells, due to trisomy of chromosome 21, gene expression profiles from clonal hAFSCs obtained both from trisomic and euploid fetuses will be compared. Next step will be to differentiate stem cells in cell populations that are considered to be target of the

DS. Several tissues and organs are indeed target of DS. We plan to primarily address the study of the two tissues that are known to be the main targets of DS: the brain and the heart, and therefore we will promote neural and cardiac differentiation of trisomic stem cells. Gene expression profiles of differentiated cells obtained both from trisomic and euploid hAFSCs will be compared. The rationale for this analysis resides in the fact that many phenotypic features of DS are determined very early in development, when the tissue specification is not completely established. Our aim is to determine how many and which chromosome 21 genes are already dysregulated in the very early steps of differentiation and whether specific categories of genes are dysregulated, such as mitochondrial enzymes or extracellular matrix proteins, that we found dysregulated in a previous study performed on fetal heart tissue [Conti et al. 2007].

Hsa21 trisomic stem cells can be also used as a model to test the significance of individual genes in determining the molecular basis of gene dosage imbalance in the most clinically relevant and common forms of aneuploidy. We could take a complementary approach to the one that was taken by De Cegli at al. (2010) who developed a mouse embryonic stem (ES) cell bank of human chromosome 21 genes. The human chromosome 21-mouse ES cell bank included 32 human chromosome 21 genes, which could be overexpressed in an inducible manner. Each clone was transcriptionally profiled in inducing versus noninducing conditions to evaluate the contribution of single genes to the trisomic mouse ES cell transcriptome. We are going to generate a similar bank of human pluripotent trisomic stem cells in which individual Hsa21 genes might be selectively inactivated to assess their contribution to the altered trisomic cell transcriptome.

ACKNOWLEDGEMENTS

At the end of this study, I would like to thank and express my gratitude to all people which, in different ways, I have been close and have allowed and encouraged both my studies and the creation and writing of this thesis.
My heartfelt thanks go to *Prof. Lucio Nitsch*, my tutor in this research work, for being always present and available with his suggestions, comments and advices, always precious for me. Thanks with sincere affection to a man and a professionist for the opportunities he has given to me.
Thanks to *Dr. Anna Conti* for the continued availability and patience shown me in clarifications and suggestions and for critical reading of all chapters of this work.
Special thanks go to *Dr. Floriana Fabbrini*, for contributing to my training and professional growth and above all for showing me respect and affection since the first moment. Her teachings and encouragement helped me to believe in my possibilities and to follow my ambitions. *To Floriana I dedicate this work for the friendship and respect that will join us forever.*
Thanks to all people of my research group, especially to *Nando* and *Rosanna*, for their help and support in the implementation of different phases of this work.
Finally, I would like to thank *Dr. Nazzareno Capitanio* and *Dr. Claudia Piccoli* for performing mitochondrial functional studies; *Dr. Marina Prisco* for electron microscope observations of mitochondrial ultrastructure; *Dr. Paolo De Coppi*, *Dr. Gabriella Rosi* and *Dr. Rita Romani* for the help in setting up the in vitro culture model of trisomic stem cells.

REFERENCES

Amano K, Sago H, Uchikawa C, Suzuki T, Kotliarova SE, Nukina N, Epstein CJ, Yamakawa K. Dosage-dependent over-expression of genes in the trisomic region of Ts1Cje mouse model for Down syndrome. Hum Mol Genet 2004, 13(13):1333-1340.

Angell JE, Lindner DJ, Shapiro PS, Hofmann ER, Kalvakolanu DV. Identification of GRIM-19, a novel cell death-regulatory gene induced by the interferon-beta and retinoic acid combination, using a genetic approach. J Biol Chem 2000; 275, 33416–33426.

Arbuzova S, Hutchin T, Cuckle H. Mitochondrial dysfunction and Down's syndrome. Bioessays 2002, 24(8):681-684.

Arron JR, Winslow MM, Polleri A, Chang CP, Wu H, Gao X, Neilson JR, Chen L, Heit JJ, Kim SK, Yamasaki N, Miyakawa T, Francke U, Graef IA, Crabtree GR. NFAT dysregulation by increased dosage of DSCR1 and DYRK1A on chromosome 21. Nature 2006, 441(7093):595-600.

Bambrick LL, Fiskum G. Mitochondrial dysfunction in mouse trisomy 16 brain. Brain Res. 2008 Jan 10;1188:9-16.

Barlow GM, Chen XN, Shi ZY, Lyons GE, Kurnit DM, Celle L, Spinner NB, Zackai E, Pettenati MJ, Van Riper AJ, Vekemans MJ, Mjaatvedt CH, Korenberg JR. Down syndrome congenital heart disease: a narrowed region and a candidate gene. Genet Med 2001, 3(2):91-101.

Barrientos A, Moraes CT. Titrating the effects of mitochondrial complex I impairment in the cell physiology. J Biol Chem. 1999 Jun 4;274(23):16188-97.

Belichenko NP, Belichenko PV, Kleschevnikov AM, Salehi A, Reeves RH, Mobley WC. The "Down syndrome critical region" is sufficient in the mouse model to confer behavioral, neurophysiological, and synaptic phenotypes characteristic of Down syndrome. The Journal of Neuroscience, May 6, 2009; 29(18):5938 –5948.

Bersu ET, Ahmad FJ, Schwei MJ, Baas PW. Cytoplasmic abnormalities in cultured cerebellar neurons from the trisomy 16 mouse. Brain Res Dev Brain Res 1998; 109:115–120.

Bhattacharyya A and Svendsen CN. Human neural stem cells: a new tool for studying cortical development in Down's syndrome. Genes, Brain and Behavior 2003; (2):179-186.

Busciglio J, Yankner BA. Apoptosis and increased generation of reactive oxygen species Down's syndrome neurons in vitro. Nature 1995;378:776–779.

Busciglio J, Pelsman A, Wong C, Pigino G, Yuan M, Mori H, Yankner BA. Altered metabolism of the amyloid beta precursor protein is associated with mitochondrial dysfunction in Down's syndrome. Neuron 2002, 33(5):677-688.

Bushdid PB, Osinska H, Waclaw RR, Molkentin JD, Yutzey KE. NFATc3 and NFATc4 are required for cardiac development and mitochondrial function. Circ Res 2003, 92(12):1305-1313.

Camello-Almaraz MC, Gomez-Pinilla PJ, Pozo MJ and Camello PJ. Mitochondrial reactive oxygen species and Ca^{2+} signaling. Am J Physiol Cell Physiol 2006, 291: C1082–C1088.

Cela O, Piccoli C, Scrima R, Quarato G, Marolla A, Cinnella G, Dambrosio M, Capitanio N. Bupivacaine uncouples the mitochondrial oxidative phosphorylation, inhibits respiratory chain complexes I and III and enhances ROS production: Results of a study on cell cultures. Mitochondrion 2010 Aug;10(5):487-96.

Chen Y, Yuen WH, Fu J, Huang G, Melendez AJ, Ibrahim FB, Lu H, Cao X. The mitochondrial respiratory chain controls intracellular calcium signaling and NFAT activity essential for heart formation in Xenopus laevis. Mol Cell Biol. 2007 Sep;27(18):6420-32. Epub 2007 Jul 16.

Chen Q, Vazquez EJ, Moghaddas S, Hoppel CL, and Lesnefsky EJ. Production of reactive oxygen species by mitochondria: central role of complex III. J Biol Chem 2003, 278: 36027–36031.

Conti A, Fabbrini F, D'Agostino P, Negri R, Greco D, Genesio R, D'Armiento M, Olla C, Paladini D, Zannini M, Nitsch L. Altered expression of mitochondrial and extracellular matrix genes in the heart of human fetuses with chromosome 21 trisomy. BMC Genomics. 2007;8:268.

Crabtree GR, Olson EN. NFAT signaling: choreographing the social lives of cells. Cell 2002, 109 [Suppl]:S67–S79.

Dauphinot L, Lyle R, Rivals I, Dang MT, Moldrich RX, Golfier G, Ettwiller L, Toyama K, Rossier J, Personnaz L, Antonarakis SE, Epstein CJ, Sinet PM, Potier MC. The cerebellar transcriptome during postnatal development of the Ts1Cje mouse, a segmental trisomy model for Down syndrome. Hum Mol Genet. 2005;14(3):373-84.

De Coppi P, Bartsch G Jr, Siddiqui MM, Xu T, Santos CC, Perin L, Mostoslavsky G, Serre AC, Snyder EY, Yoo JJ, Furth ME, Soker S, Atala A. Isolation of amniotic stem cell lines with potential for therapy. Nat Biotechnol. 2007;25(1):100-6.

De Cegli R, Romito A, Iacobacci S, Mao L, Lauria M, Fedele AO, Klose J, Borel C, Descombes P, Antonarakis SE, Di Bernardo D, Banfi S, Ballabio A and Cobellis G. A mouse embryonic stem cell bank for inducible overexpression of human chromosome 21 genes. Genome Biology 2010; 11:R64.

Delabar JM, Theophile D, Rahmani Z, Chettouh Z, Blouin JL, Prieur M, Noel B, Sinet PM: Molecular mapping of twenty-four features of Down syndrome on chromosome 21. Eur J Hum Genet 1993, 1(2):114-124.

Druzhyna NM, Wilson GL, LeDoux SP. Mitochondrial DNA repair in ageing and disease. Mech Ageing Dev. 2008 Jul-Aug; 129(7-8):383-90.

Dunlevy L, Bennett M, Slender A, Lana-Elola E, Tybulewicz VL, Fisher EM, Mohun T. Down's syndrome-like cardiac developmental defects in embryos of the transchromosomic Tc1 mouse. Cardiovasc Res. 2010 Nov 1;88(2):287-95.

Epstein CJ, Korenberg JR, Anneren G, Antonarakis SE, Ayme S, Courchesne E, Epstein LB, Fowler A, Groner Y, Huret JL et al. Protocols to establish genotype-phenotype correlations in Down syndrome. Am J Hum Genet 1991, 49(1):207-235.

Esposito LA, Melov S, Panov A, Cottrell BA, Wallace DC. Mitochondrial disease in mouse results in increased oxidative stress. Proc Natl Acad Sci USA 1999; 96:4820–4825.

Fearnley IM, Carroll J, Shannon RJ, Runswick MJ, Walker JE, Hirst J. GRIM-19, a cell death regulatory gene product, is a subunit of bovine mitochondrial NADH:ubiquinone oxidoreductase (complex I). J Biol Chem 2001; 276, 38345–38348.

Ferencz C, Neill CA, Boughman JA, Rubin JD, Brenner JI, Perry LW. Congenital cardiovascular malformations associated with chromosome abnormalities: an epidemiologic study. J Pediatr 1989, 114(1):79-86.

FitzPatrick DR, Ramsay J, McGill NI, Shade M, Carothers AD, Hastie ND. Transcriptome analysis of human autosomal trisomy. Hum Mol Genet. 2002;11(26):3249-56.

Frezza C, Cipolat S, Martins de Brito O, Micaroni M, Beznoussenko GV, Rudka T, Bartoli D, Polishuck RS, Danial NN, De Strooper B, Scorrano L. OPA1 controls apoptotic cristae remodeling independently from mitochondrial fusion. Cell 2006; 126: 177–189

Gardiner K: Predicting pathway perturbations in Down syndrome. J Neural Transm Suppl 2003(67):21-37.

Gittenberger-de Groot AC, Bartram U, Oosthoek PW, Bartelings MM, Hogers B, Poelmann RE, Jongewaard IN, Klewer SE. Collagen type VI expression during cardiac development and in human fetuses with trisomy 21. Anat Rec A Discov Mol Cell Evol Biol 2003, 275(2):1109-1116.

Gnaiger E, Forstner H, eds. Polarographic Oxygen Sensors. Aquatic and Physiological Applications. New York: Springer-Verlag; 1983.

Gnaiger E. Polarographic oxygen sensors, the oxygraph, and high-resolution respirometry to assess mitochondrial function. Drug-Induced Mitochondrial Dysfunction, Edited by James Dykens and Yvonne Will Copyright©2008 John Wiley & Sons, Inc.: pp. 327-352.

Graham BH, Waymire KG, Cottrell B, Trounce IA, MacGregor GR, Wallace DC. A mouse model for mitochondrial myopathy and cardiomyopathy resulting from a deficiency in the heart/muscle isoform of the adenine nucleotide translocator. Nat Genet 1997; 16:226–234.

Gundersen HJG. The smooth fractionator. Journal of Microscopy 2002; 207, 191–210

Gwack Y, Sharma S, Nardone J, Tanasa B, Iuga A, Srikanth S, Okamura H, Bolton D, Feske S, Hogan PG, Rao A. A genome-wide Drosophila RNAi screen identifies DYRK-family kinases as regulators of NFAT. Nature 2006 Jun 1;441(7093):646-50.

Hayat M.A. Principles and Techniques of Electron Microscopy: Biological Applications. Fourth Edition. 2000, Cambridge University Press.

Huang G, Lu H, Hao A, Ng DC, Ponniah S, Guo K, Lufei C, Zeng Q, Cao X. GRIM-19, a cell death regulatory protein, is essential for assembly and function of mitochondrial complex I. Mol Cell Biol. 2004 Oct;24(19):8447-56.

Huo L and Scarpulla RC. Mitochondrial DNA instability and peri-implantation lethality associated with targeted disruption of nuclear respiratory factor 1 in mice. Mol Cell Biol 2001, 21:644-654.

John JB, Shang Y, Li L, Renken C, Mannella CA, Selker JML, Rangell L, Bennett MJ, Zha J. The mitochondrial inner membrane protein Mitofilin controls cristae morphology. Mol Biol of the Cell 2005;16:1543-1554.

Kahlem P, Sultan M, Herwig R, Steinfath M, Balzereit D, Eppens B, Saran NG, Pletcher MT, South ST, Stetten G, Lehrach H, Reeves RH, Yaspo ML. Transcript level alterations reflect gene dosage effects across multiple tissues in a mouse model of down syndrome. Genome Res 2004, 14(7):1258-1267.

Kerstens HM, Robben JC, Poddighe PJ, Melchers WJ, Boonstra H, de Wilde PC, Macville MV, Hanselaar AG. AgarCyto: a novel cell-processing method for multiple molecular diagnostic analyses of the uterine cervix. J Histochem Cytochem. 2000 May;48(5):709-18.

Kim SH, Vlkolinsky R, Cairns N, Fountoulakis M, Lubec G. The reduction of NADH ubiquinone oxidoreductase 24- and 75-kDa subunits in brains of patients with Down syndrome and Alzheimer's disease. Life Sci 2001, 68(24):2741-2750.

Kim MS and Usachev YM. Mitochondrial Ca^{2+} Cycling Facilitates Activation of the Transcription Factor NFAT in Sensory Neurons. J Neurosci, September 30, 2009, 29(39):12101–12114

Korenberg JR, Chen XN, Schipper R, Sun Z, Gonsky R, Gerwehr S, Carpenter N, Daumer C, Dignan P, Disteche C *et al*. Down syndrome phenotypes: the consequences of chromosomal imbalance. Proc Natl Acad Sci USA 1994, 91(11):4997-5001.

Kussmaul L and Hirst J. The mechanism of superoxide production by NADH:ubiquinone oxidoreductase (complex I) from bovine heart mitochondria. Proc Natl Acad Sci USA 2006; 103, 7607–7612.

Lee M, Hyun D, Jenner P and Halliwell B. Effect of overexpression of wild-type and mutant Cu/Zn-superoxide dismutases on oxidative damage and antioxidant defences: relevance to Down's syndrome and familial amyotrophic lateral sclerosis. J. Neurochem. 2001, 76, 957–965.

Lehman JJ, Barger PM, Kovacs A, Saffitz JE, Medeiros DM, Kelly DP. Peroxisome proliferator-activated receptor gamma coactivator-1 promotes cardiac mitochondrial biogenesis. J Clin Invest. 2000 Oct;106(7):847-56.

Li CM, Guo M, Salas M, Schupf N, Silverman W, Zigman WB, Husain S, Warburton D, Thaker H, Tycko B. Cell type-specific over-expression of chromosome 21 genes in fibroblasts and fetal hearts with trisomy 21. BMC Med Genet. 2006;7:24.

Li Y and Trush MA. Diphenyleneiodonium, an NAD(P)H oxidase inhibitor, also potently inhibits mitochondrial reactive oxygen species production. Biochem Biophys Res Commun 1998; 253, 295–299.

Li Z, Yu T, Morishima M, Pao A, LaDuca J, Conroy J, Nowak N, Matsui S-I, Shiraishi I and Yu YE. Duplication of the entire 22.8 Mb human chromosome 21 syntenic region on mouse chromosome 16 causes cardiovascular and gastrointestinal abnormalities. Hum Mol Genet 2007,16(11): 1359-1366

Liesa M, Palacin M, Zorzano A. Mitochondrial dynamics in mammalian health and disease. Physiol Rev 2009. 89: 799–845

Lu H and Cao X. GRIM-19 is essential for mainenance of mitochondrial membrane potential. Mol Biol Cell 2008 May; 19:1893-1902.

Lyle R, Gehrig C, Neergaard-Henrichsen C, Deutsch S, Antonarakis SE. Gene expression from the aneuploid chromosome in a trisomy mouse model of down syndrome. Genome Res 2004, 14(7):1268-1274.

Mandarim-De-Lacerda. Stereological tools in biomedical research. An Acad Bras Cienc 2003; 75, 469-486

Mao R, Wang X, Spitznagel EL Jr, Frelin LP, Ting JC, Ding H, Kim JW, Ruczinski I, Downey TJ, Pevsner J. Primary and secondary transcriptional effects in the developing human Down syndrome brain and heart. Genome Biol 2005, 6(13):R107.

Mayhew TM. The new stereological methods for interpreting functional morphology from slices of cells and organs. Experimental Physiology 1991; 76, 639-665.

McCormick MK, Schinzel A, Petersen MB, Stetten G, Driscoll DJ, Cantu ES, Tranebjaerg L, Mikkelsen M, Watkins PC, Antonarakis SE. Molecular genetic approach to the characterization of the "Down syndrome region" of chromosome 21. Genomics 1989, 5(2):325-331.

Mensah A, Mulligan C, Linehan J, Ruf S, O'Doherty A, Grygalewicz B, Shipley J, Groet J, Tybulewicz V, Fisher E, Brandner S, Nizetic D. An additional human chromosome 21 causes suppression of neural fate of pluripotent mouse embryonic stem cells in a teratoma model. BMC Dev Biol 2007, 7:131.

Miyake M, Zenita K, Tanaka O, Okada Y, Kannagi R. Stage-specific embryonic antigens (SSEA-3 and -4) are epitopes of a unique globo-series ganglioside isolated from human teratocarcinoma cells. EMBO J. 1983; 2, 2355–2361.

Moore CS. Postnatal lethality and cardiac anomalies in Ts65Dn Down syndrome mouse model. Mammalian Genome 2006, (17) 1005-1012.

O'Doherty A, Ruf S, Mulligan C, Hildreth, V, Errington, ML, Cooke S, Sesay A, Modino S, Vanes L, Hernandez D, Linehan JM, Sharpe PT, Brandner S, Bliss TV, Henderson DJ, Nizetic D, Tybulewicz VL, Fisher EM. An aneuploid mouse strain carrying human chromosome 21 with Down syndrome phenotypes. Science 2005, 309, 2033–2037.

Olson LE, Richtsmeier JT, Leszl J, Reeves RH. A chromosome 21 critical region does not cause specific Down syndrome phenotypes. Science 2004, 306(5696):687-690.

Olson LE, Roper RJ, Sengstaken CL, Peterson EA, Aquino V, Galdzicki Z, Siarey R, Pletnikov M, Moran TH, Reeves RH. Trisomy for the Down syndrome "critical region" is necessary but not sufficient for brain phenotypes of trisomic mice. Hum Mol Genet 2007 Apr 1;16(7):774-82.

Park SC, Mathews RA, Zuberbuhler JR, Rowe RD, Neches WH, Lenox CC. Down syndrome with congenital heart malformation. Am J Dis Child 1977, 131(1):29-33.

Piccoli C, Scrima R, Quarato G, D'Aprile A, Ripoli M, Lecce L, Boffoli D, Moradpour D, Capitanio N. Hepatitis C virus protein expression causes calcium-mediated mitochondrial bioenergetic dysfunction and nitro-oxidative stress. Hepatology 2007; 46(1): 58-65.

Prince J, Jia S, Bave U, Anneren G, Oreland L. Mitochondrial enzyme deficiencies in Down's syndrome. J Neural Transm Park Dis Dement Sect 1994, 8(3):171-181.

Prusa AR, Marton E, Rosner M, Freilinger A, Bernaschek G, Hengstschläger M. Stem cell marker expression in human trisomy 21 amniotic fluid cells and trophoblasts. J Neural Transm Suppl. 2003;(67):235-42.

Rahmani Z, Blouin JL, Creau-Goldberg N, Watkins PC, Mattei JF, Poissonnier M, Prieur M, Chettouh Z, Nicole A, Aurias A *et al*. Critical role of the D21S55 region on chromosome 21 in the pathogenesis of Down syndrome. Proc Natl Acad Sci U S A 1989, 86(15):5958-5962.

Reeves RH, Irving NG, Moran TH, Wohn A, Kitt C, Sisodia SS, Schmidt C, Bronson RT and Davisson MT. A mouse model for Down syndrome exhibits learning and behaviour deficits. Nat Genet 1995, 11, 177–184.

Reeves RH. Down's syndrome. A complicated genetic insult. Lancet 2001, 358 Suppl:S23.

Reynolds ES. The use of lead citrate at high pH as an electron-opaque stain in electron microscopy. J Cell Biol 1963;17, 208-228.

Roat E, Prada N, Ferraresi R, Giovenzana C, Nasi M, Troiano L, Pinti M, Nemes E, Lugli E, Biagioni O, Mariotti M, Ciacci L, Consolo U, Balli F, Cossarizza A. Mitochondrial alterations and tendency to apoptosis in peripheral blood cells from children with Down syndrome. FEBS letters 581(2007): 521-525.

Russell LK, Mansfield CM, Lehman JJ, Kovacs A, Courtois M, Saffitz JE, Medeiros DM, Valencik ML, McDonald JA, Kelly DP. Cardiac-Specific Induction of the Transcriptional Coactivator Peroxisome Proliferator-Activated Receptor γ Coactivator-1α Promotes Mitochondrial Biogenesis and Reversible Cardiomyopathy in a Developmental Stage-Dependent Manner. Circ Res 2004; 94:525-533.

Sago H, Carlson EJ, Smith DJ, Kilbridge J, Rubin EM, Mobley WC, Epstein CJ, Huang TT. Ts1Cje, a partial trisomy 16 mouse model for Down syndrome, exhibits learning and behavioral abnormalities. Proc Natl Acad Sci USA. 1998 May 26;95(11):6256-61.

Santel A and Fuller MT. Control of mitochondrial morphology by a human mitofusin. J Cell Sci 2001. 114: 867–874

Schuchmann S and Heinemann U. Increased mitochondrial superoxide generation in neurons from trisomy 16 mice: a model of Down's syndrome. Free Radic Biol Med. 2000 Jan 15; 28(2):235-50.

Scorrano L, Ashiya M, Buttle K, Weiler S, Oakes SA, Mannella CA, Korsmeyer SJ. A distinct pathway remodels mitochondrial cristae and mobilizes cytochrome c during apoptosis. Dev Cell. 2002 Jan; 2(1):55-67.

Shapiro BL. Whither Down syndrome critical regions? Hum Genet 1997, 99(3):421-423.

Shinohara T, Tomizuka K, Miyabara S, Takehara S, Kazuki Y, Inoue J, Katoh M, Nakane H, Iino A, Ohguma A, Ikegami S, Inokuchi K, Ishida I, Reeves RH, Oshimura M. Mice containing a human chromosome 21 model behavioral

impairment and cardiac anomalies of Down's syndrome. Hum Mol Genet 2001, 10, 1163–1175.

Shukkur EA, Shimohata A, Akagi T, Yu W, Yamaguchi M, Murayama M, Chui D, Takeuchi T, Amano K, Subramhanya KH, Hashikawa T, Sago H, Epstein CJ, Takashima A and Yamakawa K. Mitochondrial dysfunction and tau hyperphosphorylation in Ts1Cje, a mouse model for Down syndrome. Hum Mol Genet 2006, 15(18):2752-2762.

Siddiqui MM and Atala A. Amniotic fluid-derived pluripotential cells: adult and fetal. In Handbook of Stem Cells, Vol. 2. (eds. R. Lanza et al.) 175–180, (Elsevier Academic Press, Amsterdam, 2004).

Siegel N, Rosner M, Hanneder M, Valli A, Hengstschläger M. Stem Cells in Amniotic Fluid as New Tools to Study Human Genetic Diseases. Stem Cell Rev (2007) 3:256–264

Smeitink J, Heuvel L and DiMauro S. The genetics and pathology of oxidative phosphorylation. Nature reviews Genetics 2001; 2:342-352

Sommer CA and Henrique-Silva F. Trisomy 21 and Down syndrome Braz. J. Biol. 2008; 68(2): 447-452, 449.

Weibel ER, Kistler GS, Scherle WF. Practical stereological methods for morphometric cytology. J Cell Biol. 1966 Jul;30(1):23-38.

Wu Z, Puigserver P, Andersson U, Zhang C, Adelmant G, Mootha V, Troy A, Cinti S, Lowell B, Scarpulla R and Spiegelman BM. Mechanisms controlling mitochondrial biogenesis and respiration trhough the termogenic coactivator PGC-1. Cell 1999; 98(1): 115-24.

Yu T, Li Z, Jia Z, Clapcote SJ, Liu C, Li S, Asrar S, Pao A, Chen R, Fan N, Carattini-Rivera S, Bechard AR, Spring S, Henkelman RM, Stoica G, Matsui S-I, Nowak NJ, Roder JC, Chen C, Bradley A and Yu YE. A mouse model of Down syndrome trisomic for all human chromosome 21 syntenic regions. Hum Mol Genet 2010, 19(14):2780-2791

Gene Expression Profile in Liver Transplantation and the Influence of Gene Dysregulation Occurring in Deceased Donor Grafts

Anna Conti[1,†], Simona Scala[2,†], Marina Romano[2,3], Antonella Izzo[1], Floriana Fabbrini[1], Floriana Della Ragione[4], Maurizio D'Esposito[4], Lucio Nitsch[1], Fulvio Calise[2,3] and Antonio Faiella[*,2]

[1]*Department of Cellular and Molecular Biology and Pathology, Federico II University, Naples, Italy*

[2]*Center of Biotechnology, "Antonio Cardarelli" Hospital, Padiglione "Y", Via A. Cardarelli, 9, 80131 Naples, Italy*

[3]*Liver Transplantation Unit, "Antonio Cardarelli" Hospital, Padiglione "Y", Via A. Cardarelli, 9, 80131 Naples, Italy*

[4]*Institute of Genetics and Biophysics, "National Research Council" Naples, Italy*

Abstract: *Background*: Brain dead patients are the main source of organs for transplants. Brain death causes changes in peripheral organs. We define modifications of gene expression in specific pathways occurring in donor livers and their influence on gene expression profile of livers after transplant.

Methods: We compared gene expression profile of both deceased donor livers and transplanted livers to gene expression data of liver tissue, retrieved from Array Express database, used as control. All expression data were obtained by microarray analysis.

Results: The expression of about 33,000 genes has been compared in liver samples from three groups: deceased donor livers, transplanted livers two hours after reperfusion, and control livers. We found that about 900 genes are dysregulated in deceased donor versus control livers. Up-regulated genes are mainly involved in apoptosis, immune response and inflammation. Down-regulated genes are mostly involved in metabolism and electron transport. We also re-evaluated a group of genes that in a previous study were found dysregulated in transplanted livers when compared to donor livers. Most of these genes, but not all, were dysregulated also when compared to control livers. Moreover 317 additional genes, dysregulated after liver transplant, were identified in this study; they were undetectable in the previous study because. They had the same dysregulation both in donor and in transplanted livers.

Conclusions: Understanding molecular mechanisms that in the donor compromise graft function is crucial in order to discriminate between basal graft damages and ischemia-reperfusion injuries and therefore to identify therapeutic targets aiming to improve liver transplantation performances.

Keywords: Liver transplantation, brain death, gene expression profiling, ischemia/reperfusion injury.

INTRODUCTION

Organs from brain dead donors are the main source for solid organ transplantation. Brain death (BD) is a complex physiological event, defined as an irreversible injury of cerebrum, cerebellum and brain stem and is associated with severe hemodynamic changes, coagulopathies, pulmonary changes, hypothermia and electrolyte imbalances. Hemodynamic instability associated with brain death can contribute to deterioration of peripheral organs. These changes may predispose the graft to increasing ischemia reperfusion injury (IRI) damages during the transplant process, accelerating organ rejection after transplantation [1]. The hemodynamic instability is well recognized as 'autonomic storm', an initial period of excessive parasympathetic activity, which is immediately followed by a sympathetic activation with high plasma levels of catecholamines, extreme arterial hypertension and tachycardia. During these phases, potential donor grafts undergo a transient period of ischemia [2]. Shock and oxidative injury during the intensive care treatment of the potential donor, followed by brain death, should be regarded as a major risk factor affecting organ viability, post-transplant function and graft survival in organ transplantation, in addition to unavoidable IRI during transplantation procedures. Donor's brain death might cause and promote organ injury altering the immunological and inflammatory status of the graft, increasing both the sensitivity of the organs towards preservation injury and acute rejection following transplantation. Despite this correlation has been experimentally shown, no clinical trials support so far this hypothesis [2].

In a previous study [3] we have compared gene expression levels in transplanted livers, soon after reperfusion, versus basal gene expression levels, before liver retrieval from the donor. About 800 genes were found dysregulated after transplantation, but we have not analyzed the potential effects of brain death on the gene expression variations.

*Address correspondence to this author at the Center of Biotechnology "Antonio Cardarelli" Hospital, Padiglione "Y", Via A. Cardarelli, 9, 80131 Naples, Italy; Tel: (+39) 39 39 130 130; Fax: +39 081 747 34 33;
E-mail: antonio.faiella@aocardarelli.it
†Both authors contributed equally to this work

1874-3005/10 2010 Bentham Open

A very recent study [4] compares gene expression patterns of transplanted livers from living donors with transplanted livers from deceased donors, defining molecular signature of both. The authors focus their attention to the pathways, which show dysregulation in the transplant process both in livers from living donors and from deceased donors; however they do not analyze the basal differences between the grafts from the two groups of donors.

The aim of the present study was to systematically define alterations of gene expression and impairment of specific pathways induced in deceased donor livers when compared to control livers. Based on these alterations an accurate analysis of genes dysregulated in transplanted livers versus control livers was carried out, in order to discriminate between transcriptional changes, due to ischemia reperfusion injuries, and variations possibly caused by brain death and other donor conditions.

We have compared gene expression profile of both deceased donor livers (DL) and transplanted livers (TL) to gene expression data of liver tissue, retrieved from Array Express database, used as control (CL) [3, 5]. This control was a set of livers from sudden death individuals without previous agonal state. Literature data demonstrate that the integrity of mRNA is scarcely affected by sudden death without agonal state. In contrast agonal state preceding death has a substantial effect on gene expression [6, 7]. A very large amount of research studies have been conducted on deceased tissues and also information included in all the databases reporting normal gene expression throughout the tissues [8] is derived from autoptic studies.

The expression of about 900 genes was found dysregulated in DL if compared to controls. This wide gene expression modification clearly affects gene regulation in TL.

The data reported in the present study give new insight to clarify the consequences of brain death and intensive care injuries on the human orthotopic liver transplantation by a molecular point of view, and help us to recognize new therapeutic targets useful to improve orthotopic liver transplantation (OLT) performance.

MATERIALS AND METHODOLOGY

Experimental Design

Gene expression profile of samples from DL and TL was compared to gene expression profile of samples from CL. The choice of sample size was performed by running p-values of expression data comparisons among groups through the PowerAtlas software [9, 10]. We selected a sample size of '5' per group to obtain an Expected Discovery Rate (EDR) > 40% (63%) and a True Positive Probability (TP) > 80% (98%) (Supplementary file **1**).

Then, five biological replicates per condition were analyzed. All expression data (DL, TL and CL) were obtained by microarray analysis, using Affymetrix gene chip HG-U133 Plus 2. Hybridization data were normalized and quantified using Robust Multiarray Analysis (RMA) software [11]. DL and TL samples were collected as previously described [3]. Briefly, 10 liver biopsies were analyzed: 5 biopsies, from the donors, collected before explantation (DL group); 5 biopsies from the transplant recipients (TL group), collected 2-3 hours after liver reperfusion. Donors were classified as 'standard' according to the criteria of the 'Italian National Transplantation Center'. Particularly, the donors' age ranged from 38 to 83 years, no hypotension, steatosis always less than 15%. Mean cold ischemia time was 8 hours (ranging from seven to ten hours), mean warm ischemia 45 min, mean hospitalization in intensive care unit was 5 days [3]. Expression data of livers, from five healthy individuals who suffered sudden death, were retrieved from Array Express database (SAMPLE ID: E-AFMX-11) [5, 12] and used as control samples. All individuals, 3 males and 2 females, suffered sudden death for reason other than their participation to the study and without any relation to the tissues used. Age was ranging from 27 to 29 and was unknown in 2 cases. Total RNAs, isolated from 200 mg of frozen tissues using the Trizol reagent, were of high and comparable quality as gauged by the ratio of 28S to 18S ribosomal RNAs estimated using the Agilent 2100 Bioanalyzer (range 1.4-1.6) [12].

In order to validate the use of deceased tissues as controls, we compared our results to a set of expression data from microarray analysis (same technology and experimental conditions) of six liver biopsies from living donors, available very recently from GEO repository [4, 13] (Supplementary file **2**).

RNA Extraction, Data Acquisition and Analysis

DL and TL samples were treated as previously described [3]. Array data have been deposited in GEO data base with accession number GSE14951 [14]. Expression data were pre-filtered to reduce noise and discard 'unreliable' genes using the Cross-Gene error model [14]. The analysis of functional clusters was performed on lists of differentially expressed genes for both Gene Ontology (GO) categories and biological pathways. GO functional class scoring was performed using the web-based GOTM software [15, 16] which visualizes differential expressed genes in the GO context, considering as gene sets all the GO categories for biological processes, molecular functions and cellular components. The list of differentially expressed genes was compared to the complete list of genes spotted on Affymetrix HG-U133 Plus 2 chip, in order to identify GO categories of genes significantly ($p < 0.01$) more represented in the list of differentially expressed genes than in the reference gene set.

Real-Time Quantitative PCR

Expression values of 26 genes chosen among the most dysregulated genes were checked by RT-PCR. The same batch of total mRNA was used for both microarray and validation experiments in DL and TL. RNAs, from five liver tissue obtained during resection of benign focal lesions, were used as controls in RT-PCR experiments. Two biopsies came from liver resections of two females (24 and 26 aged) suffering by hepatocellular adenoma. Two biopsies came from liver resections of giant hepatic cystis from two male aged respectively 39 and 43. The last biopsy came from a liver of a male suffering by liver hemangioma. cDNA was synthesized Real Time PCR were performed as previously described [3]. PCR reactions were performed in triplicate. The primers (Primm Biotech Products and Services, Milan -

Table 1. Primer Pairs Used for Real-Time Quantitative PCR

Probe Set	Gene Name	Ensembl Gene ID	Left Primer	Right Primer
205364_at	ACOX2	ENSG00000168306	CGGAGTCTTCAGGACCACAC	GCAGGAAGCCATTGTCTGTT
231587_at	APOC3	ENSG00000110245	CAGCCCCGGGTACTCCTT	TTGGTGGCGTGCTTCATGTA
209186_at	ATP2A2	ENSG00000174437	TGAAACAGTTCATCCGCTACC	AATCAAAGCCTCGGGAAATC
228876_at	BAIAP2L2	ENSG00000128298	AGAACGTGCGGGAGATGAAG	CAGACACGAAGGCCTGCAT
212952_at	CALR	ENSG00000179218	CCTGAGTACAAGGGTGAGTGGAA	GCCCAGCACGCCAAAGT
204093_at	CCNH	ENST00000256897	CAGAAGTTGGAGCGATGTCA	GTCCATTCTTCCTCCTCATGTT
220046_s_at	CCNL1	ENSG00000163660	GAACTCCAGCCCTTTCAACC	TTGGTGATTTCTCTTCAGCTTTT
228766_at	CD36	ENSG00000135218	GCTGAGGACAACACAGTCTCTTTC	AGCCTCTGTTCCAACTGATAGTGA
213279_at	DHRS1	ENSG00000157379	TGGCCGTGGCATTGC	AGATGGCGGCCAGTGATG
1555612_s_at	G6PC	ENSG00000131482	TCCGTCAGTGTCATCCCCTACT	CCGAAGACTCCACATCTCTTACAA
210328_at	GNMT	ENSG00000124713	ATCATCGCAACTACGACCACAT	GTCCTTGGTCAAGTCACTCTTATAGTAGAT
215554_at	GPLD1	ENSG00000112293	GGGACCAGTGACTGCAACCT	GCCCTGGGTGTGGTTTTG
241945_at	HECTD1	ENSG00000092148	ACTAATGCCACGAACAACATGAAT	TGATGTAGTACCAGGTGTGGTCAA
201466_s_at	JUN	ENSG00000177606	AGAAAGTCATGAACCACGTTAACAGT	CCCCCGACGGTCTCTCTT
205222_at	LBP	ENSG00000129988	CCGACTGACCACCAAGTCCTT	GGCACTGATCCCTGGAGTTC
203675_at	NUCB2	ENSG00000070081	GAAAAGGCAAGAAGTAGGAAGGTT	GTCAGGATTCAGGTGGTTTAGG
206278_at	PTAFR	ENSG00000169403	CCTGCCACTTTGGATTGTCTACT	GCCACGTTGCACAGGAATTT
210479_s_at	RORA	ENSG00000069667	TCATTCTCCACCCAGCTGTTG	CTGTGCTTTGCCCCAGTGTA
222226_at	SAA3P	ENSG00000166787	GCCAGGCTACCAACAAATGG	GCAGATTGAAAAGGAAGCTCAGTAT
213874_at	SERPINA4	ENSG00000100665	TCAAAGCCCTGTGGGAGAAA	CGGACTGTTGTGTTCTCATCAAC
222705_s_at	SLC25A15	ENSG00000102743	CAGCCGCCGGTTCCTT	ACACTGTATTCTGGCTCTTGGCTAT
215223_s_at	SOD2	ENSG00000112096	TGGTGGTGGTCATATCAATCA	GCCGTCAGCTTCTCCTTAAA
217040_x_at	SOX15	ENSG00000129194	CAGCGGATTTTGCATTCGA	GCTTAAACCGGAGCCTTTGC
207306_at	TCF15	ENSG00000125878	CCAGAGGGTATGTGTTGAAAAGTCT	CCCTAGGCTGCTTGCAGAGA
201042_at	TGM2	ENSG00000198959	CTTTGACGTCTTTGCCCACAT	CGGTGCGGGCACAGA
239818_x_at	TRIB1	ENSG00000173334	GGGCGCTGTGCATCCA	AAGGCCTGATTTTGTCCTGGTA

Italy) used for amplification are listed in Table **1**. Primer pairs were designed using the Primer 3 software [17] in order to obtain amplicons ranging from 100 and 150 bp, and specifically designed to span introns or cross intron/exon boundaries. Data normalization was performed using *GAPDH* as housekeeping gene [18]. Experiments were performed twice, in triplicate. The amplification protocol was: 1 cycle of 10 min at 95 °C, 40 cycles of 95 °C for 15 sec, 58-60 °C for 20 sec, 72 °C for 20 sec, plus an extension at 72 °C for 3 min. The relative expression value was calculated with the formula 2^{DDct}

Statistics

Expression data from different groups were compared using the ANOVA test, with Benjamini and Hochberg false discovery rate as multiple testing corrections. Statistical significance was established at $p < 0.01$. Genes were considered differentially expressed with a fold change > 1.5 between two conditions. Gene sets were considered enriched with a $p < 0.01$ when compared to the reference gene list.

Liver biopsies were collected in different hospitals, including the "Liver Transplantation Center" of the "Cardarelli Hospital". All biopsies were obtained with informed consent given according to protocols approved by the Institutional Ethics Committee of the "Antonio Cardarelli Hospital."

RESULTS

The expression of about 33,000 genes, represented on the Affymetrix chip HG-U133 Plus 2, has been evaluated in liver samples from three groups: DL, TL 2 hours after reperfusion, and CL. The groups were compared each other for gene expression. Expression of about 900 genes was dysregulated in DL compared to control ones. Table **2** shows the 40 most up-regulated and the 40 most down-regulated genes. Table **3a** and Table **3b** report the distribution of the dys-

Table 2. The Most up- and Down-Regulated Genes in DL Group *vs*. CL Group

Up-Regulated Genes		Down-Regulated Genes	
Gene Name	**Fold Change**	**Gene Name**	**Fold Change**
SPINK1	95.29	LOC283130	0.0555
APOC3	9.516	MALAT-1	0.0612
RPS11	8.807	TF	0.084
SOD2	7.177	KCNN2	0.0927
PLEKHG5	6.343	ID2	0.106
LOC440836	6.052	H19	0.112
ATP2A2	5.483	CAT	0.116
APOA1	5.461	GNMT	0.117
TOMM40	5.194	G6PC	0.13
SAP30L	5.043	CD36	0.131
TMEFF2	5.042	RORA	0.135
APOC2	4.937	C8orf4	0.139
TMEM151	4.83	SLC6A1	0.145
RBP4	4.765	HECTD1	0.146
C9ORF44	4.72	KIAA0293	0.155
FAM84A	4.72	C6orf71	0.159
SLC39A8	4.689	GPLD1	0.164
LTB4R2	4.59	TRIB1	0.168
RP3-402G11.12	4.375	DKFZP586A0522	0.176
RPS19	4.354	MBNL2	0.177
PTAFR	4.323	SERPINA4	0.185
TCF15	4.236	FGD4	0.186
FTL	4.157	CYP3A5	0.19
LBP	4.083	CYP3A4	0.195
SAA3P	4.069	DHRS1	0.195
TGM2	4.062	C10orf65	0.202
BAIAP2L2	4.039	SLC25A15	0.203
SOX15	3.996	JUN	0.204
DLG4	3.995	RCL1	0.204
SLC35C1	3.919	ZGPAT	0.204
ELMOD2	3.911	DSIPI	0.207
DDX54	3.9	KLF6	0.209
AMBP	3.876	CYP26A1	0.21
SCUBE1	3.874	NDUFS1	0.213
SFXN4	3.865	AASS	0.218
TAOK2	3.782	CYP4A11	0.218
VWA1	3.779	TMEM16A	0.22
SRCRB4D	3.744	BAAT	0.221
ATF5	3.709	HGD	0.221
BBC3	3.678	PSMAL	0.232

Table 3a. Enriched GO Categories of Genes Up-Regulated in Donor Livers *versus* Controls

List Name	Description	Total Probes	Expected By Chance	Actual	Enrichment	P-Value
Regulation of JNK cascade	Any process that modulates the frequency, rate or extent of signal transduction mediated by the JNK cascade	37	1.06	8	7.51	0.00000859
DNA damage response, signal transduction by p53 class mediator	A cascade of processes induced by the cell cycle regulator phosphoprotein p53, or an equivalent protein, in response to the detection of DNA damage	44	1.27	8	6.32	0.00003298
DNA damage response, signal transduction resulting in induction of apoptosis	A cascade of processes initiated by the detection of DNA damage and resulting in the induction of apoptosis (programmed cell death)	48	1.38	7	5.07	0.00042682
Regulation of binding	Any process that modulates the frequency, rate or extent of binding, the selective interaction of a molecule with one or more specific sites on another molecule	59	1.70	7	4.12	0.00150276
Stress-activated protein kinase signaling pathway	A series of molecular signals in which a stress-activated protein kinase (SAPK) cascade relays one or more of the signals	136	3.91	15	3.83	0.00000995
JNK cascade	A cascade of protein kinase activities, culminating in the phosphorylation and activation of a member of the JUN kinase subfamily of stress-activated protein kinases	130	3.74	14	3.74	0.00002546
DNA damage response, signal transduction	A cascade of processes induced by the detection of DNA damage within a cell	115	3.31	12	3.63	0.00012753
Induction of apoptosis by intracellular signals	Any process induced by intracellular signals that directly activates any of the steps required for cell death by apoptosis	82	2.36	8	3.39	0.00252772

Table 3b. Enriched GO Categories of Genes Down-Regulated in Donor Livers *versus* Controls

List Name	Description	Total Probes	Expected by Chance	Actual	Enrichment	p-Value
Heterocycle metabolic process	The chemical reactions and pathways involving heterocyclic compounds, those with a cyclic molecular structure and at least two different atoms in the ring (or rings)	146	3.93	17	4.33	0.00000050
Monocarboxylic acid metabolic process	The chemical reactions and pathways involving monocarboxylic acids, any organic acid containing one carboxyl (COOH) group or anion (COO-)	396	10.65	41	3.85	0.00000000
Fatty acid metabolic process	The chemical reactions and pathways involving fatty acids, aliphatic monocarboxylic acids liberated from naturally occurring fats and oils by hydrolysis	283	7.61	29	3.81	0.00000000
Aromatic compound metabolic process	The chemical reactions and pathways involving aromatic compounds, any organic compound characterized by one or more planar rings, each of which contains conjugated double bonds and delocalized pi electrons	211	5.68	20	3.52	0.00000142
Sterol metabolic process	The chemical reactions and pathways involving sterols, steroids with one or more hydroxyl groups and a hydrocarbon side-chain in the molecule	147	3.95	13	3.29	0.00018779
Electron transport	The transport of electrons from an electron donor to an electron acceptor	599	16.11	48	2.98	0.00000000
Alcohol metabolic process	The chemical reactions and pathways involving alcohols, any of a class of alkyl compounds containing a hydroxyl group	541	14.55	39	2.68	0.00000005
Glucose metabolic process	The chemical reactions and pathways involving glucose, the aldohexose gluco-hexose, D-glucose is dextrorotatory and is sometimes known as dextrose	195	5.25	14	2.67	0.00090344

regulated genes in GO biological process categories, showing that apoptosis and stress activated protein kinase activities are the most affected pathways by up-regulated genes (Table **3a**), whereas down-regulated genes are involved in metabolic pathways and electron transport (Table **3b**). At least 30 mitochondrial enzymes, involved in oxidative chain, are from 2 to 5 folds down-regulated, in deceased DL, if compared to CL (Table **4**). Comparison between TL and CL samples demonstrated that 855 genes were dysregulated in TL versus CL. Condition tree from hierarchical clustering of these genes (Fig. **1**) clearly shows that about 1/3 of these genes were already dysregulated in DL if compared to controls: 182 genes, (mainly involved in oxidoreductase, electron transport and metabolic activity), were already down-regulated in DL group versus CL group and 135 genes, (involved in inflammatory pathways and cell adhesion), were already up-regulated in DL group versus CL group.

In conclusion, the present study demonstrated that: 1) 900 genes were dysregulated in DL if compared to controls; 2) 855 genes were dysregulated in TL if compared to CL. At least 400 of these genes were already dysregulated in DL.

A comparison of expression data between biopsies of living donors and livers from sudden death individuals is shown in the supplemental section (Supplementary file **2**).

Briefly, even though 217 genes are differentially expressed with fold change >1.75 and $p<0.01$ between livers

Table 4. Oxidative Phosphorilation Genes Down-Regulated in Donor Livers *versus* Controls

Gene Name	Gene Bank	Description	Fold Change DL *vs*. CL
AASS	AK023446	aminoadipate-semialdehyde synthase	0.218
ACOX1	BF435852	acyl-Coenzyme A oxidase 1, palmitoyl	0.296
ACOX3	BF055171	acyl-Coenzyme A oxidase 3, pristanoyl	0.534
ALDH5A1	NM_001080	aldehyde dehydrogenase 5 family, member A1	0.336
CAT	AW015521	catalase	0.266
CHDH	AA609488	choline dehydrogenase	0.493
COX15	AF026850	COX15 homolog, cytochrome c oxidase assembly protein (yeast)	0.358
COX7A2L	NM_004718	cytochrome c oxidase subunit VIIa polypeptide 2 like	0.547
CYP26A1	NM_000783	cytochrome P450, family 26, subfamily A, polypeptide 1	0.21
CYP2B7	M29873	cytochrome P450, family 2, subfamily B, polypeptide 7 pseudogene	0.349
CYP3A4	AV650252	cytochrome P450, family 3, subfamily A, polypeptide 4	0.195
CYP3A43	NM_022820	cytochrome P450, family 3, subfamily A, polypeptide 43	0.305
CYP3A5	AW964006	cytochrome P450, family 3, subfamily A, polypeptide 5	0.19
CYP3A7	AF315325	cytochrome P450, family 3, subfamily A, polypeptide 7	0.297
CYP4A11	BC041158	cytochrome P450, family 4, subfamily A, polypeptide 11	0.218
DAO	NM_001917	D-amino-acid oxidase	0.499
FLJ22378	NM_025078	hypothetical protein FLJ22378	0.524
HAO2	NM_016527	hydroxyacid oxidase 2 (long chain)	0.322
IBRDC2	AI953847	IBR domain containing 2	0.502
IVD	NM_002225	isovaleryl Coenzyme A dehydrogenase	0.488
KMO	NM_003679	kynurenine 3-monooxygenase (kynurenine 3-hydroxylase)	0.291
NDUFA2	BC003674	NADH dehydrogenase (ubiquinone) 1 alpha subcomplex, 2, 8kDa	0.514
NDUFB7	NM_004146	NADH dehydrogenase (ubiquinone) 1 beta subcomplex, 7, 18kDa	0.376
NDUFB8	AA723057	NADH dehydrogenase (ubiquinone) 1 beta subcomplex, 8, 19kDa	0.455
NDUFV1	AF092131	NADH dehydrogenase (ubiquinone) flavoprotein 1, 51kDa	0.504
NISCH	NM_007184	nischarin	0.549
PAOX	AI743990	polyamine oxidase (exo-N4-amino)	0.523
PIPOX	AF136970	pipecolic acid oxidase	0.437
UQCRB	BC005230	ubiquinol-cytochrome c reductase binding protein	0.437
ZDHHC4	NM_018106	zinc finger, DHHC domain containing 4	0.556

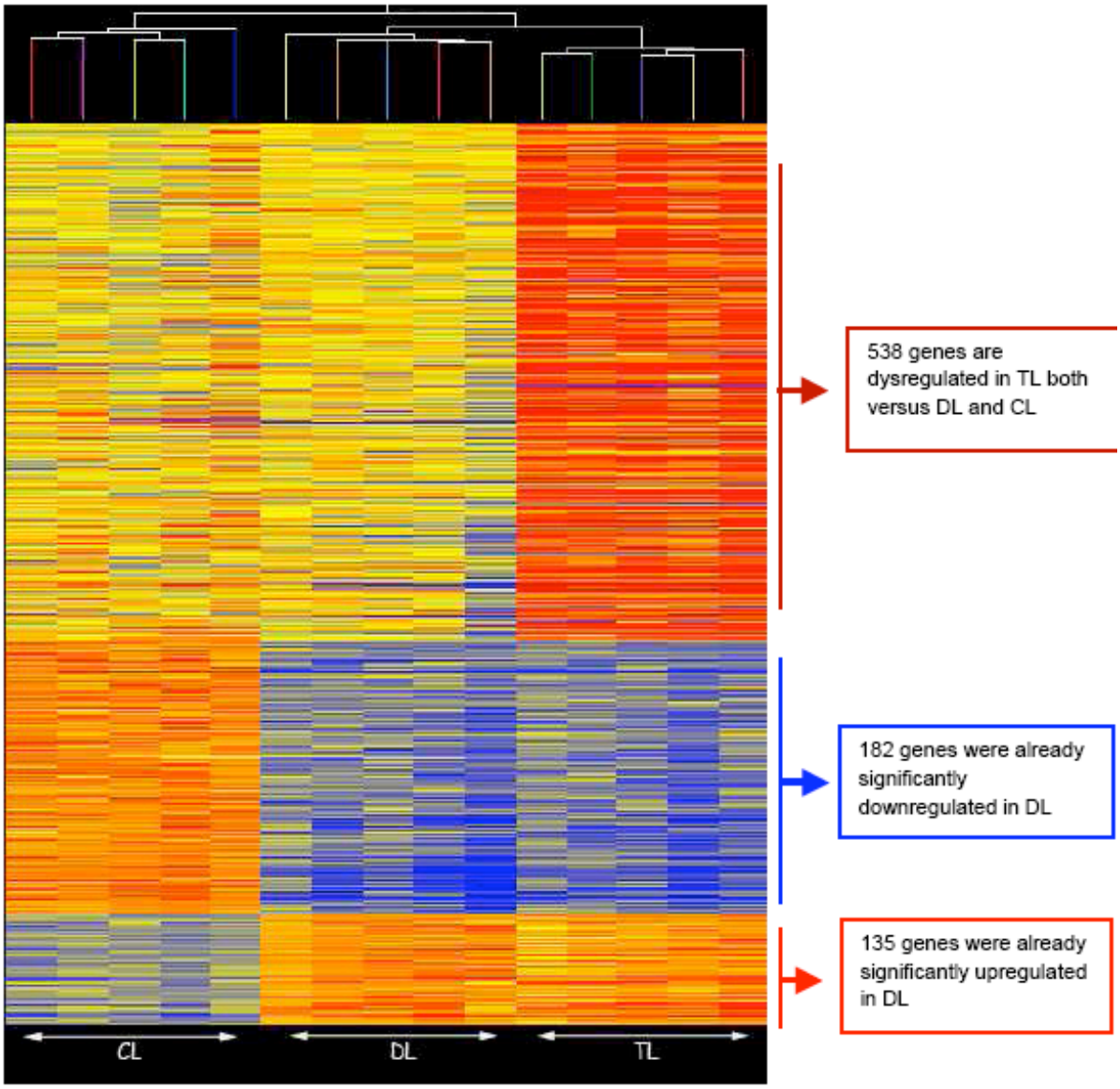

Fig. (1). Condition tree from hierarchical clustering of genes differentially expressed between TL and CL groups.

Samples from each group are well clustered together according to the expression level of these genes. The figure shows that many genes (in the lower part of the graphic), differentially expressed between TL and CL, were already dysregulated in the DL. Therefore their dysregulation might be due to brain death more than to ischemia/reperfusion injury. The genes in the upper part of the tree are dysregulated only in TL group both versus CL and DL samples.

Genes were considered differentially expressed with $p < 0.01$ using ANOVA test with Benjamini and Hochberg false discovery rate correction.

CL=Control livers, DL=Donor livers, TL=Transplanted livers.

from living donors and livers from deceased subjects (CL) only 54 (63 probe sets) out of these genes are included in the set of 900 genes we found differentially expressed in DL *vs*. CL.

Quantitative RT-PCR analysis of 26 genes, chosen among the most dysregulated genes, was carried out in order to validate the results of microarray analysis. The RT-PCR experiments confirm the microarray data for these genes. Correlation between quantitative RT-PCR and microarray data was satisfactory for all the tested genes ($r > 0.85$) (Table **5**).

DISCUSSION

Clinical studies on humans have shown that allograft from unrelated living donors have better graft function and survival than allograft from deceased donors [19-21]. This difference could be attributed to the pathophysiological changes derived from brain death and donor condition more than to the influence of cold ischemia times [22-24].

In this study we have demonstrated that brain death, together with other factors related to donor condition (shock, intensive care treatment, parenteral nutrition, etc.) causes the dysregulation of at least 900 genes in human liver tissue. The

Table 5. Comparison between Quantitative Real Time PCR and Microarray Data

Probe Set	Gene Name	Microarray Fold Change DL/CL	RT Fold Change DL/CL
205364_at	ACOX2 acyl-Coenzyme A oxidase 2	0.27	0.27
231587_at	APOC3 apolipoprotein C-III	9.51	14.25
209186_at	ATP2A2 ATPase, Ca++ transporting	5.48	1.90
228876_at	BAIAP2L2 BAI1-associated protein 2-like 2	4.04	3.50
212952_at	CALR calreticulin	9.41	21.75
204093_at	CCNH cyclin H	1.06	0.90
220046_s_at	CCNL1 cyclin L1	0.47	0.30
228766_at	CD36 CD36 molecule	0.13	0.25
213279_at	DHRS1 dehydrogenase/reductase	0.20	0.28
1555612_s_at	G6PC glucose-6-phosphatase	0.13	0.08
210328_at	GNMT glycine N-methyltransferase	0.12	0.30
215554_at	GPLD1 glycerol-3-phosphate dehydrogenase 1	0.16	0.28
241945_at	HECTD1 HECT domain-containing 1	0.15	0.34
201466_s_at	JUN jun oncogene	0.20	0.18
205222_at	LBP lipopolysaccharide binding protein	4.08	6.55
203675_at	NUCB2 nucleobindin 2	3.95	3.90
206278_at	PTAFR platelet-activating factor receptor	4.32	7.80
210479_s_at	RORA RAR-related orphan receptor A	0.14	0.33
222226_at	SAA3P serum amyloid A3 pseudogene	4.07	6.05
213874_at	SERPINA4 serpin peptidase inhibitor	0.19	0.20
222705_s_at	SLC25A15 solute carrier family 25	0.20	0.65
215223_s_at	SOD2 superoxide dismutase 2	2.04	2.40
217040_x_at	SOX15SRY (sex determining region Y)-box 15	4.00	5.50
207306_at	TCF15 transcription factor 15 (basic helix-loop-helix)	4.24	7.45
201042_at	TGM2 transglutaminase 2 (C polypeptide, protein-glutamine-gamma-glutamyltransferase)	4.06	4.65
239818_x_at	TRIB1 Tribless homolog 1 (Drosophila m.)	0.17	0.10

validation study (Supplementary file 2) demonstrates that 54 of them (6/%) might be affected by the choice of deceased tissues, as they are already dysregulated between CL and living donor tissues. Subtraction of these genes from the set of 900 genes does not affect at all the following considerations about injuries occurring in donor livers. Up-regulated genes are mainly involved in immune response, cytoskeletal remodelling, inflammation, apoptosis and cell adhesion. Down-regulated genes are mostly involved in mitochondrial activities and metabolism, being members of metabolic pathways of aminoacids, such as Gly, Ser and Cys, fatty acids (*HNF4alpha*) and vitamins. Metabolism might be also affected by starvation and stress, due to a long stay in intensive care unit. Molecular and cellular alterations triggered by brain death itself may significantly alter both early and long-term results of transplantation if compared to organs harvested from living donors [25].

Apoptosis induction and increased expression of apoptosis related proteins were observed in hepatocytes from brain dead animals [26]. A recent study on molecular changes induced in the heart by brain death [27], evaluates the variation in the expression levels of 5 genes involved in apoptotic processes: *BAX*, *BCL2*, *CASP3*, Cytochrome C (*CYCS*) and *FAS* and one gene induced by hypoxia (*HIF1A*) concluding that brain death mainly induces the expression of 3 out of these genes: *BAX*, *FAS* and *CASP3* involved in apoptosis activation. *HIF1A* is not significantly induced, excluding hypoxic damages. Our results show that *BAX* and *FAS* are induced in liver samples from deceased donors. Moreover in our experiments the anti-apoptotic *BCL2* gene is induced much more than in the heart as like as *HIF1A*, indicating that hypoxic injuries are already present in DL.

Our study unraveled that in deceased DL at least 30 mitochondrial enzymes, involved in oxidative chain, are from 2 to 5 fold down-regulated if compared to CL (Table **4**). It is known that during ischemia oxidative phosphorylation and ATP level decrease producing ischemic damage. The

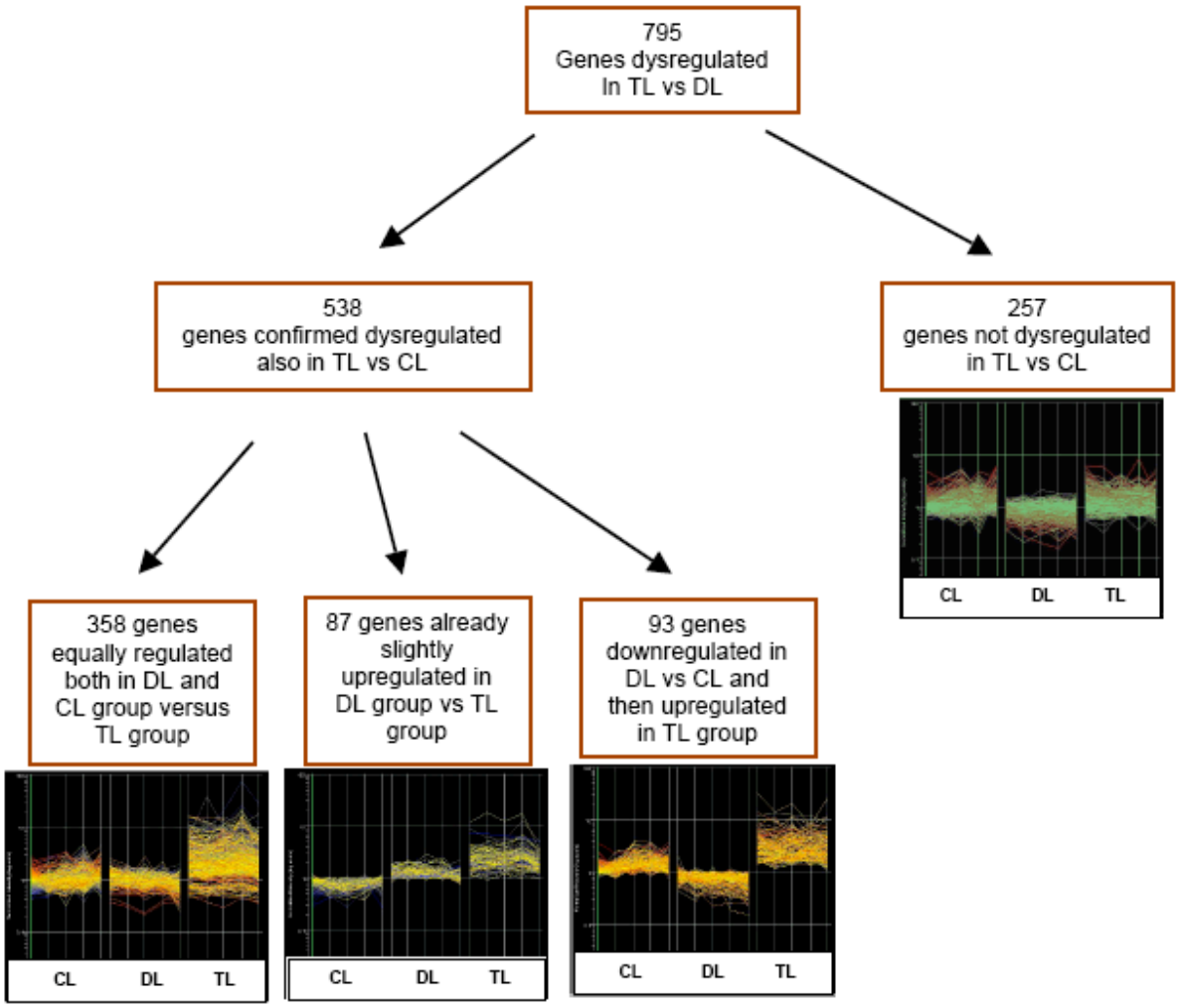

Fig. (2). Expression profiles of 795 genes previously found dysregulated in livers after transplant.

The figure shows on the left the expression profiles of 538 genes found dysregulated in a previous study, in TL *versus* DL, and now confirmed as dysregulated in TL if compared to CL. Detailed analysis of these genes, dysregulated both *versus* DL and CL, shows three different behaviors:

- 358 genes were normoregulated between DL and CL groups;

- 87 genes were already slightly up-regulated in DL group.

- 93 genes were down-regulated in DL group versus CL group and highly up-regulated after transplantation in TL group.

On the right side of the figure are shown expression profiles of 257 genes dysregulated in TL *versus* DL, but not confirmed as dysregulated in TL when compared to CL.

Genes were considered differentially expressed with $p < 0.01$ using ANOVA test with Benjamini and Hochberg false discovery rate correction.

CL=Control livers, DL=Donor livers, TL=Transplanted livers.

situation might be deeply compromised if the expression of oxidative enzymes is down-regulated.

A detailed analysis of 795 genes previously found dysregulated in TL when compared to DL [3], in the new perspective of the comparison between transplanted and control liver tissues shows that about 250 genes, mainly involved in angiogenesis, lipid metabolism, growth, cell cycle, were not confirmed as dysregulated in our study when compared to CL (Fig. **2**). For these genes we hypothesize that their dysregulation is due to events related to brain death instead of IRI. However many genes reported as dysregulated in the previous study are dysregulated even when TL are compared to CL: 87 of them were already slightly up-regulated in DL group. These genes are mainly apoptotic regulators, proteolytic enzymes, chemokines, cytokines and stress responsive genes. Ninetythree more genes, down-regulated in DL, are essentially involved in growth, angiogenesis, mitosis initiation, cell cycle regulation and metabolism. We demonstrate that c-*FOS* and *c-JUN* are down-regulated by brain death causing inhibition of cell proliferation and *VEGF* signaling (angiogenesis). This might explain the better graft function and survival of allograft from living donors if compared to

Table 6. 15 Out of 78 Genes Predictive for IPGF, Already Dysregulated in Donor Livers *versus* Controls

Gene Name	Gene Bank	Description	Fold Change DL *vs.* CL
SOD2	R34841	Superoxide dismutase 2, mitochondrial	7.177
FCAMR	AW028140	FKSG87 protein	2.332
STCH	NM_006948	Stress 70 protein chaperone, microsome-associated, 60kDa	2.161
SOD2	BF575213	Superoxide dismutase 2, mitochondrial	1.898
ADAMTS1	AF060152	A disintegrin-like and metalloprotease with thrombospondin type 1 motif, 1	1.892
VNN2	NM_004665	Vanin 2	1.874
OSGIN2	BC031054	Chromosome 8 open reading frame 1	1.807
RAB31	BF510937	Homo sapiens transcribed sequences	1.802
IL-7	NM_000880	Interleukin 7	1.708
FLJ22684	NM_025048	Hypothetical protein FLJ22684	1.635
IFI16	AF208043	Interferon, gamma-inducible protein 16	1.62
NCOA7	AL035689	Nuclear receptor coactivator 7	1.564
LCP1	AW205969	Homo sapiens transcribed sequences	1.54
MAP4K4	NM_017792	Hypothetical protein FLJ20373	0.528
BAAT	NM_001701	Bile acid Coenzyme A: amino acid N-acyltransferase	0.221

deceased donors. All these genes are very highly up-regulated after transplantation and reperfusion.

In addition to the genes already found dysregulated in the previous study and confirmed in this study, we found 317 additional genes differentially expressed between TL and CL (Fig. **1**); these genes were not detected in our previous study [3] because they were already dysregulated in DL, therefore no differences between DL and TL group were detectable. In detail, 135 genes were equally up-regulated in DL and TL group versus controls. They are mainly anti-apoptotic genes, *NFKB* subunits, *BCL2*, *BCLXL*, cell adhesion molecules. 182 genes were equally down-regulated in DL and TL group versus controls. Most of them are involved in fatty acid, glucose and aminoacid metabolism and electron transport activities. Thus, inflammatory processes and oxidative phosphorylation activities are impaired in the liver since the pre-explant period, and continue to be impaired after transplant and reperfusion.

Functional analysis of the remaining genes dysregulated in TL group versus CL group completely confirms the results of our previous study [3]. Many authors agree with the idea that understanding molecular bases of graft failure is crucial to identify therapeutic targets able to improve transplant performance [28]. In this respect, a recent study identifies 78 classifier genes whose dysregulation after liver transplantation is able to predict initial poor graft function (IPGF) [29]. Our study demonstrated that 15 of these genes resulted already dysregulated in DL (Table **6**); molecular pathways involved in IPGF might be compromised before the organ is explanted and preventing these mechanisms in the donors possibly results in better graft function.

Recently De Jonge *et al.* [4] have been carried out in human OLT a study which analyzes the differential gene expression between donor baseline biopsies and post-reperfusion biopsies in two groups of liver transplantations: from living donors and from deceased donors. The authors find a large number of genes differentially expressed in both graft types following reperfusion when compared to the pre biopsies, more in the living transplant than in the deceased one. Among the group of genes differentially expressed in post-reperfusion biopsies of both groups they find a significant up-regulation of genes involved in inflammatory and immune processes, both in deceased and in living donor grafts.

CONCLUSIONS

Brain death and intensive care injuries induce stress in DL, affecting liver gene transcriptional profile both in donors and in recipients, and many genes dysregulated in TL *versus* CL are already dysregulated in DL before transplantation. On these bases we hypothesize that the dysregulation of these genes, mainly involved in inflammatory pathways, cell adhesion and electron transport, might affect graft function and organ survival in OLT. The insight of these mechanisms is crucial for the identification of therapeutic targets, aiming to improve OLT performances.

ACKNOWLEDGEMENT

The authors thank R.A. Chamuleau (Academic Medical Center, University of Amsterdam, The Netherlands) for helpful comments and suggestions and A. Ceriello and V. Scuderi (Liver Transplantation Unit, "Antonio Cardarelli" Hospital - Naples, Italy) for their precious surgical assistance. This work has been supported by grants from "*Alto Comitato per i Trapianti Regione Campania"*.

ABBREVIATIONS

BD = Brain death

CL = Control Livers

DL = Donor livers

EDR = Expected Discovery Rate

GO = Gene Ontology

IRI = Ischemia Reperfusion Injury

OLT = Orthotopic Liver Transplantation

RMA = Robust Multiarray Analysis

TL = Transplanted Livers

SUPPLEMENTARY MATERIAL

Supplementary material is available on the publishers Web site along with the published article.

REFERENCES

[1] Colombo G, Gatti S, Turcatti F, *et al.* Alteration in the transcriptional profile of livers from brain-dead organ donors. Transplantation 2006; 82: 69-79.

[2] Weiss S, Kotsch K, Francuski M, *et al.* Brain death activates donor organs and is associated with a worse I/R injury after liver transplantation. Am J Transplant 2007; 7: 1584-93.

[3] Conti A, Scala S, D'Agostino P, *et al.* Wide gene expression profiling of ischemia-reperfusion injury in human liver transplantation. Liver Transpl 2007; 13: 99-113.

[4] de Jonge J, Kurian S, Shaked A, *et al.* Unique early gene expression patterns in human adult-to-adult living donor liver grafts compared to deceased donor grafts. Am J Transplant 2009; 9: 758-72.

[5] Parkinson H, Kapushesky M, Kolesnikov N, *et al.* ArrayExpress update—from an archive of functional genomics experiments to the atlas of gene expression. Nucl Acids Res 2009; 37: 868-72.

[6] Franz H, Ulmann C, Becker A, *et al.* Systematic analysis of gene expression in human brains before and after death. Genome Biol 2005; 6: R112

[7] Li JZ, Vawter MP, Walsh DM, *et al.* Systematic changes in gene expression in postmortem human brains associated with tissue pH and terminal medical conditions. Hum Mol Genet 2004; 13: 609-16.

[8] Wu C, Orozco C, Boyer J, *et al*. BioGPS: an extensible and customizable portal for querying and organizing gene annotation resources. Genome Biol 2009, 10: RI30.

[9] Gadbury GL, Garrett KA, Allison DB. Challenges and approaches to statistical design and inference in high-dimensional investigations. Methods Mol Biol 2009; 553: 181-206.

[10] Page GP, Edwards JW, Gadbury GL, *et al*. The PowerAtlas: a power and sample size atlas for microarray experimental design and research. BMC Bioinformatics 2006; 7: 84.

[11] Wu Z, Irizarry RA. Preprocessing of oligonucleotide array data. Nat Biotechnol 2004; 22: 656-8; author reply 658.

[12] Khaitovich P, Hellmann I, Enard W, *et al.* Parallel patterns of evolution in the genomes and transcriptomes of humans and chimpanzees. Science 2005; 309: 1850-4.

[13] Edgar R, Domrachev M, Lash AE. Gene Expression Omnibus: NCBI gene expression and hybridization array data repository. Nucleic Acids Res 2002; 30(1): 207-10.

[14] Rocke DM, Lorenzato S. A two component model for measurement error in analytical chemistry. Technometrics 1995; 37: 176-84.

[15] Zhang B, Kirov S, Snoddy J. WebGestalt: an integrated system for exploring gene sets in various biological contexts. Nucleic Acids Res 2005; 33: 741-8.

[16] Zhang B, Schmoyer D, Kirov S, Snoddy J. GOTree Machine (GOTM): a web-based platform for interpreting sets of interesting genes using Gene Ontology hierarchies. BMC Bioinformatics 2004; 5: 16.

[17] Rozen S, Skaletsky H. Primer3 on the WWW for general users and for biologist programmers. Methods Mol Biol 2000; 132: 365-86.

[18] Vandesompele J, De Preter K, Pattyn F, *et al.* Accurate normalization of real-time quantitative RT-PCR data by geometric averaging of multiple internal control genes. Genome Biol 2002; 3: 0034.1-11.

[19] U.S. department of health and human services: 2004 annual report of the U.S. organ procurement and transplantation network and the scientific registry of transplant recipients: Transplant data 1994-2003.

[20] Terasaki PI, Cecka JM, Gjertson DW, Takemoto S. High survival rates of kidney transplants from spousal and living unrelated donors. N Engl J Med 1995; 333: 333-6.

[21] Jassem W, Koo DD, Cerundolo L, Rela M, Heaton ND, Fuggle SV. Cadaveric versus living donor livers: differences in inflammatory markers after transplantation. Transplantation 2003; 76:1599-603.

[22] Boom H, Mallat MJ, de Fijter JW, Zwinderman AH, Paul LC. Delayed graft function influences renal function, but not survival. Kidney Int 2000; 58: 859-66.

[23] Koning OH, Ploeg RJ, van Bockel JH, *et al*. Risk factors for delayed graft function in cadaveric kidney transplantation: a prospective study of renal function and graft survival after preservation with University of Wisconsin solution in multi-organ donors. European Multicenter Study Group. Transplantation 1997; 63: 1620-8.

[24] Offermann G. What is a reasonably short cold ischemia time in kidney transplantation? Transplant Proc 1998; 30: 4291-3.

[25] Audibert G, Charpentier C, Seguin-Devaux C, *et al.* Improvement of donor myocardial function after treatment of autonomic storm during brain death. Transplantation 2006; 82: 1031-6.

[26] van Der Hoeven JA, Ter Horst GJ, Molema G, *et al.* Effects of brain death and hemodynamic status on function and immunological activation of the potential donor liver in the rat. Ann Surg 2000; 232: 804-13.

[27] Pérez López S, Vazquez Moreno N, Escudero Augusto D, *et al.* A molecular approach to apoptosis in the human heart during brain death. Transplantation 2008; 86: 977-82.

[28] Boutros T, Nantel A, Emadali A, *et al.* The MAP kinase phosphatase-1 MKP-1/DUSP1 is a regulator of human liver response to transplantation. Am J Transplant 2008; 8: 2558-68.

[29] Defamie V, Cursio R, Le Brigand K, *et al.* Gene expression profiling of human liver transplants identifies an early transcriptional signature associated with initial poor graft function. Am J Transplant 2008; 8: 1221-36.

Received: July 15, 2010 Revised: September 30, 2010 Accepted: December 16, 2010

Prenatal diagnosis of an inverted duplication of chromosome 5p arm with terminal deletion

Izzo A.[1], Genesio R. [1], Ronga V. [1], Nocera V. [1], Marullo L. [1], Cicatiello R. [1], Sglavo G. [2], Paladini D. [2], Conti A. [1] and Nitsch. L. [1]

1. Dept. of Cellular and Molecular Biology and Pathology

2. Dept. of Obstetric, Gynecologic and Pathophysiology of Reproduction

University of Naples "Federico II"

ABSTRACT

Objective

Partial or complete trisomies of short arm of chromosome 5 are rare chromosomal abnormalities. We report a prenatal case of trisomy 5p due to a de novo inverted duplication with subtelomeric deletion in a fetus with mild phenotype anomalies. The characterization of the present case and the correlation between genotype and phenotype might help to identify the critical region for more severe anomalies such as cardiopathy and cerebral anomalies described in large 5p duplications.

Methods

The diagnosis was made by standard and molecular cytogenetic techniques on fetal lymphocytes at 22 weeks of gestation following the discovery of ultrasonographic abnormalities. The fetus presented short femur, bilateral clubfoot, pielectasy, broad anterior fontanelle and facial dysmorphisms.

Results

Molecular cytogenetics investigations and CGH array revealed an inverted duplication of the short arm of chromosome 5 spanning from 5p13.1 to 5p15.33 with a 600kb deletion of 5pter.

Conclusions

The absence of heart and brain anomalies, that should be ultrasonographically evident at 22 weeks of gestation, suggests that the critical region for severe abnormalities in 5p arm is smaller than the region previously described including only a portion of 5p13.1 band.

INTRODUCTION

Trisomies of short arm of chromosome 5 are uncommon abnormalities. Less than 50 subjects with complete or partial duplications have been described in medical literature since 1964. For the majority of them, 5p duplications were generated from structural chromosomal rearrangements or were due to chromosome markers. Only three cases with inverted duplication of chromosome 5p with or without terminal deletion were described (Wang et al. 2008; Cervera et al. 1999; Sreekantaiah et al. 1999). The extension of both the duplicated and the deleted regions is different in size in all cases, including our case. On the contrary the phenotype features are very similar all over the cases. Since the first description of the trisomy 5p syndrome by Lejeune et al. in 1964, various clinical features associated with segmental aneusomy on chromosome 5p have been delineated (Avansino et al. 1999, Velagaleti et al. 2000). Patients with duplications spanning from 5p15.3 to 5p13.3 have mild and relatively indistinct phenotypes, while in presence of complete 5p trisomy as well as proximal duplications to cytogenetic band 5p13, the phenotype is more severe.

Our case is the first prenatal detection of 5p duplication, not involving other chromosomes, in a fetus with very mild phenotype anomalies.

Case description

A 26 year old gravida 3 para 2 woman was referred to our unit for prenatal diagnosis because of fetal malformations. The family history of both the mother and her husband was not remarkable. Ultrasonographic examination showed short femur, bilateral clubfoot, pielectasy and broad anterior fontanelle. Tridimensional sonography showed facial dysmorphisms such as low-set ears, exophthalmos and sloping forehead (fig.1). The association of multiple soft markers suggested the opportunity of a fetal karyotyping. Therefore a cordocentesis was performed at 22 weeks of gestation.

MATERIALS AND METHODS

Karyotyping and FISH

Fetal blood was cultured for 48hr in Chromosome Medium (Euroclone). Metaphase chromosomes were analyzed by standard G-banding technique. FISH analysis was performed with the commercial probe LSI D5S23 for the Cri-du-Chat syndrome critical region 5p15.2 and for whole chromosome 5 (wcp5,Vysis) according to the manufacturer's protocols. The 5p15.33 region was hybridized with BAC clone probe RP11-94J21. BAC location was mapped according to UCSC Genome Bioinformatics (http://genome.ucsc.edu) and EMBL-EBI and Sanger Institute Genome Database (http://www.ensembl.org). The BAC clone was extracted using standard methods (Birnboim 1993), labeled by random priming with CY3-dCTP and hybridized as for the LSI probe. The analysis was performed on metaphases. Image acquisition was performed using an Olympus BX61 Microscope with CytoVision 3.7 software.

Array CGH

Comparative genomic hybridization (array-CGH) was performed using the Constitutional Chip® 4.0 including approximately 5000 BAC clones (PerkinElmer, USA) with a mean 500 kb resolution. The array-CGH was performed in dye swap according to manufacturer's instructions. The hybridization data were analyzed with OneClickCGH® software (Infoquant, UK). Control genome was a standard of female DNA (Promega).

BACs-on-Beads (BoBs) tecnique

BACs-on-Beads™ is a technology where probes generated from selected BACs are immobilized onto Luminex encoded beads. The resulting bead sets are used to assay chromosomal gains and losses from minute amounts with high throughput. The assay was performed according to manufacturer's instructions. The kit that we used gave information about 13, 18, 21, X and Y aneuploidies and about the 9 most frequent

microdeletion/duplication syndromes: Wolf-Hirschhorn, Cri-du-chat, Williams-Beuren, Langer-Giedion, Prader-Willi, Angelman, Miller-Dieker, Smith-Magenis, DiGeorge. One male and one female control genomes were used as reference samples.

RESULTS

CYTOGENETIC STUDIES

BACs-on-Beads (BoBs) assay was performed within 48 hours on DNA extracted from fetal blood in order to quickly detect aneuploidies of chromosomes 13, 18, 21, X and Y, as well as copy number variations in 9 microdeletion syndrome regions. The BoBsoft software analysis showed that the whole Cri-du-Chat syndrome region was clearly duplicated (Fig. 2). Eight independent BAC probes are included in the BoBs panel for chromosome 5p, spanning 7,7 Mb from 5p15.2 to 5p15.33.

High resolution G banding of chromosomes from fetal lymphocytes showed additional material on the short arm of one chromosome 5 (Fig. 3). The whole chromosome painting for chromosome 5 (wcp5; Vysis) demonstrated that the additional material was derived from chromosome 5 only. No additional hybridization signals were seen on other chromosomes (Fig. 4). Dual FISH using both a Cri-du-Chat (Vysis) unique sequence (green signal), mapping to the p15.2 region of chromosome 5, and the BAC clone (red signal) mapping to p15.33 showed two fluorescent green signals on the short arm of the abnormal chromosome with a double red signal in between demonstrating that the duplication was inverted (Fig. 5). Array CGH with Constitutional Chip® 4.0 (Perkin Elmer) showed a 40 Mb duplication from 5p13.1 to 5p15.33 with a 5pter deletion spanning about 600 Kb (Fig. 6).

The complete karyotype formula was 46,XY,add(5)(p15.3).ish der(5)(5p1.3->5p1.5::5p1.5->5qter)(wcp5+,D5S23++,5ptel-).arr 5p15.33(RPI-24H17)x1, 5p15.33->5p13.1(RP11-94J21->CTD-2142G21)x3.

DISCUSSION

We have characterized, by molecular cytogenetics, the first prenatal case of inverted duplication with terminal deletion (inv dup del) of a large trait of the chromosome 5 short arm. FISH and CGH array analyses demonstrated that the duplication was inverted, spanning 40Mb from 5p13.1 to 5p15.33, including the critical region for cri-du-chat syndrome. Furthermore there was a terminal deletion of about 600 kb.

Our case did not involve other chromosomes and presented with very mild ultrasonographic anomalies. The comparison with three previously reported cases of invdup, with or without terminal deletion (Sreekantaiah et al. 1999, Cervera et al. 2005 and Wang et al. 2008), has shown that clinical features often found in these patients, like hypotonia, speech delay and mental retardation, are not assessable in prenatal diagnosis. Phenotypic characteristics associated with duplication involving chromosomal regions from 5p13.1 to centromere are, for example, congenital heart defect and brain abnormalities, not reported in our case even though a segment of 5p13.1 is duplicated. The absence of these severe anomalies, that should be ultrasonographically evident at 22 weeks of gestation, suggests that the critical region for severe abnormalities in 5p arm is smaller than the region previously described (Velagaleti et al. 2000) and it includes only a portion of 5p13.1 band.

It was hypothesized that inverted duplication with terminal deletion could arise from three mechanisms, all involving the formation of a dicentric chromosome which subsequently breaks during meiosis to form a monocentric duplicated and deleted chromosome. The most frequent mechanism, the *"classical" model* (Weleber et al. 1976, Jenderny et al. 1998), suggests that inv dup del occurs from an unusual intrachromosomal meiotic recombination in two homologous chromosomes after a double-strand break. This recombination process is called a *U-type exchange* because the ends of broken chromosomes fuse together and a dicentric chromosome is produced. After division one daughter cell contains a recombinant

chromosome with one centromere and a region with a symmetric inverted duplication accompanied by a concomitant distal deficiency together with the lack of telomeric sequences.

Several studies on inverted 8p duplication/deletions have suggested a second mechanism identified as *"modified" model* (Gorinati et al., 1991; Minelli et al., 1993; Mitchell et al., 1994; Guo et al., 1995; Floridia et al., 1996; Giglio et al., 2001; Shimokawa et al., 2004; Ciccone et al., 2006; Zuffardi et al., 2009). Abnormal meiotic alignment between two homologous chromosomes, followed by a non-allelic homologous recombination (NAHR), determine the formation of a dicentric chromosome. Subsequently, breakage of the dicentric outside the inverted repeats leads to a monocentric chromosome with a terminal deletion and an inverted duplication with a single copy region between duplication. This mechanism involves the presence of inverted low-copy repeats (LCRs) spanning about 10-500kb, with a sequence homology greater than 95% (Stankiewicz et al. 2002, Rowe et al. 2009) outside the specific segment involved in the rearrangement. In case of tandem LCRs, Gorinati et al. (1991) suggest the possibility of a paracentric inversion in one parent.

Two different couples of LCRs in tandem with high similarities in the breakpoint region of the described rearrangement (Fig. 7) support the hypothesis that in this case the mechanism of inv dup del 5p will be most likely consistent with the modified model. In this case a single copy region, spanning less than 50 kb, between LCRs in 5p15.33 might be identified only with a very high resolution array CGH (about 10 kb).

Finally our study demonstrates the utility of a new technology, called *"Bac-on-Beads"*, that allows to quickly detect in 48hr the most frequent aneuploidies as well as many microdeletions and microduplications in prenatal diagnosis.

REFERENCES

Avansino J.R., Dennis T.R., Spallone P., Stock D.A., Levin M.L., Proximal 5p trisomy resulting from a marker chromosome implicates band 5p13 in 5p trisomy syndrome, Am. J. Med. Genet. 1999 87:6–11.

Birnboim HC. A rapid alkaline extraction method for the isolation of plasmid DNA. Methods Enzymol 1993 100:243-255.

Cervera M, Sanchez S, Molina B, Alcantara MA, Del Castillo V, Carnevale A, Gonzales-del Angel A. Trisomy of the short arm of chromosome 5 due to a de novo inversion and duplication (5)(p15.3 p13.3). Am J Med Genet 2005 136A:381-385.

Ciccone R, Mattina T, Giorda R, Bonaglia MC, Rocchi M, Pramparo T, Zuffardi O. Inversion polymorphisms and noncontiguous terminal deletions: The cause and the (unpredicted) effect of our genome architecture. J Med Genet 2006 43:e19.

Floridia G, Piantanida M, Minelli A, Dellavecchia C, Bonaglia C, Rossi E, Gimelli G, Croci G, Franchi F, Gilgenkrantz S, Grammatico P, Dalpra L, Wood S, Danesino C, Zuffardi O. The same molecular mechanism at the maternal meiosis I produces mono- and dicentric 8p duplications. 1996 Am J Hum Genet 58:785–796.

Giglio S, Broman KW, Matsumoto N, Calvari V, Gimelli G, Neumann T, Ohashi H, Voullaire L, Larizza D, Giorda R, Weber JL, Ledbetter DH, Zuffardi O. Olfactory receptor-gene clusters, genomic-inversion polymorphisms, and common chromosome rearrangements. Am J Hum Genet 2001 68:874–883.

Gorinati M, Caufin D, Minelli A, Memo L, Gaspardo G, Dodero A. Inv dup (8) (p21.1----22.1): further case report and a new hypothesis on the origin of the chromosome abnormality. Clin Genet. 1991 Jan;39(1):55-9.

Guo WJ, Callif-Daley F, Zapata MC, Miller ME. Clinical and cytogenetic findings in seven cases of inverted duplication of 8p with evidence of a telomeric deletion using fluorescence in situ hybridization. Am J Med Genet 1995 58:230–236.

Jenderny J, Poetsch M, Hoeltzenbein M, Friedrich U, Jauch A. Detection of a concomitant distal deletion in an inverted duplication of chromosome 3. Is there an overall mechanism for the origin of such duplications/deficiencies? European Journal of Human Genetics (1998) 6, 439–444.

Minelli A, Floridia G, Rossi E, Clementi M, Tenconi R, Canurri L, Bernardi F, Hoeller H, Previde Re C, Maraschio P, Wood S, Zuffardi O, Danesino C.D8S7 is consistently deleted in inverted duplications of the short arm of chromosome 8 (invdup 8p). Hum Genet 1993 92:391–396.

Mitchell JJ, Vekemans M, Luscombe S, Hayden M, Weber B, Richter A, Sparkes R, Kojis T, Watters G, Der Kaloustian VM. U-type exchange in a paracentric inversion as a possible mechanism of origin of an inverted tandem duplication of chromosome 8. Am J Med Genet 1994 49:384–387.

Rowe LR, Lee JY, Rector L, Kaminsky EB, Brothman AR, Martin CL, South ST. U-type exchange is the most frequent mechanism for inverted duplication with terminal deletion rearrangements. J Med Genet 2009 46(10):694-702.

Shimokawa O, Kurosawa K, Ida T, Harada N, Kondoh T, Miyake N, Yoshiura K, Kishino T, Ohta T, Niikawa N, Matsumoto N. Molecular characterization of inv dup del(8p): Analysis of five cases. Am J Med Genet Part A 2004 128A:133–137.

Sreekantaiah C, Kronn D, Marinescu RC, Goldin B, Overhauser J. Characterization of a complex chromosomal rearrangement in a patient with a typical catlike cry and no other clinical findings of Cri-du-chat Syndrome. Am. J. Med. Genet. 1999 86:264-268.

Stankiewicz P, Lupski JR. Genome architecture, rearrangements and genomic disorders. Trends Genet 2002 18(2):74-82.

Velagaleti GVN, Morgan DL, Tonk VS. Trisomy 5p. A case report and review. Ann. Génét. 2000 43:143–145.

Wang J, Coe BP, Lomax B, MacLeod PM, Parslow MI, Schein JE, Lam WL, Eydoux P. Inverted duplication with terminal deletion of 5p and no cat-like cry. Am J Med Genet 2008 146A:1173-1179.

Weleber RG, Verma RS, Kimberling WJ, Fieger HG Jr, Iubs HA. Duplication-deficiency of the short arm of chromosome 8 following artificial insemination. Ann Genet. 1976 Dec;19(4):241-7.

Zuffardi O, Bonaglia M, Ciccone R, Giorda R. Inverted duplications deletions: underdiagnosed rearrangements?? Clin Genet 2009: 75:505-513

FIGURES

Figure 1

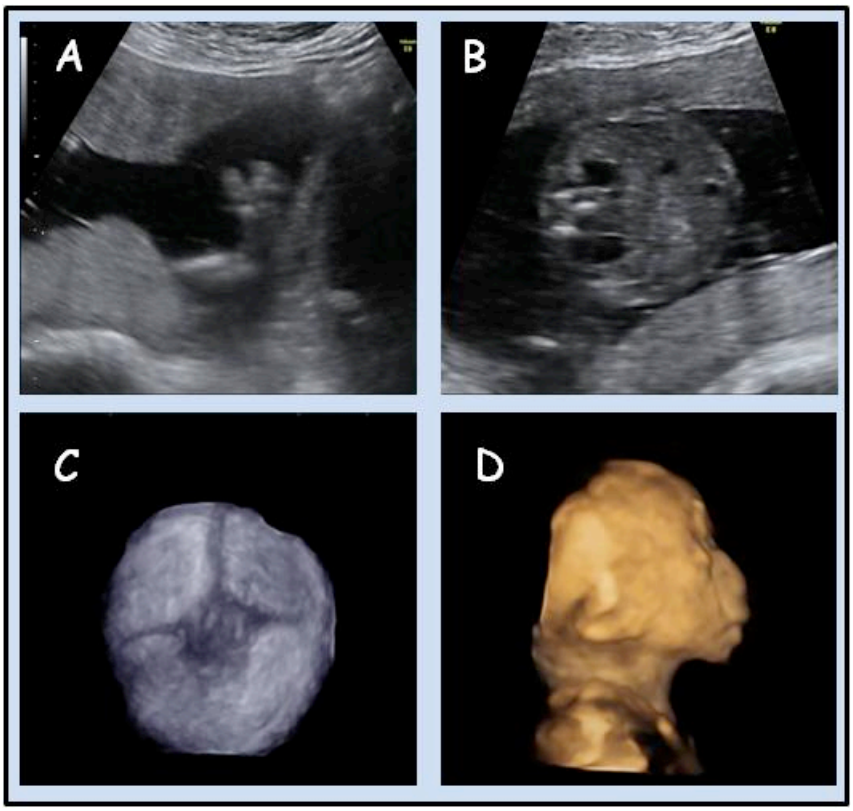

Ultrasonographic examination images of fetus showing bilateral clubfoot (A), pielectasy (B) and broad anterior fontanelle (C). Tridimensional sonography shows facial dysmorphisms such as low-set ears, exophthalmos and sloping forehead (D).

Figure 2

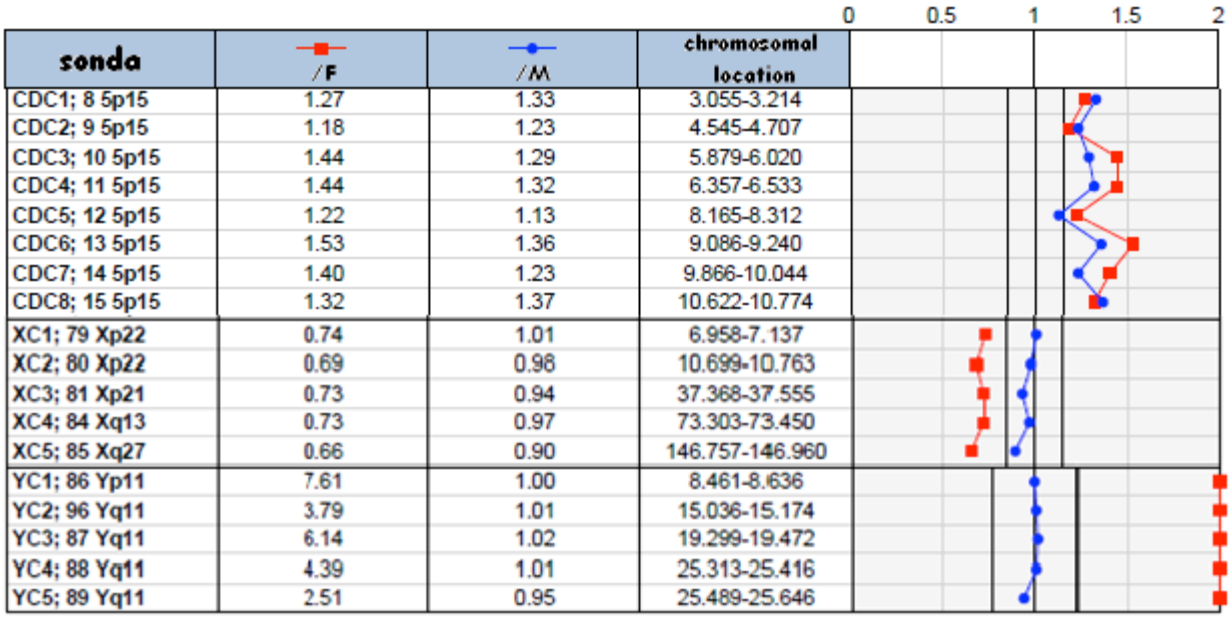

sonda	/F	/M	chromosomal location
CDC1; 8 5p15	1.27	1.33	3.055-3.214
CDC2; 9 5p15	1.18	1.23	4.545-4.707
CDC3; 10 5p15	1.44	1.29	5.879-6.020
CDC4; 11 5p15	1.44	1.32	6.357-6.533
CDC5; 12 5p15	1.22	1.13	8.165-8.312
CDC6; 13 5p15	1.53	1.36	9.086-9.240
CDC7; 14 5p15	1.40	1.23	9.866-10.044
CDC8; 15 5p15	1.32	1.37	10.622-10.774
XC1; 79 Xp22	0.74	1.01	6.958-7.137
XC2; 80 Xp22	0.69	0.98	10.699-10.763
XC3; 81 Xp21	0.73	0.94	37.368-37.555
XC4; 84 Xq13	0.73	0.97	73.303-73.450
XC5; 85 Xq27	0.66	0.90	146.757-146.960
YC1; 86 Yp11	7.61	1.00	8.461-8.636
YC2; 96 Yq11	3.79	1.01	15.036-15.174
YC3; 87 Yq11	6.14	1.02	19.299-19.472
YC4; 88 Yq11	4.39	1.01	25.313-25.416
YC5; 89 Yq11	2.51	0.95	25.489-25.646

Profile of the patient analyzed with BoBs, showing duplication of BAC clones in 5p15 (CDC probes). Patient DNA was compared to a female reference (in red) and to a male reference (in blue). The analysis showed a male karyotype.

Figure 3

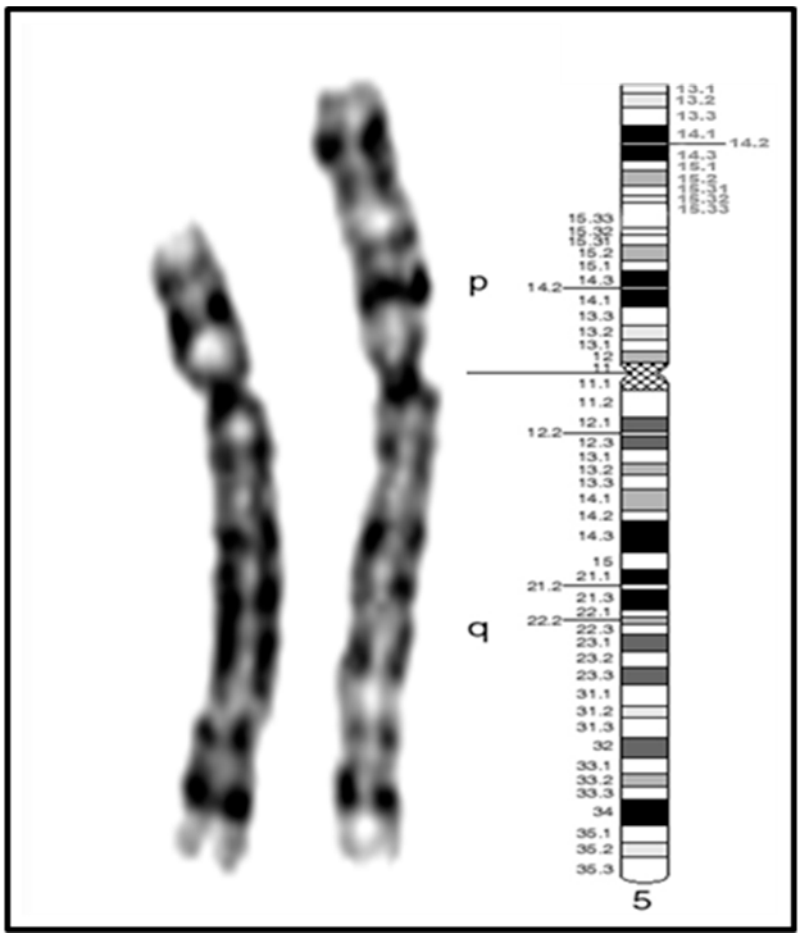

High resolution G-banding and ideogram of the derived chromosome 5 from fetal lymphocytes showing the presence of additional material on the short arm of one chromosome 5.

Figure 4

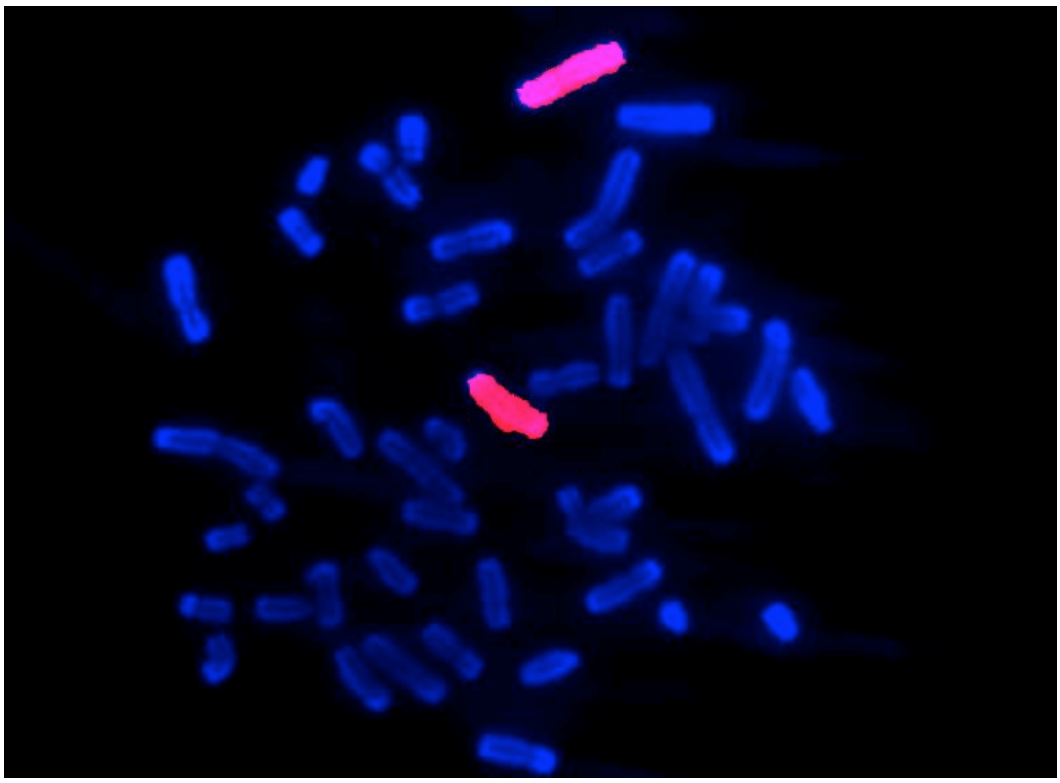

Fluorescent In Situ Hybridization (FISH) performed on metaphases with whole chromosome painting for chromosome 5 showed that the additional material was derived from chromosome 5 only (red signals).

Figure 5

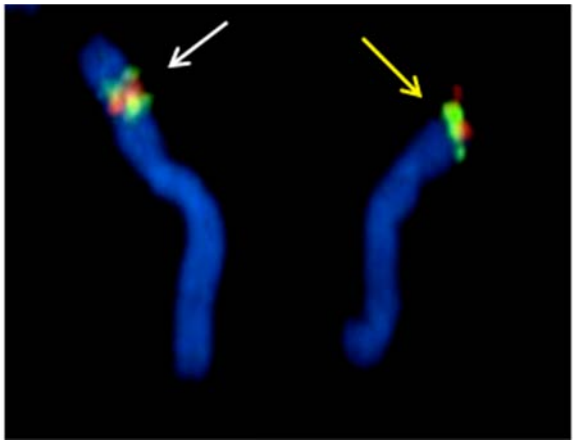

Dual FISH using both a Cri-du-Chat unique sequence (green signal), mapping to the p15.2 region of chromosome 5, and the RP11-94J21 BAC clone (red signal) mapping to p15.33 showed two fluorescent green signals on the short arm of the abnormal chromosome (indicated by white arrow) with a double red signal in between demonstrating that the duplication was inverted.

Figure 6

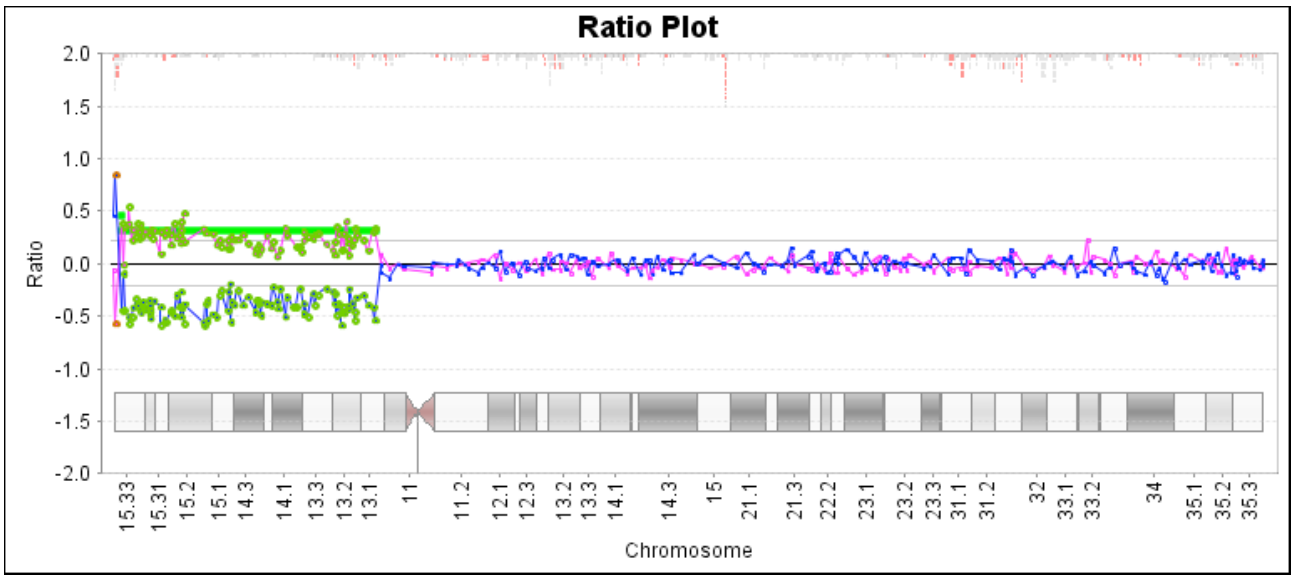

Array-CGH profile in dye swap of chromosome 5 showed a 40Mb duplication (green line) from 5p13.1 to 5p15.33 and a 5pter deletion spanning about 600kb (red line).

Figure 7

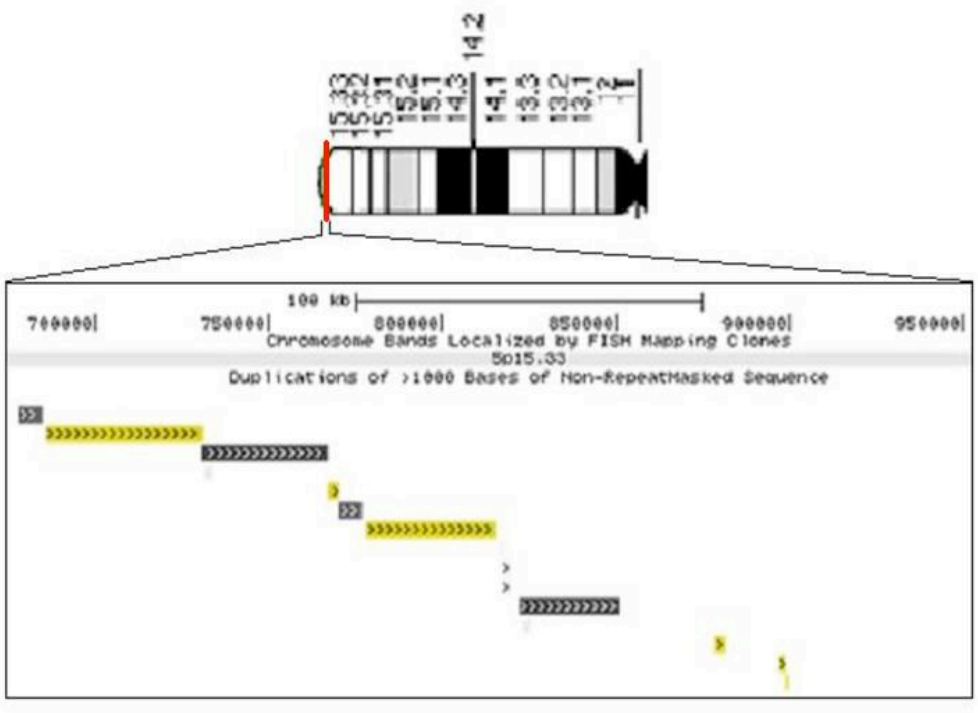

Breakpoint region in 5p15.33 is indicated as red line. In this region, two different couples of LCRs in tandem with high similarity are located, supporting the hypothesis of a modified model. Yellow LCR region spans about 40kb while the gray one spans about 30kb.